

博士論文

Studies on bioactive peptides from the marine sponge *Theonella swinhoei*

(カイメン *Theonella swinhoei* 由来の生物活性ペプチドに関する研究)

福原 和哉

Kazuya Fukuhara

Studies on bioactive peptides from the marine sponge *Theonella swinhoei*

Laboratory of Aquatic Natural Products Chemistry

Graduate School of Agricultural and Life Sciences

The University of Tokyo

Supervisor: Professor Shigeki Matsunaga

By
Kazuya Fukuhara

Acknowledgements

First of all, I am deeply grateful to Professor Shigeki Matsunaga for inviting me to dive into the world of marine natural products. Moreover, I thank him for supporting my whole research and giving me countless valuable advice, especially about isolation and structure elucidation. I would like to thank Associate Professor Shigeru Okada for insightful comments about my research and letting me to use HPLC-MS many times. I owe my deepest gratitude to Assistant Professor Kentaro Takada for encouragement and helps throughout my research, and giving me many opportunities for discussion, constructive advice, and incisive criticisms.

I would like to express appreciation to two graduates of the laboratory of aquatic natural products chemistry: Mr. Masashi Suzuki for giving me the foundation of experiments and kind helps through my undergraduate research; Dr. Yuki Hitora for giving me practical advice even after his graduation. Also, I want thank all members of the laboratory for supporting my research. I would like to particularly thank three members: Dr. Raku Irie, Dr. Akihiro Ninomiya, and Ms. Rei Suo for wide-ranging discussions and moral supports.

I would like to express my gratitude to Dr. Kazuo Furihata for letting me to use NMR and giving me many constructive and practical advice about NMR.

I would like to offer my special thanks to Dr. Katherine Duncan, Dr. Micheal Wilson, and all staffs of Gordon Research Seminar (Marine Natural Products, 2016) for inviting me to the seminar and giving me the opportunity for oral presentation in front of young and energetic researchers.

I would like to thank many great professors for discussion and giving me valuable advice: Professor Ryuichi Sakai, Associate Professor Masaki Fujita, and Professor Toshiyuki Wakimoto, Hokkaido University; Professor Hiroshi Nagai and Assistant Professor Michiya Kamio, Tokyo University of Marine Science and Technology; Assistant Professor Shinichi Nishimura, Kyoto University.

I am deeply grateful to Dr. Yuji Ise, Nagoya University for letting me use beautiful pictures of sponges (Figure 1-2, Chapter 1) and giving knowledge of sponges.

I want to thank Ms. Shiho Obonai for providing me excellent figure (Figure 1-1, Chapter 1) and lots of moral supports.

I would like to thank JSPS for financial supports.

Finally, I would like to offer my special thanks to my parents and grandparents for allowing me going on to graduate school, financial supports, and lots of encouragement.

List of Abbreviations (I)

^{13}C	carbon thirteen
^1H	proton
BuOH	butanol
calcd	calculated
COSY	correlation spectroscopy
DMSO	dimethyl sulfoxide
DTT	dithiothreitol
Et ₂ O	diethyl ether
EtOH	ethanol
FABMS	fast atom bombardment mass spectroscopy
FDAA	<i>N</i> ^α -(5-fluoro-2,4-dinitrophenyl)-alaninamide
FDNP	<i>N</i> ^α -[2,4-dinitro-5-fluorophenyl]
HMBC	heteronuclear multiple bond coherence spectroscopy
HPLC	high performance liquid chromatography
HRESIMS	high resolution electrospray ionization mass spectroscopy
HSQC	heteronuclear multiple quantum coherence spectroscopy
LC-MS	liquid chromatography-mass spectrometry
MeCN	acetonitrile
MeOH	methanol
min	minute
<i>m/z</i>	mass-to-charge ratio

List of Abbreviations (II)

NMR	nuclear magnetic resonance
NOESY	nuclear Overhauser enhancement spectroscopy
rRNA	ribosomal RNA
ODS	octadecylsilyl
obsd	observed
PrOH	propanol
ROESY	rotating frame nuclear Overhauser enhancement spectroscopy
RP-HPLC	reversed phase high performance liquid chromatography
TOCSY	total correlation spectroscopy
UV	ultraviolet

Table of Contents

Acknowledgements	a
List of abbreviations (I)	b
List of abbreviations (II)	c
Table of Contents	d
Chapter 1. Introduction	1
Chapter 2. Nazumazoles A–C, cyclic pentapeptides dimerized through a disulfide bond from the marine sponge <i>Theonella swinhoei</i>	14
Chapter 3. Nazumazoles D–F, cyclic pentapeptides that inhibit chymotrypsin, from the marine sponge <i>Theonella swinhoei</i>	59
Chapter 4. Theonellamide H, a cytotoxic peptide with colony dependent distribution from the marine sponge <i>Theonella swinhoei</i>	94
Chapter 5. Conclusion	127
Reference and Notes	132

Chapter 1.

Introduction

Sponges (phylum Porifera) are one of the simplest and most primitive animals on earth. They appeared in the world at least 600 million years ago, 50–100 million years before the Cambrian explosion.^{1,2} They can be found in oceans all around the world and even in freshwaters. Today, more than 8500 species of sponges are identified.³ Although only a few species of sponges are movable and carnivorous, almost all sponges are benthos and filter-feeders.⁴

Neither nerve system, musculature, nor organs are observed in sponges, but they have cells which have specialized functions (Figure 1-1).^{4,5,6} Sponges have many “mouths” (ostia) on the “epidermis” (pinacoderm), take waters in their bodies, and capture organic particles in water by cells with flagellates (choanocytes). Taken water is excreted from relatively larger “mouth” (oscula) and this flow of water is supported by flagellates of choanocytes. Adjacent to pinacoderm and choanocytes, there is a gelatinous and non-living layer, called mesohyl. In this layer, sponge cells called

archeocytes are wandering and these cells are multi-functional: storage and digestion of food materials; metamorphosis into other specific cells, sperms and eggs; formation of the sponge body by secreting spicules and spongin, a kind of collagen protein.

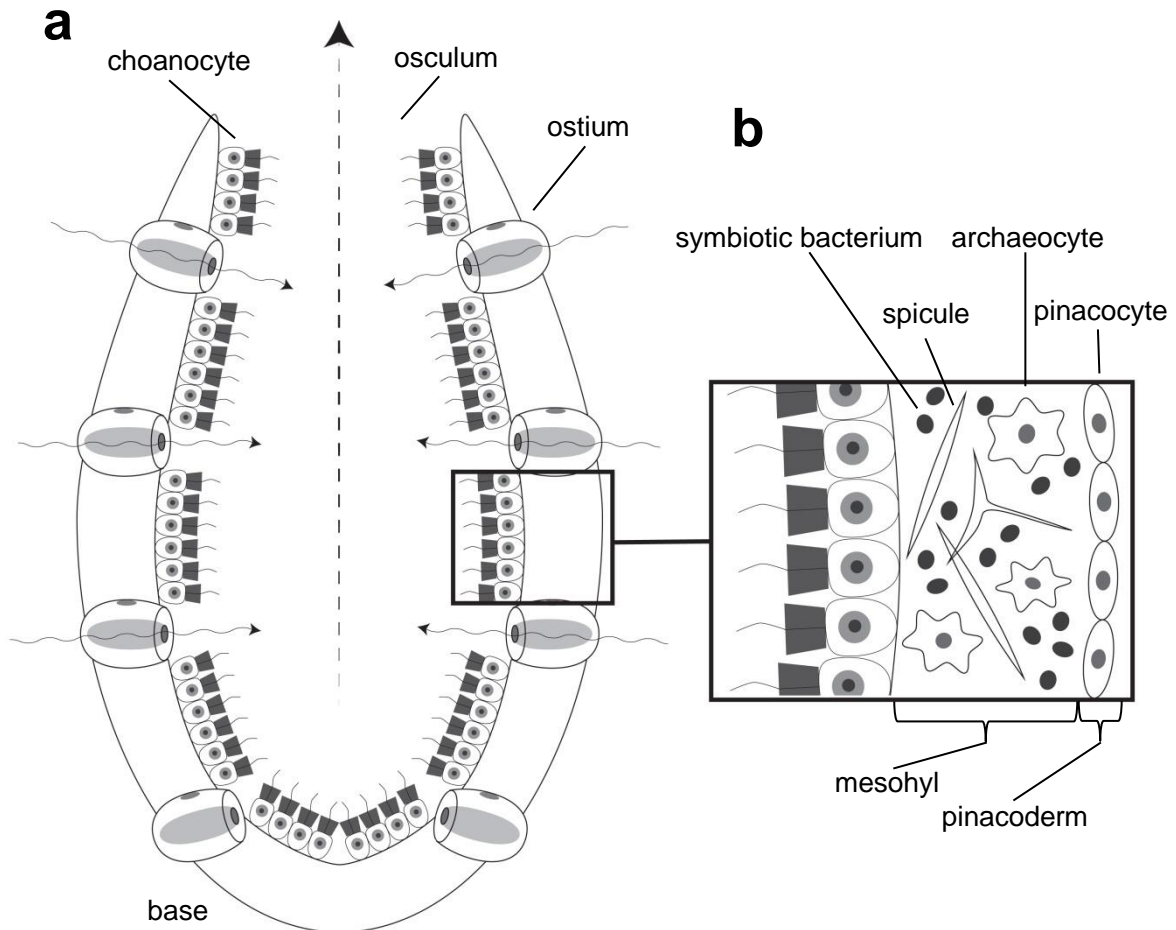


Figure 1-1. (a) A schematic figure of a typical sponge (arrows indicate flow of water) and (b) an enlarged view of the internal structure of a typical sponge.

From ecological aspects, sponges provide habitats and shelters for other animals.⁵ Moreover, there is a variety of cyanobacteria and other bacteria in the mesohyl layer (Figure 1-1b).^{6,7} Although the percentages somehow differ among literatures, the amount of symbiotic bacteria can be up to 35–50% of total biomass of

sponges.^{6,7} These bacteria have been thought as a great source of bioactive compounds.⁸ From sponges' view, these compounds may work as anti-predators⁹, anti-competitors¹⁰, or anti-harmful microorganisms.¹¹ One of the reasons why these simple and immovable animals can flourish in water environment is thought to be that sponges have these diverse “chemical weapons” in their body.¹² On the other hand, from humans' view, these compounds can be new pharmacologically active compounds.¹³ Actually, a number of reports about search for bioactive compounds from sponges have been published.¹⁴

The subject of this doctoral thesis is to search for new bioactive compounds from the sponge *Theonella swinhoei*. To show that this sponge is a promising source of beneficial bioactive compounds, two aspects of this sponge are described in this chapter: (1) diversity and structural complexity of secondary metabolites in this sponge; (2) progress of research about biosynthesis of metabolites and biology of symbiotic bacteria in the sponge.

Metabolites of the marine sponge *Theonella swinhoei*

The sponges of the genus *Theonella* are one of the greatest sources of bioactive secondary metabolites among sponges. Today, more than 300 compounds

isolated from “*Theonella*” sponge are registered in the database.¹⁵

There are several “subspecies” of the sponge *Theonella swinhoei*. We can find two types of sponges, *T. swinhoei* with white interior (*T. swinhoei* W) and *T. swinhoei* with yellow interior (*T. swinhoei* Y), at Hachijo Island, Tokyo, Japan (Figure 1-2). These sponges are different not only by their colors and shapes, but also by their metabolic profiles (Figure 1-3).

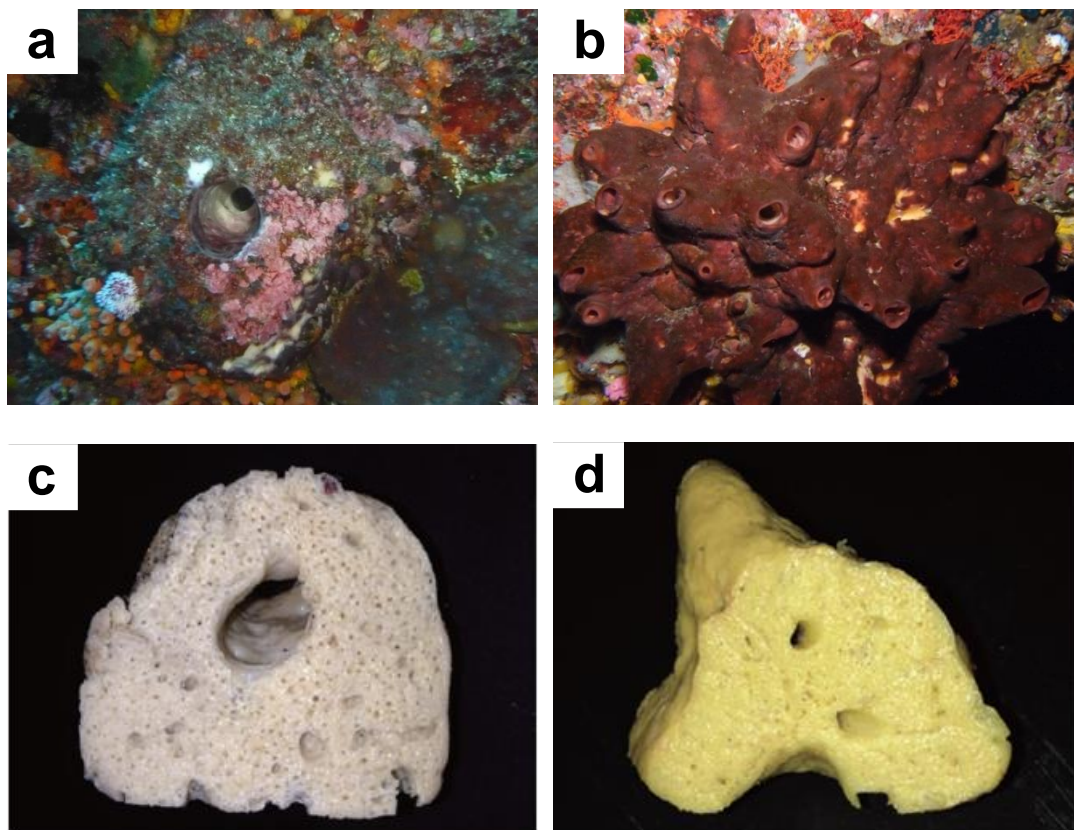
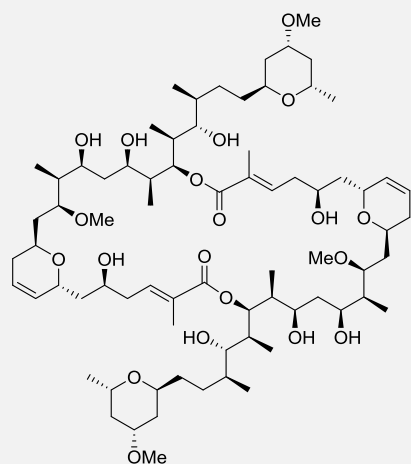
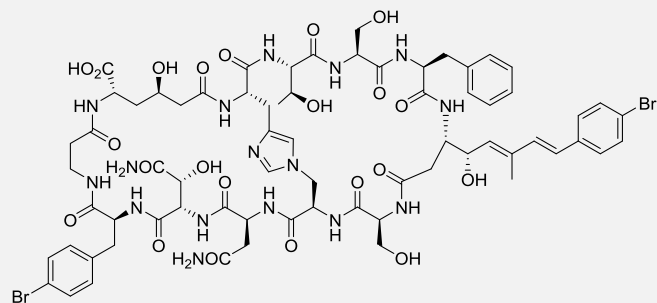


Figure 1-2. Two types of the sponge *Theonella swinhoei*; their underwater photos (**a**: white interior; **b**: yellow interior) at Hachijo Island, Tokyo, Japan and their cross sections (**c**: white interior; **d**: yellow interior). Photos were taken by Dr. Yuji Ise, Nagoya University.

a (from *T. swinhoei* W)

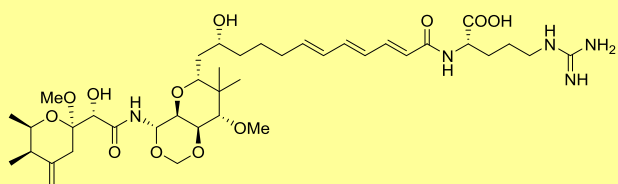


Misakinolide A (1)

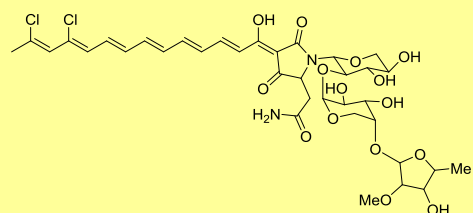


Theonellamide F (2)

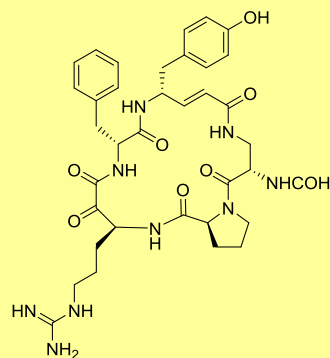
b (from *T. swinhoei* Y)



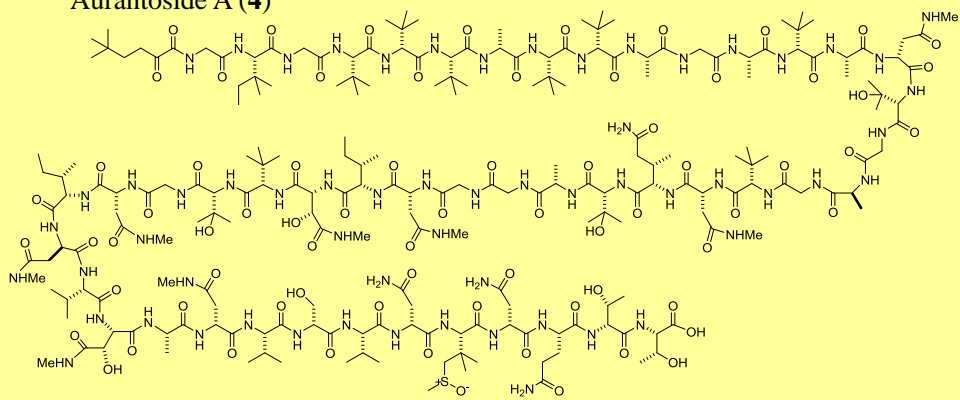
Onnamide A (3)



Aurantoside A (4)



Cyclotheonamide A (5)



Polytheonamide B (6)

Figure 1-3. Bioactive secondary metabolites from the sponge *Theonella swinhoei* (white and yellow)

From the sponge *T. swinhoei* W, structurally complex and bioactive macrolides, such as misakinolide A (**1**), and peptides, such as theonellamide F (**2**), were identified.

Misakinolide A (**1**) was first reported as an antitumor compound from Okinawan *T. swinhoei* W¹⁶, and its structure was determined as a 20-membered macrolide (Figure 1-4). One year later from the report, the compound which showed identical ¹H and ¹³C NMR spectra as those of **1** was found in *T. swinhoei* W collected at Hachijo Island.¹⁷ In this report, the structure of misakinolide A was revised as a 40-membered macrolide, which is the dimerized structure of the originally proposed 20-membered macrolide. Finally, the absolute configuration of **1** was established by comparison of spectroscopic data of **1** with those of swinholide A, which is closely related compound of **1**.^{18,19}

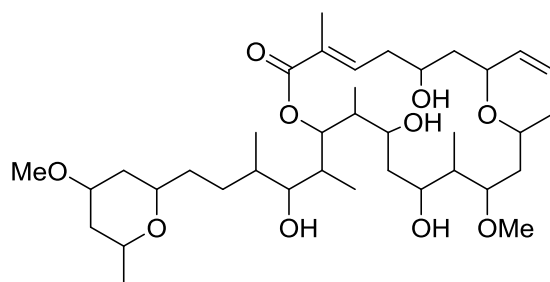


Figure 1-4. Originally proposed structure of misakinolide A.

Theonellamide F (**2**) was found in *T. swinhoei* collected at Hachijo Island.²⁰ This peptide has bicyclic structure containing characteristic unusual amino acids and histidinoalanine bridge, and exhibited bioactivities including antifungal activity and

cytotoxicity against some cancer cell lines. The structure of **2** was determined by careful analysis of the hydrolysate and 2D NMR spectra. Molecular target of **2** is revealed as 3 β -hydroxysterol, including ergosterol, in cell membranes and it is expected that **2** would be used as a research tool for exploring the function of sterols in cell membranes.²¹

Similarly, the sponge *T. swinhoei* Y contains a variety of secondary metabolites, which include some nitrogenous metabolites, such as onnamide A (**3**) and aurantoside A (**4**), and peptides, such as cyclotheonamide A (**5**) and polytheonamide B (**6**). As shown in Figure 1-3, structural features of metabolites in *T. swinhoei* Y are clearly different from those in *T. swinhoei* W.

Onnamide A (**3**) was isolated from Okinawan *T. swinhoei* and exhibited potent antiviral activity against herpes simplex virus type-1, vesicular stomatitis virus, and coronavirus A-59.²² Later, it was revealed that **3** had cytotoxicity against murine and human tumor cells.²³ The toxicity was exhibited by inhibition of protein synthesis²³ and activation of stress-activated protein kinases.²⁴ In addition, **3** is the first compound which was revealed to be biosynthesized by symbiotic bacteria in the sponge (described in the next part of the introduction).²⁵

Aurantioside A (**4**) and B were found in *T. swinhoei* collected at Hachijo Island.²⁶ Compound **4** exhibits orange color because it contains a conjugated heptaene system. Yellow color of *T. swinhoei* Y is due to the presence of this compound. Compound **4** showed cytotoxicity against P388 and L1210 leukemia cells.

Cyclotheonamide A (**5**) and B were also found in *T. swinhoei* collected at Hachijo Island.²⁷ Compound **5** contains two characteristic amino acids, α -keto- β -arginine (Kar) and α,β -unsaturated- γ -tyrosine (Figure 1-5). The absolute configuration of Kar residue in **5** was established by total synthesis.²⁸ Compound **5** inhibits the activity of serine proteases such as thrombin and trypsin, because Kar residue covalently bonds to the active sites of the enzymes.²⁹

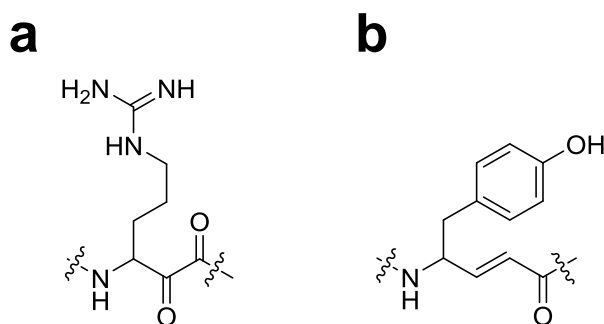


Figure 1-5. The structures of (a) α -keto- β -arginine and (b) α,β -unsaturated- γ -tyrosine.

Polytheonamide B (**6**) was isolated from *T. swinhoei* collected at Hachijo Island.³⁰ The structure of **6** is a linear peptide constructed by 48 amino acids with *N*-terminus blocked by 5,5-dimethyl-2-oxoheptanoyl group and has D/L alternating

stereochemistry. In solution, compound **6** adopts a β -helical structure and forms channels in cell membranes.³¹ This accounts for the potent cytotoxicity of **6** (IC₅₀ values was 68 pg/mL against P388 leukemia cells). Polytheonamides had been thought to be biosynthesized by non-ribosomal peptide synthase (NRPS).³² However, it was revealed by metagenome analysis that the peptides are ribosomal.³³

As described, the sponge *T. swinhoei* is one of the most important sources to provide bioactive secondary metabolites among marine invertebrates. Therefore, many studies about biosynthesis of these compounds and symbiotic bacteria in the sponge are conducted.

Symbiotic bacteria in the marine sponge *Theonella swinhoei*

Some sponge metabolites have structural similarity with those of bacterial origin, so it had been hypothesized that these compounds were biosynthesized by the symbiotic bacteria and not by the sponges themselves.^{34,35}

In the sponge *T. swinhoei*, there is a large amount of cyanobacteria, and they had been thought to be the producer of bioactive compounds.^{19c} However, Bewley *et al.* reported suggestive results about symbiotic bacteria in the sponge *T. swinhoei*.³⁶ They separated symbiotic bacteria in Palauan *T. swinhoei* W and analyzed their metabolites.

They revealed that bioactive secondary metabolites, such as swinholide A and theopalauamide³⁷, an analogue of theonellamides, were not detected from the cyanobacteria fraction, but from the filamentous bacterial fraction. Four years later, Schmidt *et al.* reported the result of 16S rRNA analysis of the bacterium, and identified the bacterium as a novel species, named “*Candidatus Entotheonella palauensis*”.³⁸

In 2002, Piel identified the biosynthetic gene cluster of the cytotoxic polyketide, pederin (Figure 1-6a), from uncultured symbiotic bacteria in the beetle *Paederus fuscipes*.³⁹ Pederin is closely related to the metabolites, theopederin⁴⁰ and onnamide A, in *T. swinhoei* Y (Figures 1-6b and 1-6c), and this research showed the first evidence that symbiotic bacteria produce bioactive secondary metabolites. Two years later, Piel *et al.* identified the biosynthetic gene cluster of onnamide A from the metagenome of *T. swinhoei* Y, as mentioned above.²⁵ Metagenomics is an efficient method to explore the biosynthesis of metabolites produced by uncultured symbiotic bacteria, as evidenced by the demonstration that polytheonamides are ribosomal.³³

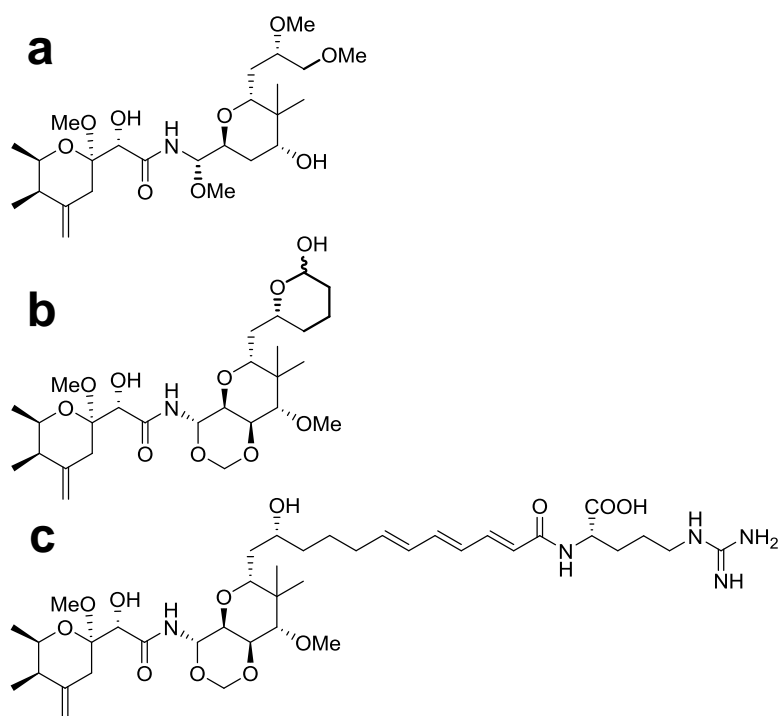


Figure 1-6. The structures of (a) pederin, (b) theopederin A, and (c) onnamide A.

In 2013, Piel's group and Japanese research groups reported that the filamentous bacteria, *Candidatus Entotheonella factor*, is the sole producer of bioactive secondary metabolites in *T. swinhoei* Y (Figure 1-7).⁴¹ Based on single cell genomics and metagenomics, this research revealed that almost all secondary polyketides and peptides identified in *T. swinhoei* Y, except for aurantosides, are biosynthesized by this bacterium.

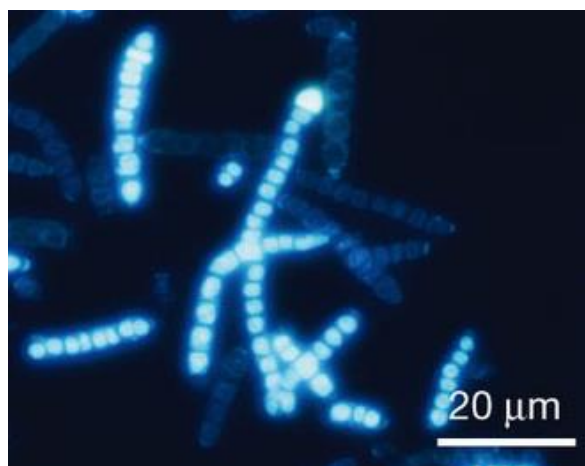


Figure 1-7. Florescence micrograph of filamentous bacteria, *Candidatus Entotheonella* factor (cited from reference 42).

With this great breakthrough, genus *Ca. Entotheonella* bacteria were observed in some sponges which contain bioactive secondary metabolites, and biosynthetic gene clusters of some metabolites were identified in the genome of *Ca. Entotheonella* sp., such as misakinolide A in *T. swinhoei* W⁴², and calyculin A⁴³ and kasumigamide⁴⁴ in the sponge *Discodermia calyx*.^{45,46} Recently, some biological aspects of *Ca. Entotheonella* bacteria in *T. swinhoei* Y were reported⁴⁷, and this bacterial group is becoming a bright resource of bioactive natural products.

The bottleneck of the pharmaceutical use of sponge metabolites is the limitation of the amount of biomass and metabolites, so it is challenging to provide these metabolites for clinical trial and long-term supplies. Chemical synthesis is one of the ways to resolve the problem, but synthesis of complex natural products is sometimes not economical. Another way is cultivating the chemical producer or transferring the

biosynthetic genes to a culturable host.⁷ From this view, as biosynthetic research about metabolites of *T. swinhoei* is advanced, it is expected that bioactive compounds from the sponge could be easily applied to drug candidates or biological research tools. Therefore, I searched for novel bioactive compounds from *T. swinhoei* Y.

In this doctoral thesis, the studies about bioactive peptides found in the sponge *T. swinhoei* Y are described. The second chapter describes the structures and biological activities of the new class of cyclic peptides, nazumazoles A–C. The third chapter illustrates nazumazoles D–F, monomeric analogue of nazumazoles A–C. The fourth chapter reports a new analogue of theonellamides, theonellamide H, which is contained in only several colonies and is the first compound of the theonellamide family which was identified in *T. swinhoei* Y.

The contents of chapters 2 and 3 have been published as follows.

- (I) Fukuhara, K.; Takada, K.; Okada, S.; Matsunaga, S. *Org. Lett.* **2015**, *17*, 2646–2648.
- (II) Fukuhara, K.; Takada, K.; Okada, S.; Matsunaga, S. *J. Nat. Prod.* **2016**, *79*, 1694–1697.

Chapter 2.

Nazumazoles A–C, cyclic pentapeptides dimerized through a disulfide bond from the marine sponge *Theonella swinhoei*

2.1. Introduction

We have analyzed the extracts of marine invertebrates by LC-MS and found that the extract of *T. swinhoei* Y contained unidentified metabolites, among which was an extraordinarily broad peak in ODS-HPLC (Figure 2-1, Figure S2-1). We successfully purified the peak, which exhibited cytotoxicity against P388 murine leukemia cells. We describe the isolation, structure elucidation, and biological activity of the constituents of the peak, nazumazoles A, B, and C (2-1–2-3) in this chapter.

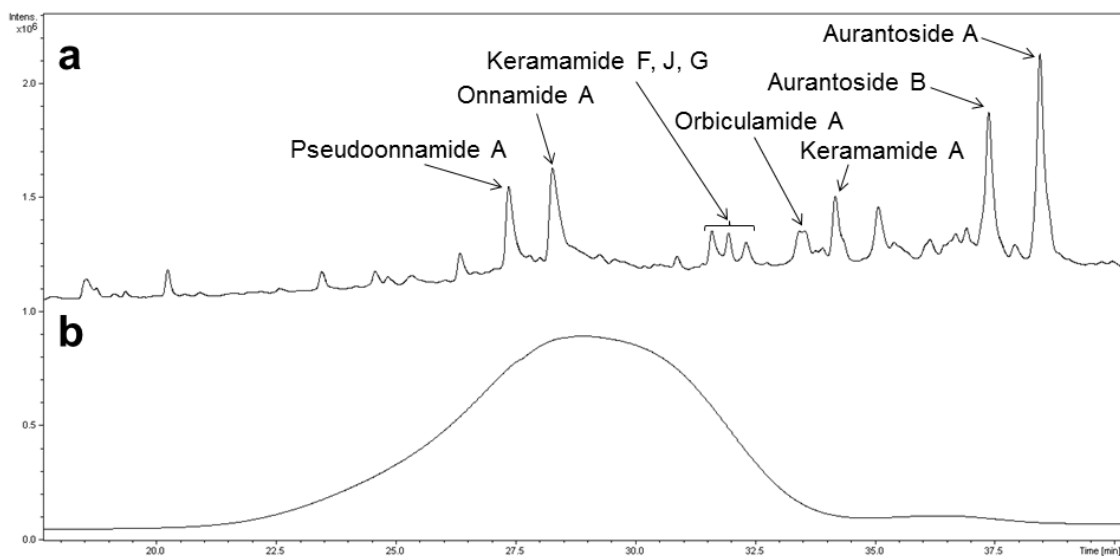


Figure 2-1. LC-MS charts of the crude fraction of *T. swinhoei* Y: **a)** UV-VIS chromatogram (integration of 210–400 nm) with assignments of some known compounds^{22,26,48,49,50} and **b)** MS chromatogram of a sum of the responses of the ions at m/z 1185, 1199, and 1213.

in the ESIMS when the solvent of the sample and the carrier liquid was altered from MeCN to MeOH or EtOH. For example, the protonated ion peaks of nazumazole C (2-3) were observed at m/z 1213, 1277, and 1305, respectively, when using MeCN, MeOH, and EtOH, indicating that two molecules of MeOH or EtOH were incorporated into the molecular ion, reminiscent of the FABMS data of cyclotheonamide A, in which alcohol adducts were formed at the α -keto- β -amino acid residue.²⁷

¹H and ¹³C NMR data (Table 2-1) suggested the peptide nature of the molecules with several amide ¹H signals and carbonyl ¹³C signals. Interpretation of the COSY, HSQC, and TOCSY spectra revealed the presence of Cys, 2,3-diaminopropionic acid (Dpr), and 4-methylproline (Mpr) residues (Figure 2-2a and 2-2b). The α -amino group of the Dpr residue was formylated as indicated by the HMBC correlations between H-14 (δ_H 4.76) and the formyl ¹³C signals (δ_C 160.7), and between the formyl ¹H (δ_H 7.99) and C-14 (δ_C 50.5) signals (Figure 2-3). There were ¹H NMR spin systems attributable to leucine and norvaline residues, for which nitrogen substituted methine ¹H signals were correlated to a ¹³C signal at δ_C 197.3 (197.2), suggesting the presence of α -ketoleucine (Kle) and α -ketonorvaline (Knv) residues (Figure 2-2c and 2-2d).⁵¹ The presence of a disubstituted oxazole ring was deduced from the HMBC data, in which a singlet aromatic ¹H signal (δ_H 8.54) directly coupled to a ¹³C signal at δ_C 142.4 by 213

Hz was correlated to ^{13}C signals at δ_{C} 134.5 and δ_{C} 163.5.⁵⁰ Further HMBC correlations from H-23 (δ_{H} 5.01) and H-24 (δ_{H} 1.54) signals to C-22 (δ_{C} 163.4) signal suggested that the oxazole ring was a part of an alanine derived oxazole (Aox, Figure 2-2e). At this moment, two amide carbonyl ^{13}C (δ_{C} 159.6 and δ_{C} 163.5) signals were left unassigned, one of which was in the α -keto- β -amino acid residue and the other attached to the Aox residue as inferred from a process of elimination.

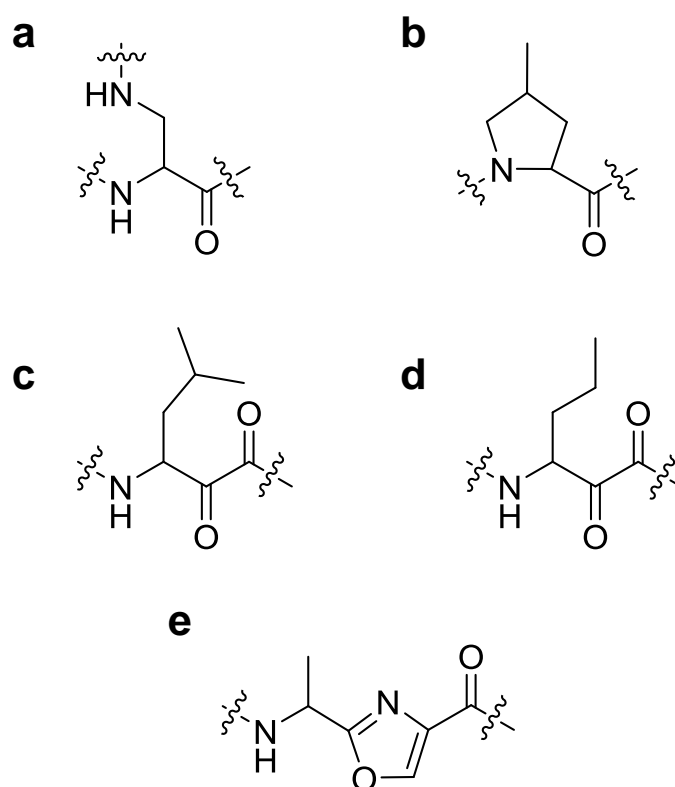


Figure 2-2. The structures of constituent amino acids in nazumazoles A–C (**2-1-2-3**): (a) 2,3-diaminopropionic acid (Dpr); (b) 4-methylproline (Mpr); (c) α -ketoleucine (Kle); (d) α -ketonorvaline (Knv); (e) alanine derived oxazole (Aox).

Table 2-1. ^1H and ^{13}C NMR Data for the Mixture of Nazumazoles A (**2-1**)–C (**2-3**) in DMSO- d_6 .

residue	position	$\delta_{\text{C}}^{\text{a}}$, type	$\delta_{\text{H}}^{\text{a}}$ (J in Hz)	residue	position	$\delta_{\text{C}}^{\text{a}}$, type	$\delta_{\text{H}}^{\text{a}}$ (J in Hz)
Knv	1	163.5, ^b C		Mpr	7	172.4, C	
	2	197.2, C			8	59.5, CH	4.44, m
	3	54.6, CH	4.82, m		9	37.1, CH ₂	2.42, m
	4	31.4, CH ₂	1.94, m				1.29, m
			1.56, m		10	33.2, CH	2.21, m
	5	19.1, CH ₂	1.48, m		11	53.9, CH ₂	3.90, m
			1.40, m				2.94, m
	6	13.3, CH ₃	0.90, m		12	15.8, CH ₃	0.99, d (6.4)
3-NH		8.59, d (6.0)	<i>N</i> -CHO-Dpr	13	167.0, C		
Kle	1	163.5, C		14	50.5, CH	4.76, m	
	2	197.3, C		15	38.7, CH ₃	3.68, m	
	3	53.3, CH	4.87, m			3.45, m	
	4	38.0, CH ₂	1.76, m	14-NH		7.98, m	
			1.46, m	15-NH		7.48, m	
	5	24.8, CH	1.78, m	CHO	160.7, CH	7.99, s	
	6	21.0, CH ₃	0.90, m	Aox	19	159.6, C	
	5-Me	22.9, CH ₃	0.93, m	20	134.5, C		
3-NH		8.56, m	21	142.4, CH	8.54, s		
			22	163.5, ^b C			
			23	43.7, CH	5.01, m		
			24	15.7, CH ₃	1.54, d (6.9)		
			23-NH		8.95, m		

^aRecorded at 150 MHz for ^{13}C and 600 MHz for ^1H at 40 °C.

^bChemical shifts of C-1 and C-22 overlapped each other.

The amino acid sequences of **2-1-2-3** were determined by HMBC and NOESY data (Figure 2-3). HMBC correlations 3-NH/C-7, H-11a/C-13, H-14/C-13, H-15b/C-16, H-18b/C-16, and H-17a,b/C-19 suggested the sequence of -K_{nv} (Kle)-M_{pr}-N-CHO-D_{pr}-C_{ys}-. The amide ¹H signal of the Cys residue was correlated to a ¹³C signal at δ_C 159.6 and the nitrogen substituted methine ¹H signal of the Aox residue was correlated to a ¹³C signal at δ_C 163.5 in the HMBC spectrum. Therefore, the Cys residue was shown to be connected to the Aox residue via a carbonyl carbon and the Aox residue was linked to the K_{nv}/Kle residue.

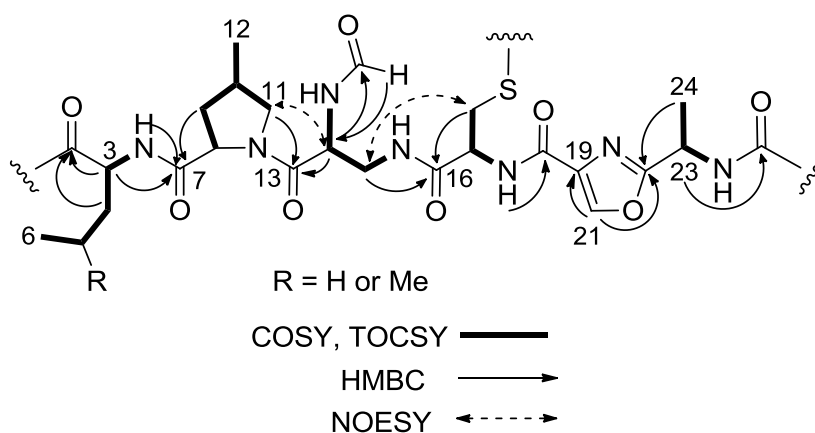
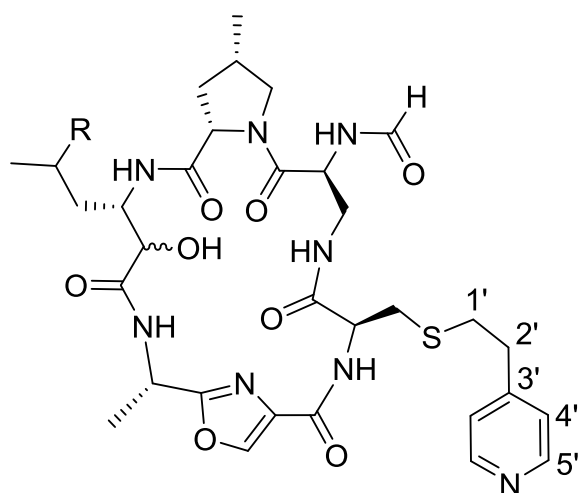


Figure 2-3. Key COSY, TOCSY, HMBC, and NOESY correlations in **2-1-2-3**.

Because the sizes of the resulting pentapeptide fragments were about half of the molecular weights of nazumazoles A–C, we considered that these peptides were either cyclic decapeptides or cyclic pentapeptides dimerized through a disulfide bond. In order to clarify this issue, the mixture of **2-1-2-3** was reduced consecutively with NaBH₄ and DTT, and subjected to alkylation with 4-vinylpyridine to afford a mixture of **2-4a** and **2-4b** and that of **2-5a** and **2-5b**, for which HRESIMS suggested that they were reduced cyclic pentapeptides with an *S*-pyridylethyl group.⁵² In **2-4a** and **2-4b**, the α -carbon of Knv residue was reduced to a secondary alcohol (rKnv residue), whereas in **2-5a** and **2-5b**, the pertinent residue was replaced by the reduced Kle (rKle) residue. Even though the structures of **2-4a**, **2-4b**, **2-5a**, and **2-5b** were confirmed by the 2D NMR data, each pair of diastereomers was inseparable by HPLC. Therefore, **2-1-2-3** were cyclic pentapeptides dimerized through a disulfide bond. We then examined the mode of dimerization by analyzing the NaBH₄ reduction products of the mixture of nazumazoles A–C, which gave three sharp HPLC peaks (Figure S2-2, **2-6-2-8**). The ESIMS and 2D NMR data demonstrated that the smallest congener (peak A, Figure S2-2) contained two rKnv residues, the second congener contained (peak B, Figure S2-2) one each of rKnv and rKle residue, and the largest congener (peak C, Figure S2-2) contained two rKle residues.⁵³



2-4a and **2-4b**: R = H
2-5a and **2-5b**: R = Me

The absolute configuration of the amino acid residues in **2-1–2-3** was determined by Marfey's method.⁵⁴ Ala, Cys, Dpr, and Mpr were liberated by standard acid hydrolysis. Knv and Kle residues were analyzed as Nva and Leu residues, respectively, by oxidation with H₂O₂. Two diastereomers of 4-methylproline were synthesized from *trans*-4-hydroxy-L-proline as described in the literature and used as standards.⁵⁵ Marfey's analysis with detection by ESIMS revealed the presence of L-Ala, D-Cys, L-Dpr, *cis*-4-methyl-L-proline, L-Leu, and L-Nva (Figure S2-30–S2-35).

The mixture of nazumazoles A–C (**2-1–2-3**) exhibited cytotoxicity against P388 murine leukemia cells with an IC₅₀ value of 0.83 μM. The cytotoxicity was diminished when the ketone in **2-1–2-3** was reduced, whereas the cytotoxicity was lost by further reduction and alkylation of the thiol group (Table S2-7).

2.3. Experimental Section

General Experimental Procedure.

UV spectra were measured on a Shimadzu BioSpec-1600 spectrophotometer. Optical rotations were measured on a Jasco DIP-1000 polarimeter. NMR spectra were measured on a JEOL delta 600 NMR spectrometer and referenced to residual solvent DMSO-*d*₆ (δ_{H} 2.49 for ¹H and δ_{C} 39.5 for ¹³C). ESI mass spectra were recorded on a JEOL JMS-T100LC mass spectrometer. LC-MS experiments were performed on a Shimadzu LC-20AD solvent delivery pump with a Nacalai Tesque Cosmosil 2.5C₁₈-MS-II column (ϕ 2.0 mm \times 100 mm) and interfaced to Bruker amaZon SL mass spectrometer. The results of XTT assay were recorded by Molecular Devices SPECTRA max M2.

Extraction and Isolation of Nazumazoles A–C (2-1–2-3).

The marine sponge *Theonella swinhoei* (22 kg) was collected at Hachijo Island. The sponge was extracted with MeOH at ambient temperature. The extract was dried in vacuo and partitioned between H₂O and Et₂O. The organic layer was further partitioned between 90% MeOH and *n*-hexane. The H₂O and 90% MeOH layers were combined and subjected to ODS column chromatography by elution with H₂O, MeOH-H₂O (1:1),

and CHCl₃-MeOH (1:1). The CHCl₃-MeOH (1:1) fraction was subjected to ODS column chromatography with *n*-PrOH-H₂O (2:3 and 3:1) and CHCl₃-MeOH (1:1). The *n*-PrOH-H₂O (2:3) fraction was subjected to gel permeation chromatography (Sephadex LH-20) with CHCl₃-MeOH (1:1) to afford 3 fractions. The fraction that eluted after polytheonamides³⁰ in the Sephadex LH-20 chromatography was subjected to ODS column chromatography with MeCN-H₂O (1:9, 1:3, 2:3), MeCN, and MeOH. The MeCN-H₂O (1:3) fraction was subjected to gel permeation HPLC on TOSOH TSK gel α -2500 (ϕ 20 mm \times 300 mm) at a flow rate of 2.8 mL min⁻¹ with detection at 235 nm, eluted with MeOH-H₂O (3:7) to afford 7 fractions.

Each fraction was analyzed by LC-MS, and the fractions that contain **2-1-2-3** were combined and purified by ODS-HPLC on Cosmosil 5C₁₈-AR-II (ϕ 10 mm \times 250 mm) at a flow rate of 4 mL min⁻¹ with detection at 220 nm. Gradient elution was performed using solvent A (0.2% acetic acid in H₂O/MeCN = 9:1) and solvent B (0.15% acetic acid in MeCN) with the following linear gradient program: at 0 min, 94% A; at 10 min, 94% A; at 35 min, 66% A; at 45 min; 66% A. As a result, we obtained the mixture of compounds **2-1-2-3** (43.4 mg).

Nazumazoles A–C (2-1–2-3): yellow powder; $[\alpha]_D = +22.4^\circ$ (c 0.05, MeOH); UV (MeOH) λ_{\max} ($\log \epsilon$) 216 (4.13); ^1H NMR and ^{13}C NMR (DMSO- d_6) see Table 2-1; HRESIMS obsd m/z 1207.4293 ($\text{M} + \text{Na}$) $^+$ ($\text{C}_{50}\text{H}_{68}\text{N}_{14}\text{NaO}_{16}\text{S}_2$ requires m/z 1207. 4277) for **2-1**, 1221.4464 ($\text{M} + \text{Na}$) $^+$ ($\text{C}_{51}\text{H}_{70}\text{N}_{14}\text{NaO}_{16}\text{S}_2$ requires m/z 1221. 4433) for **2-2**, and 1235.4560 ($\text{M} + \text{Na}$) $^+$ ($\text{C}_{52}\text{H}_{72}\text{N}_{14}\text{NaO}_{16}\text{S}_2$ requires m/z 1235. 4590) for **2-3**.

Reduction of the Mixture of 2-1–2-3 with DTT.

0.2 M DTT in H_2O (100 μL) was added to the mixture of **2-1–2-3** (100 μg) in MeOH (100 μL) and kept at 37 $^\circ\text{C}$ for 2 hours under N_2 . The reaction mixture was dried with a stream of N_2 and applied to a column of ODS (ϕ 5 mm \times 10 mm) and eluted with MeCN- H_2O (1:19, 3:2). The fraction eluted with MeCN- H_2O (3:2) was dried in vacuo and analyzed by LC-MS.

Reduction and Alkylation of the Mixture of 2-1–2-3.

NaBH_4 (2 mg) was added to the mixture of **2-1–2-3** (20 mg) in MeOH (1 mL) and left for 10 min at ambient temperature. To the reaction mixture, 5% acetic acid in H_2O (1 mL) was added. The solution was applied to a column of ODS (ϕ 5 mm \times 10 mm) and eluted with H_2O and MeCN- H_2O (3:2). The fraction eluted with MeCN- H_2O (3:2) was dried in vacuo to give a mixture of the reduced peptides (16 mg). To the

mixture dissolved in MeOH (1 mL) was added 1 M dithiothreitol (DTT) in H₂O (1 mL) and kept at 37 °C for 2 hours under N₂. 4-Vinylpyridine (100 μL) was added to the reaction mixture and incubated at rt in the dark for 24 hours under N₂. The reaction mixture was dried with a stream of N₂ and partitioned between H₂O and CHCl₃. The H₂O layer was then purified by ODS-HPLC on Cosmosil 5C₁₈-AR-II (ϕ 10 mm \times 250 mm) at a flow rate of 2.8 mL min⁻¹ with detection at 235 nm. Gradient elution was performed using solvent A (0.5% acetic acid in H₂O/MeCN = 9:1) and solvent B (0.45% acetic acid in MeCN) with the following linear gradient combination: at 0 min, 100% A; at 10 min, 100 % A; at 55 min, 50 % A. As a result, we obtained alkylated peptides **2-4** (4.2 mg) and **2-5** (1.9 mg). For the sake of clarity, the mixture of **2-4a** and **2-4b** and that of **2-5a** and **2-5b** were indicated as **2-4** and **2-5**, respectively.

2-4: yellow powder; $[\alpha]_D = +57.6^\circ$ (c 0.1, MeOH); ¹H NMR and ¹³C NMR (DMSO-*d*₆) see Table S2-1; HRESIMS obsd *m/z* 723.28813 (M + Na)⁺, C₃₂H₄₄N₈NaO₈S requires *m/z* 723.29005.

2-5: yellow powder; $[\alpha]_D = +81.2^\circ$ (c 0.05, MeOH); ¹H NMR and ¹³C NMR (DMSO-*d*₆) see Table S2-2; HRESIMS obsd *m/z* 715.32535 (M + H)⁺, C₃₃H₄₇N₈O₈S requires *m/z* 715.32375

Purification of the NaBH₄ Reduction Products of the Mixture of 2-1–2-3.

The mixture of reduced peptide (6.6 mg) was separated by ODS-HPLC on Cosmosil 5C₁₈-AR-II (ϕ 10 mm \times 250 mm) at a flow rate of 4 mL min⁻¹ with detection at 235 nm. Gradient elution was performed using solvent A (0.5% acetic acid in H₂O/MeCN = 9:1) and solvent B (0.45% acetic acid in MeCN) with the following linear gradient combination: at 0 min, 100% A; at 10 min, 100% A; at 20 min, 89% A; at 40 min, 89% A; at 50 min, 78% A; at 60 min, 78% A. As a result, we obtained **2-6** (0.9 mg), **2-7** (1.2 mg), and **2-8** (0.7 mg). Each of **2-6**, **2-7**, and **2-8** was an inseparable mixture of four compounds.

2-6: pale yellow powder; ¹H NMR (DMSO-*d*₆) see Table S2-3; HRESIMS obsd *m/z* 1211.45526 (M + Na)⁺, C₅₀H₇₂N₁₄NaO₁₆S₂ requires *m/z* 1211.45898.

2-7: pale yellow powder; ¹H NMR (DMSO-*d*₆) see Table S2-4 and S2-5; HRESIMS obsd *m/z* 1225.47719 (M + Na)⁺, C₅₁H₇₄N₁₄NaO₁₆S₂ requires *m/z* 1225.47463.

2-8: pale yellow powder; ¹H NMR (DMSO-*d*₆) see Table S2-6; HRESIMS obsd *m/z* 1239.48263 (M + Na)⁺, C₅₂H₇₆N₁₄NaO₁₆S₂ requires *m/z* 1239.49028

Marfey's Analysis of 2-1-2-3.

To the mixture of **2-6-2-8** (100 μg) in MeOH (1 mL) was added 0.1 M dithiothreitol (DTT) in H₂O (1 mL) and kept at 37 °C for 2 hours under N₂. The product was dried, redissolved in 6 N HCl, and kept at 110 °C for 3 hours. The reaction mixture was dried by a stream of N₂ and dissolved in H₂O (100 μL), to which were added 1% L-FDAA in acetone (100 μL) and 1 M NaHCO₃ in H₂O (20 μL) and kept at 55 °C for 30 min. After addition of 2 N HCl (10 μL), the reaction mixture was analyzed by LC-MS at a flow rate of 0.5 mL min⁻¹. Gradient elution was performed using solvent A (0.5% acetic acid in H₂O) and solvent B (0.45% acetic acid in MeCN) with the following linear gradient combination: at 0 min, 90% A; at 2 min, 90% A; at 32 min, 30% A. Retention times of amino acids (min): 6.6 (*m/z* 374, Cys), 9.7 (*m/z* 342, Ala), 12.4 (*m/z* 382, Mpr), and 15.7 (*m/z* 609, Dpr). Reduced Knv and Kle were detected by this analysis: 11.0 and 12.1 (*m/z* 400, rKnv), 12.8 and 13.8 (*m/z* 414, rKle).

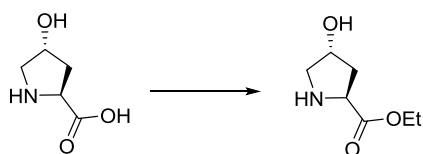
Absolute Configuration of the Knv and Kle Residues in 2-1-2-3.

The mixture of compounds **2-1-2-3** (50 μg) was dissolved in 5% NaOH in 30% H₂O₂ (250 μL) and kept at 65 °C for 45 min. The solution was dried with a stream of N₂, and the product was subjected to acid hydrolysis, derivatization with L-FDAA, and

analysis by LC-MS as described above. Retention times for amino acids (min): 13.4 (m/z 370, Nva), 15.4 (m/z 384, Leu). Standard amino acids of L-Nva, D-Nva, L-Leu, and DL-Leu were derivatized with L-FDAA and analyzed by LC-MS. Retention times (min) for standard amino acids were 13.4 (L-Nva), 14.9 (D-Nva), 15.4 (L-Leu), and 17.8 (D-Leu), so the absolute configuration of Knv and Kle were determined as L (Figure S2-34 and S2-35).

***trans*-4-Hydroxy-L-proline Ethyl Ester.**

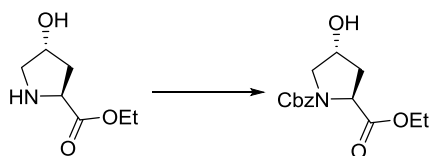
To a solution of *trans*-4-hydroxy-L-proline (100 mg) in EtOH (10 mL) was added SOCl_2 (1.0 g) at 0 °C and refluxed for 4 h. The reaction mixture was diluted with petroleum ether and the product was filtered to afford *trans*-4-hydroxy-L-proline ethyl ester (95 mg). This material was used without further purification.



***N*-Cbz-*trans*-4-Hydroxy-L-proline Ethyl Ester.**

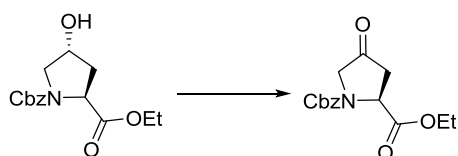
trans-4-Hydroxy-L-proline ethyl ester (95 mg) in MeOH (2 mL) was cooled to 0 °C, to which was added triethylamine (TEA, 215 μL) and carbobenzyloxy chloride (CbzCl, 65 μL), and stirred at rt for 16 h. The mixture was dried in vacuo, and the

product was dissolved in ethyl acetate (3 mL) and washed with 5% citric acid in H₂O (3 mL, 3 times) and H₂O (3 mL, twice). The organic layer was dried with MgSO₄. The product was subjected to silica gel column chromatography with petroleum ether/ethyl acetate (19:1, 4:1, 1:1) to afford *N*-Cbz-*trans*-4-hydroxy-L-proline ethyl ester (110 mg) as colorless oil from the petroleum ether/ethyl acetate (1:1) fraction.



***N*-Cbz-4-Keto-L-proline Ethyl Ester.**

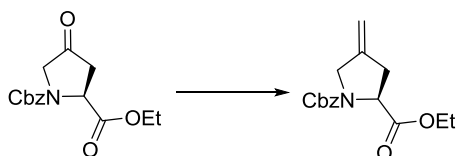
CrO₃ (0.6 g) was dissolved in the mixture of CH₂Cl₂ (5 mL) and pyridine (1 mL). *N*-Cbz-*trans*-4-hydroxy-L-Pro ethyl ester (110 mg) in CH₂Cl₂ (2 mL) was added to the solution, and the mixture was stirred at rt for 16 h. The mixture was filtered on silica pad with petroleum ether/ethyl acetate (1:1) to afford *N*-Cbz-4-keto-L-proline ethyl ester (100 mg) which was used without further purification.



***N*-Cbz-4-Exomethylene-L-proline Ethyl Ester.**

To a solution of *N*-Cbz-4-keto-L-proline ethyl ester (100 mg) in anhydrous

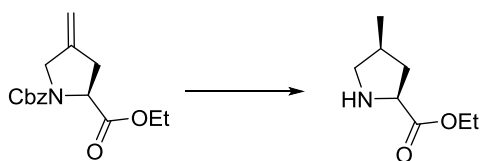
toluene (1 mL) was added dimethyltitanocene (1 mL) and kept at 90 °C for 3 h. After cooled to rt, petroleum ether (50 mL) was added to the mixture and stirred for 30 min. The mixture was filtered on Celite and the solvent was dried in vacuo. The product was subjected to silica gel column chromatography with petroleum ether/diethyl ether (49:1, 19:1, 9:1) to afford *N*-Cbz-4-exomethylene-L-proline ethyl ester (24 mg) as colorless oil from the petroleum ether/diethyl ether (9:1) fraction.



***cis*-4-Methyl-L-proline.**

To a solution of *N*-Cbz-4-exomethylene-L-proline ethyl ester (4.0 mg) in CH₂Cl₂ (1 mL) was added 10 % Pd/C (1.5 mg), and the mixture was stirred for 16 h under an atmosphere of H₂. The product was filtered on Celite to afford *cis*-4-methyl-L-proline ethyl ester (2.0 mg) as colorless oil.

cis-4-Methyl-L-proline ethyl ester (2.0 mg) was dissolved in 6N HCl (300 μL) and kept at 70 °C for 6 h. After cooled to rt, the mixture was washed with ethyl acetate (300 μL, twice). The aqueous layer was dried under a stream of N₂ to afford *cis*-4-methyl-L-proline (1.4 mg) as white powder.



***trans*-4-Methyl-L-proline.**

To *N*-Cbz-4-exomethylene-L-proline ethyl ester (3.5 mg) in CHCl_3 was added Crabtree's catalyst, and the mixture was stirred for 5 d under an atmosphere of H_2 . The product was subjected to silica gel column chromatography with petroleum ether/diethyl ether (49:1, 24:1, 47:3) to afford *N*-Cbz-*trans*-4-methyl-L-proline ethyl ester (3.6 mg) as colorless oil from the petroleum ether/diethyl ether (47:3) fraction.

N-Cbz-*trans*-4-Methyl-L-proline ethyl ester (3.6 mg) was subjected to deprotection and hydrolysis as described above to afford *trans*-4-methyl-L-proline (1.9 mg) as white powder.



Absolute Configuration of Cys, Ala, Mpr, and Dpr Residues in 2-1–2-3.

To a solution of *cis*-4-methyl-L-proline (0.7 mg) in H_2O (100 μL) was added 1% L-FDAA in acetone (100 μL) and 1 M NaHCO_3 in H_2O (20 μL) and kept at 55 $^\circ\text{C}$ for 30 min. After addition of 2 N HCl (10 μL), the reaction mixture was analyzed by

LC-MS. *cis*-4-Methyl-L-proline (0.7 mg) was derivatized with D-FDAA in the same manner. *trans*-4-Methyl-L-proline (0.9 mg, respectively) was derivatized similarly. Standard amino acids of L-Cys, D-Cys, L-Ala, D-Ala, L-Dpr, DL-Dpr, L-Nva, D-Nva, L-Leu, and DL-Leu were derivatized with L-FDAA and analyzed by LC-MS. Retention times (min) for standard amino acids were 5.2 (L-Cys), 6.7 (D-Cys), 9.8 (L-Ala), 11.8 (D-Ala), 12.5 (*cis*-4-methyl-L-proline), 12.6 (*trans*-4-methyl-L-proline), 13.5 (*trans*-4-methyl-D-proline), 13.6 (*cis*-4-methyl-D-proline), 15.8 (L-Dpr), and 16.6 (D-Dpr). Thus, the absolute configurations of amino acids in **2-1-2-3** were determined as D-Cys (6.6), L-Ala (9.7), *cis*-4-methyl-L-proline (12.4), L-Dpr (15.7), L-Nva (13.4) and L-Leu (15.4) (Figure S2-30–S2-35).

XTT Assay against P388 Cells.

P388 murine leukemia cells were cultured in PRMI 1640 (Wako Chemical) medium, supplemented with 100 µg/mL of kanamycin (Wako Chemical) and 10% fetal bovine serum (ThermoFisher Scientific), at 37 °C under a 5% CO₂ atmosphere. To each well of the 96-well microplate containing 100 µL of 2×10^4 cells/mL, 100 µL of test solution dissolved in PRMI-1640 medium was added, and the plate were incubated for 3 days. After the addition of 50 µL of 3'-[1-(phenylaminocarbonyl)-3,4-tetrazolium]-bis(4-methoxy-6-nitro)benzenesulfonic acid hydrate (XTT) solution (1 mg/mL)

containing 4% of phenazine methosulfate (PMS) solution (0.153 mg/mL) to each well, the plates were further incubated for 4 h. The absorbance at 450 nm was measured with a microplate reader.

2.4. Supporting Information

Table S2-1. ^1H and ^{13}C NMR Data for **2-4a** and **2-4b** in $\text{DMSO-}d_6$.

2-4a ^a					2-4b ^a			
residue	position	$\delta_{\text{C}}^{\text{b}}$, type	$\delta_{\text{H}}^{\text{b}}$ (J in Hz)	HMBC	residue	position	$\delta_{\text{C}}^{\text{b}}$, type	$\delta_{\text{H}}^{\text{b}}$ (J in Hz)
rKnv	1	172.4, C			rKnv	1	171.9, C	
	2	73.3, CH	3.83, m	1, 3	2	72.6, CH		3.62, d (8.9)
	3	50.1, CH	4.12, m		3	50.6, CH		3.95, ddd (8.3, 8.3, 7.6)
	4	35.4, CH ₂	1.47, m	6	4	33.2, CH ₂		1.75, m
	5	18.4, CH ₂	1.32, m		5	17.7, CH ₂		1.20, m
			1.25, m	6				1.35, m
Mpr	6	13.6, CH ₃	0.82, m	4, 5	6	13.7, CH ₃		1.20, m
	3-NH		7.90, m		3-NH			0.79, m
	7	171.0, C			7	170.6, C		8.23, m
	8	60.0, CH	4.42, t (8.9)	7, 9	8	60.2, CH		4.26, t (8.9)
	9	36.2, CH ₂	2.23, dddd (7.6, 6.2, 6.2, 5.5)		9	36.2, CH ₂		2.12, dddd (8.3, 6.9, 6.2, 5.5)
			1.14, ddd (11.7, 11.7, 11.0)					0.95, ddd (11.7, 11.7, 10.3)
N-CHO-Dpr	10	32.9, CH	2.03, m		10	32.9, CH		2.03, m
	11	54.3, CH ₂	3.83, m	10, 12	11	54.2, CH ₂		3.77, m
	12	15.5, CH ₃	0.70, d (5.5)	9, 10, 11	12	15.3, CH ₃		2.73, m
	13	168.3, C			13	168.3, C		0.84, m
	14	48.5, CH	4.55, m		14	48.9, CH		4.49, m
	15	40.5, CH ₂	3.77, m	14, 16	15	40.5, CH ₂		3.81, m
Cys			2.96, m	13, 14				2.96, m
	14-NH		8.42, m		14-NH			8.40, m
	15-NH		8.54, m	16	15-NH			8.56, m
	CHO	160.3, CH	7.95, s	14	CHO	160.3, CH		7.95, s
	16	169.8, C			16	170.0, C		
	17	53.6, CH	4.67, m	18, 19	17	52.8, CH		4.70, m
ethyl-pyridine	18	34.4, CH ₂	2.98, m	16, 17, 1'	18	34.4, CH ₂		3.00, m
			2.82, m	16, 17, 1'				2.88, m
	17-NH		8.26, d (9.6)	17, 19	17-NH			8.10, d (9.6)
	1'	31.4, CH ₂	2.76, dd (8.3, 7.6)	18, 3'	1'	31.5, CH ₂		2.76, dd (8.3, 7.6)
	2'	33.8, CH ₂	2.83, m	3', 4', 7'	2'	33.8, CH ₂		2.82, m
	3'	149.0, C			3'	149.0, C		
Aox	4', 7'	123.7, CH	7.22, d (3.6)	2', 5', 6'	4', 7'	123.7, CH		7.22, d (3.6)
	5', 6'	149.1, CH	8.42, d (3.6)	4', 7'	5', 6'	149.1, CH		8.42, d (3.6)
	19	160.0, C			19	160.0, C		
	20	135.0, C			20	135.3, C		
	21	142.1, CH	8.57, s	20, 22	21	142.7, CH		8.53, s
	22	163.8, C			22	164.2, C		
23-NH	23	42.8, CH	4.82, dddd (7.6, 6.9, 6.2, 6.2)	1, 24	23	43.2, CH		4.70, m
	24	16.6, CH ₃	1.53, d (6.9)	22, 23	24	16.2, CH ₃		1.53, d (6.9)
	23-NH		7.91, m	1, 23, 24	23-NH			8.55, m

^a**2-4a** is major isomer and **2-4b** is minor isomer of alkylated nazumazoles A–C, respectively. ^bRecorded at 600 MHz and 25 °C.

Table S2-2. ^1H and ^{13}C NMR Data for **2-5a** and **2-5b** in $\text{DMSO-}d_6$.

2-5a^a					2-5b^a				
residue	position	$\delta_{\text{C}}^{\text{b}}$, type	$\delta_{\text{H}}^{\text{b}}$ (J in Hz)	HMBC	residue	position	$\delta_{\text{C}}^{\text{b}}$, type	$\delta_{\text{H}}^{\text{b}}$ (J in Hz)	
rKle	1	172.2, C			rKle ^c	1	unassigned		
	2	73.7, CH	3.81, m	1, 4		2	72.7, CH	3.54, d (8.9)	
	3	48.7, CH	4.21, m			3	49.2, CH	3.93, m	
	4	42.6, CH ₂	1.57, m			4	41.1, CH ₂	1.60, m	
				1.21, m				1.18, m	
	5	23.5, CH	1.66, m			5	23.5, CH	1.74, m	
	6	24.0, CH ₃	0.84, m	4, 5, 5-Me		6	23.3, CH ₃	0.85, m	
	5-Me	21.7, CH ₃	0.84, m	4, 5, 6	5-Me	21.1, CH ₃	0.76, d (6.2)		
	3-NH		7.91, m		3-NH		8.19, m		
Mpr	7	171.0, C			Mpr ^c	7	unassigned		
	8	60.0, CH	4.43, t (8.9)	7		8	60.2, CH	4.21, m	
	9	36.0, CH ₂	2.21, dddd (7.6, 6.9, 6.9, 5.5)			9	36.0, CH ₂	2.05, m	
			1.12, ddd (11.7, 11.7, 11.0)					0.87, m	
	10	32.9, CH	2.01, m			10	32.9, CH	2.02, m	
	11	54.6, CH ₂	3.84, m			11	54.2, CH ₂	3.75, t (7.6)	
			2.68, ddd (11.0, 10.3, 9.6)					2.72, m	
	12	15.3, CH ₃	0.67, d (6.2)	9, 10, 11	12	15.1, CH ₃	0.82, m		
N-CHO-Dpr	13	169.5, C			N-CHO-Dpr ^c	13	unassigned		
	14	48.3, CH	4.51, dddd (6.9, 6.9, 4.8, 4.1)			14	48.7, CH	4.41, m	
	15	40.7, CH ₂	3.84, m	14, 16		15	40.7, CH ₂	3.90, m	
			2.83, m					2.78, m	
		14-NH		8.48, d (7.6)			14-NH		8.48, d (7.6)
		15-NH		8.58, m		16	15-NH		8.64, m
		CHO	160.6, CH	7.94, s		14	CHO	160.4, CH	7.93, s
Cys	16	169.8, C			Cys	16	169.5, C		
	17	53.6, CH	4.68, m	19		17	52.8, CH	4.71, m	
	18	34.6, CH ₂	2.94, m	16, 17, 1'		18	34.4, CH ₂	2.96, m	
			2.83, m	16, 17		17-NH		8.17, d (9.6)	
ethyl-pyridine	17-NH		8.31, d (9.6)	19	ethyl-pyridine	1'	31.7, CH ₂	2.77, m	
	1'	31.7, CH ₂	2.77, m	2', 3'		2'	33.8, CH ₂	2.81, t (6.6)	
	2'	33.8, CH ₂	2.81, t (6.6)	1', 4', 7'		3'	149.0, C		
	3'	149.0, C				4', 7'	123.7, CH	7.22, d (4.2)	
	4', 7'	123.7, CH	7.22, d (4.2)	2', 5', 6'		5', 6'	149.1, CH	8.42, d (4.2)	
	5', 6'	149.1, CH	8.42, d (4.2)	4', 7'	Aox	19	160.2, C		
Aox	19	160.0, C				20	135.3, C		
	20	135.1, C				21	141.5, CH	8.50, s	
	21	141.9, CH	8.57, s	20, 22		22	164.1, C		
	22	163.6, C				23	43.4, CH	4.63, qui (6.9)	
	23	42.9, CH	4.81, qui (6.9)	1		24	16.1, CH ₃	1.54, m	
	24	16.4, CH ₃	1.53, m	22, 23		23-NH		8.63, m	
	23-NH		8.63, m	1, 22, 23					

^a**2-5a** is major isomer and **2-5b** is minor isomer of alkylated nazumazoles A–C, respectively. ^bRecorded at 600 MHz and 25 °C.

^cNo HMBC correlation to amide carbonyl carbon was observed.

Table S2-3. ¹H NMR Data for the Mixture of the Reduction Products of Nazumazole A (2-6) in DMSO-*d*₆.

major signals			minor signals		
amino acid	position	δ _H ^a (J in Hz)	amino acid	position	δ _H ^a (J in Hz)
rKnv	1		rKnv	1	
	2	3.84, m		2	3.64, d (6.9)
	3	4.13, m		3	4.00, m
	4	1.50, m		4	1.76, m
	5	1.35, m			1.22, m
			1.26, m		5
	6	0.85, m			1.24, m
	3-NH	7.75, d (7.8)		6	0.85, m
Mpr	7			3-NH	8.14, m
	8	4.40, dd (8.7, 9.2)	Mpr	7	
	9	2.21, m		8	4.27, dd (8.2, 9.6)
		1.09, m		9	2.14, m
	10	2.03, m			0.99, m
	11	3.80, m		10	2.05, m
		2.72, m		11	3.77, m
	12	0.75, d (6.0)			2.75, m
<i>N</i> -CHO-Dpr	13			12	0.86, m
	14	4.55, m	<i>N</i> -CHO-Dpr	13	
	15	3.75, m		14	4.52, m
		3.04, m		15	3.74, m
	14-NH	8.33, d (7.8)			3.07, m
	15-NH	8.45, m		14-NH	8.31, m
	CHO	7.95, s		15-NH	8.42, m
Cys	16			CHO	7.95, s
	17	4.76, m	Cys	16	
	18	3.10, m		17	4.79, m
		2.94, m		18	3.12, m
	17-NH	8.21, d (9.6)			2.96, m
Aox	19			17-NH	8.06, d (9.6)
	20		Aox	19	
	21	8.47, s		20	
	22			21	8.46, s
	23	4.81, m		22	
	24	1.53, m		23	4.74, m
				24	1.51, m
	23-NH	7.92, d (7.3)		23-NH	8.45, m

^aRecorded at 600 MHz and 40 °C.

Table S2-4. ¹H NMR Data for the Minor Signals of the Mixture of the Reduction Products of Nazumazole B (**2-7**) in DMSO-*d*₆.

amino acid	position	δ _H ^a (J in Hz)	amino acid	position	δ _H ^a (J in Hz)
rKlv	1		rKle ^b	1'	
	2	3.85, m		2'	unassigned
	3	4.12, m		3'	4.20, m
	4	1.50, m		4'	1.54, m
	5	1.34, m			1.27, m
		1.27, m		5'	1.64, m
	6	0.84, m		6'	0.83, m
	3-NH	7.93, m		5'-Me	0.85, d (7.8)
Mpr	7			3'-NH	7.88, d (8.7)
	8	4.40, dd (8.7, 8.2)	Mpr	7'	
	9	2.21, m		8'	4.40, dd (8.7, 8.2)
		1.10, m		9'	2.21, m
	10	2.01, m			1.10, m
	11	3.80, m		10'	2.01, m
		2.70, m		11'	3.80, m
	12	0.74, d (6.0)			2.70, m
N-CHO-Dpr	13			12'	0.70, d (6.0)
	14	4.54, m	N-CHO-Dpr	13'	
	15	3.75, m		14'	4.51, m
		3.02, m		15'	3.81, m
	14-NH	8.33, m			2.91, m
	15-NH	8.43, m		14'-NH	8.38, m
	CHO	7.95, s		15'-NH	8.46, m
Cys	16			CHO	7.95, s
	17	4.74, m	Cys	16'	
	18	3.09, m		17'	4.78, m
		2.92, m		18'	3.09, m
	17-NH	8.24, d (9.6)			2.92, m
Aox	19			17'-NH	8.29, d (9.6)
	20		Aox	19'	
	21	8.47, s		20'	
	22			21'	8.47, s
	23	4.80, m		22'	
	24	1.52, m		23'	4.80, m
	23-NH	7.98, m		24'	1.52, d (6.9)
				23'-NH	7.98, m

^aRecorded at 600 MHz and 40 °C. ^bNeither COSY or TOCSY correlation to H-2' were not observed.

Table S2-5. ^1H NMR Data for the Minor Signals of the Mixture of the Reduction Products of Nazumazole B (2-7) in $\text{DMSO-}d_6$.

amino			amino				
acid	position	$\delta_{\text{H}}^{\text{a}}$ (J in Hz)	acid	position	$\delta_{\text{H}}^{\text{a}}$ (J in Hz)		
rKlv	1		rKle	1'			
	2	3.67, m		2'	3.59, m		
	3	4.00, m		3'	3.95, m		
	4	1.76, m		4'	1.62, m		
		1.22, m			1.19, m		
	5	1.51, m		5'	1.74, m		
		1.37, m			0.84, m		
	6	0.86, m		5'-Me	0.78, d (6.4)		
		8.39, m			3'-NH	8.29, d (8.7)	
	Mpr	7			Mpr	7'	
8		4.29, dd (9.2, 8.7)	8'	4.23, m			
9		2.16, m	9'	2.09, m			
		0.99, m		0.95, m			
10		2.05, m	10'	2.01, m			
		3.79, m		3.75, m			
11		2.75, m	11'	2.71, m			
		0.83, m		12'		0.83, m	
N-CHO-Dpr		13		N-CHO-Dpr		13'	
		14	4.43, m			14'	4.43, m
	15	3.85, m	15'		3.85, m		
		2.86, m			2.86, m		
	14-NH	8.38, d (7.8)	14'-NH		8.38, d (7.8)		
	15-NH	8.53, m	15'-NH		8.53, m		
CHO	7.95, s	CHO	7.95, s				
Cys	16		Cys	16'			
	17	4.78, m		17'	4.79, m		
	18	3.10, m		18'	3.10, m		
		2.94, m			3.00, m		
	17-NH	8.10, d (8.2)		17'-NH	8.18, d (8.7)		
Aox	19		Aox	19'			
	20			20'			
	21	8.46, s		21'	8.46, s		
	22			22'			
	23	4.75, m		23'	4.66, m		
	24	1.53, m		24'	1.53, m		
	23-NH	8.61, m		23'-NH	8.64, m		

^aRecorded at 600 MHz and 40 °C.

Table S2-6. ¹H NMR Data for the Mixture of the Reduction Products of Nazumazole C (2-8) in DMSO-*d*₆.

major signals			minor signals			
amino acid	position	$\delta_{\text{H}}^{\text{a}}$ (J in Hz)	amino acid	position	$\delta_{\text{H}}^{\text{a}}$ (J in Hz)	
rKle	1		rKle	1		
	2	3.83, m		2	3.56, m	
	3	4.19, m		3	3.95, m	
	4	1.55, m		4	1.73, m	
		1.27, m			1.19, m	
	5	1.65, m		5	1.65, m	
	6	0.86, m		6	0.86, m	
	5-Me	0.85, d (6.9)		5-Me	0.78, d (5.5)	
	3-NH	7.78, d (10.0)		3-NH	8.13, m	
	Mpr	7		Mpr	7	
8		4.40, t (8.7)		8	4.22, m	
9		2.20, m		9	2.08, m	
		1.08, m			0.91, m	
10		2.00, m		10	2.01, m	
11		3.79, m		11	3.74, m	
		2.68, m			2.72, m	
12		0.71, d (6.0)		12	0.85, m	
N-CHO-Dpr		13		N-CHO-Dpr	13	
		14	4.50, m		14	4.43, m
	15	3.79, m		15	3.81, m	
		2.90, m			2.86, m	
	14-NH	8.38, d (6.0)		14-NH	8.38, d (6.0)	
	15-NH	8.44, m		15-NH	8.51, m	
	CHO	7.94, s		CHO	7.94, s	
Cys	16		Cys	16		
	17	4.76, m		17	4.78, m	
	18	3.09, m		18	3.12, m	
		2.94, m			3.00, m	
17-NH	8.27, d (9.6)		17-NH	8.15, d (9.6)		
Aox	19		Aox	19		
	20			20		
	21	8.46, s		21	8.46, s	
	22			22		
	23	4.80, m		23	4.66, m	
	24	1.53, d (6.9)		24	1.53, d (6.9)	
	23-NH	7.93, m		23-NH	8.55, m	

^aRecorded at 600 MHz and 40 °C.

Table S2-7. IC₅₀ Values of Nazumazoles and Their Derivatives against P388 Cells.

	IC ₅₀ (μM)
2-1-2-3	0.83
2-6	28
2-7	20
2-8	17
2-4a, 2-4b, 2-5a, and 2-5b	>50

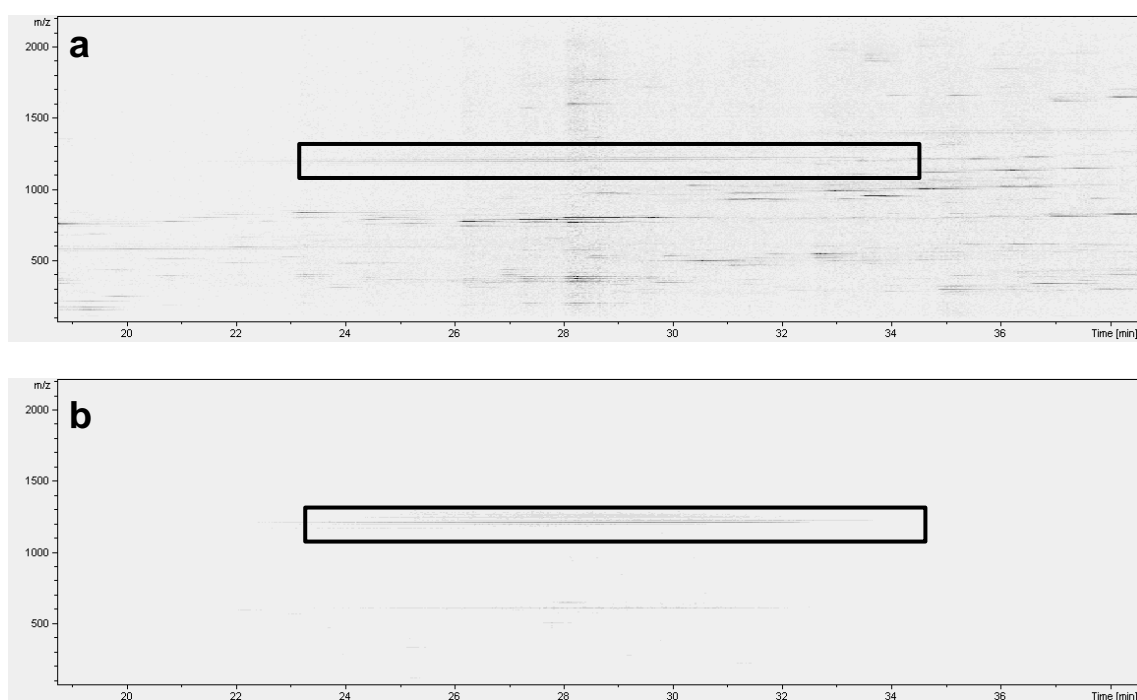


Figure S2-1. Two-dimensional LC-MS charts of **2-1-2-3** (in rectangle) in (a) crude sample and (b) purified sample; x-axis is retention time and y-axis is *m/z*.

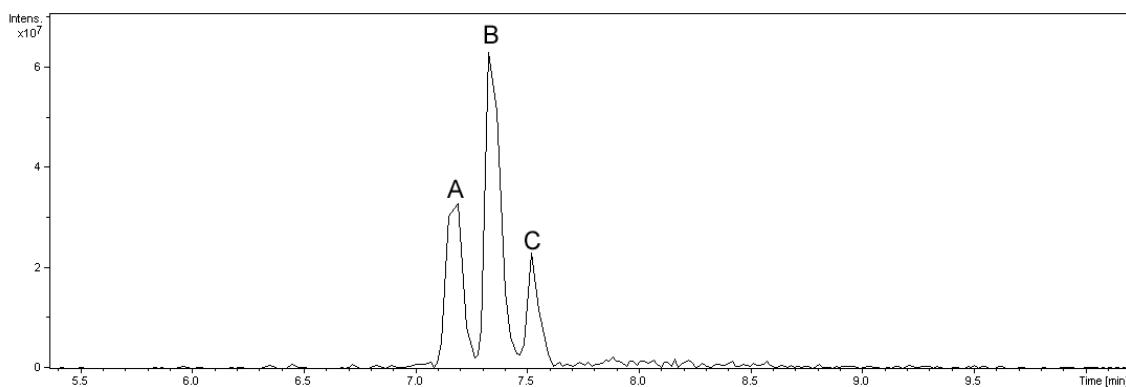


Figure S2-2. LC-MS chart of the mixture of **2-6-2-8**.

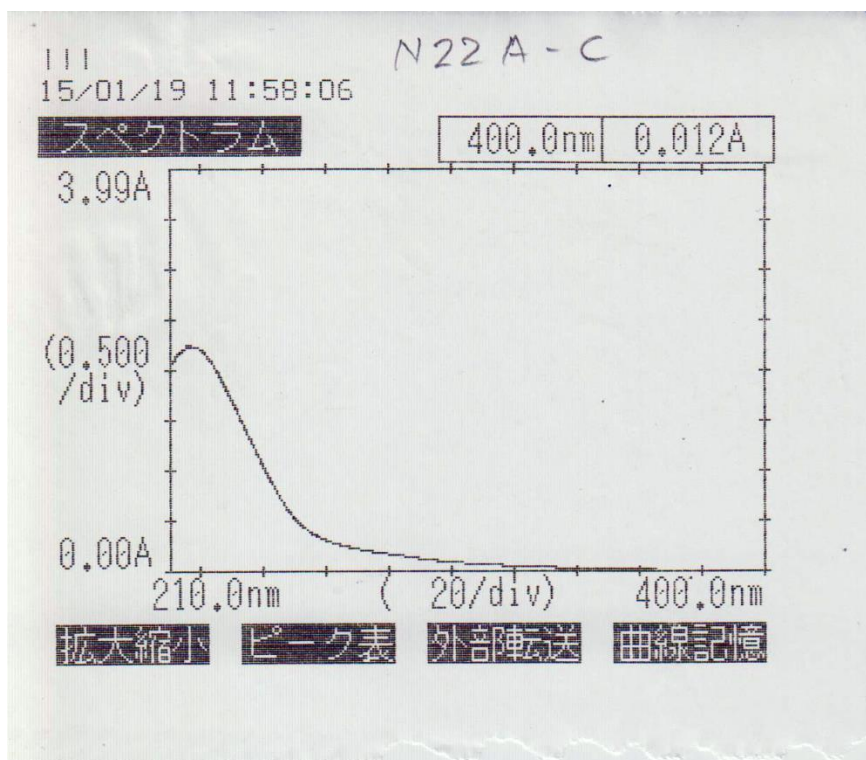


Figure S2-3. UV-VIS spectrum of the mixture of **2-1-2-3** (MeOH, 210–400 nm).

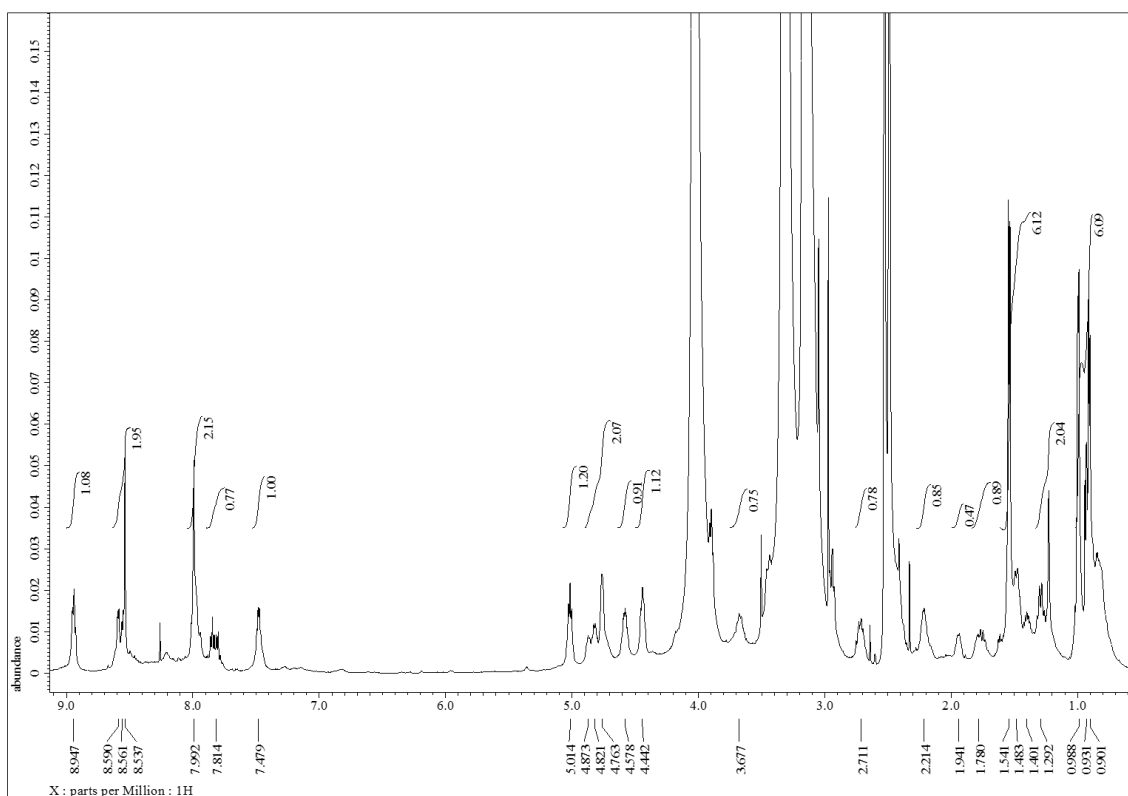


Figure S2-4. ^1H NMR spectrum of the mixture of 2-1-2-3 in $\text{DMSO-}d_6$ (600 MHz).

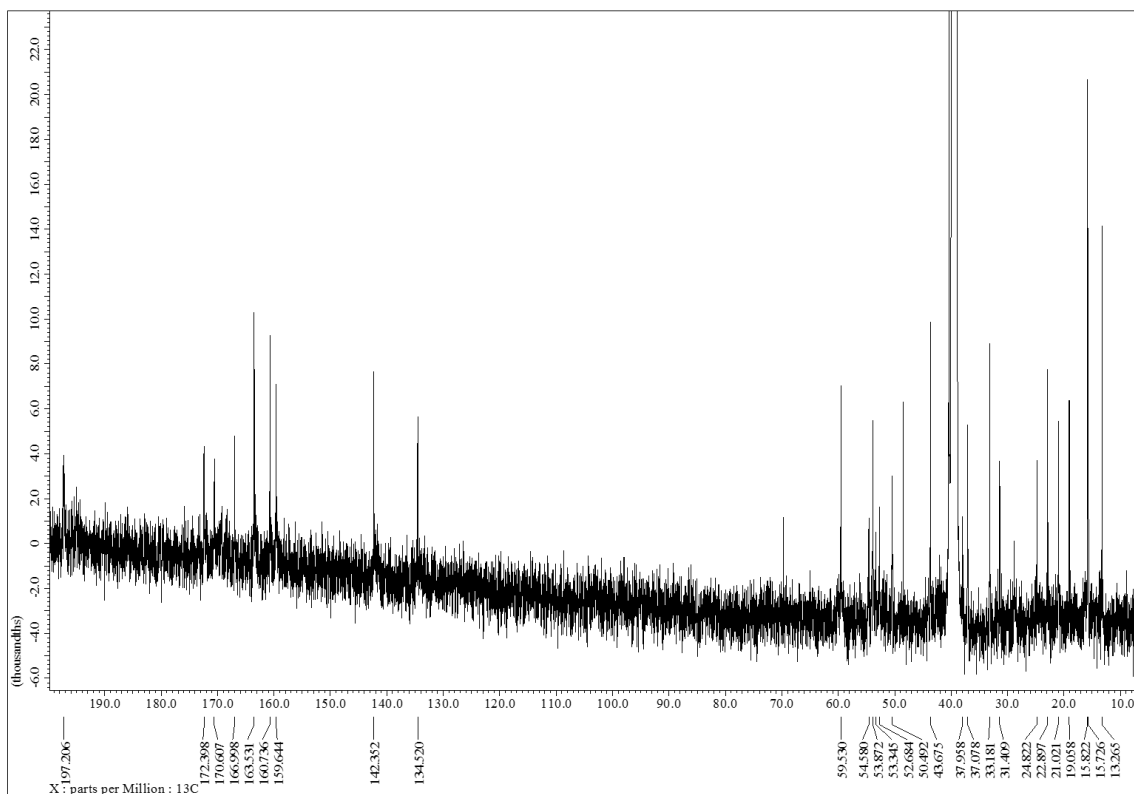


Figure S2-5. ^{13}C NMR spectrum of the mixture of 2-1-2-3 in $\text{DMSO-}d_6$ (150 MHz).

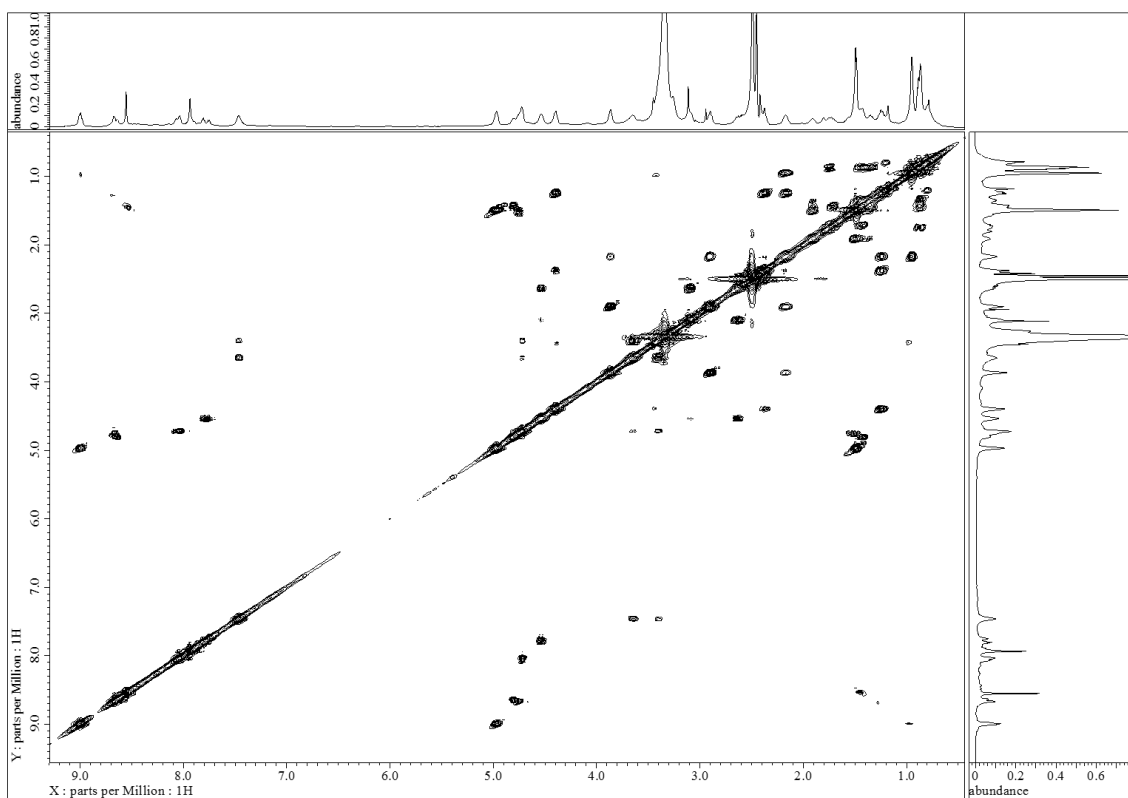


Figure S2-6. COSY spectrum of the mixture of **2-1-2-3** in DMSO- d_6 (600 MHz).

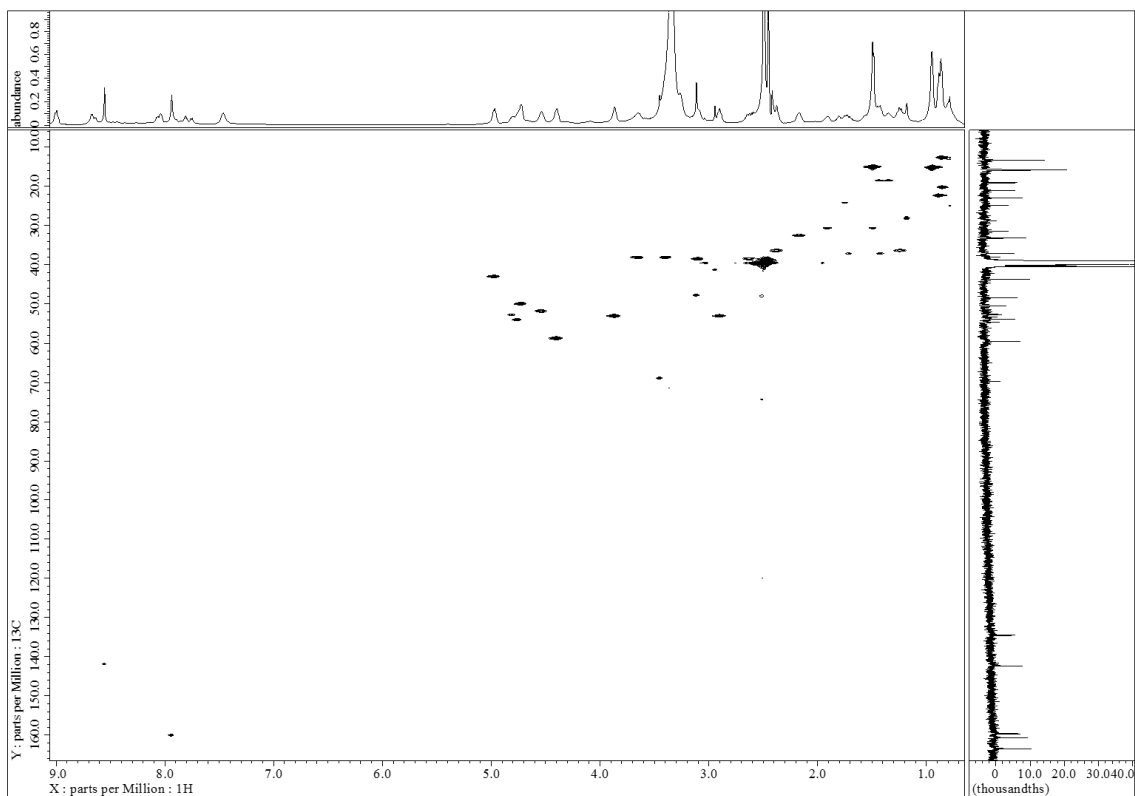


Figure S2-7. HSQC spectrum of the mixture of **2-1-2-3** in DMSO- d_6 (600 MHz).

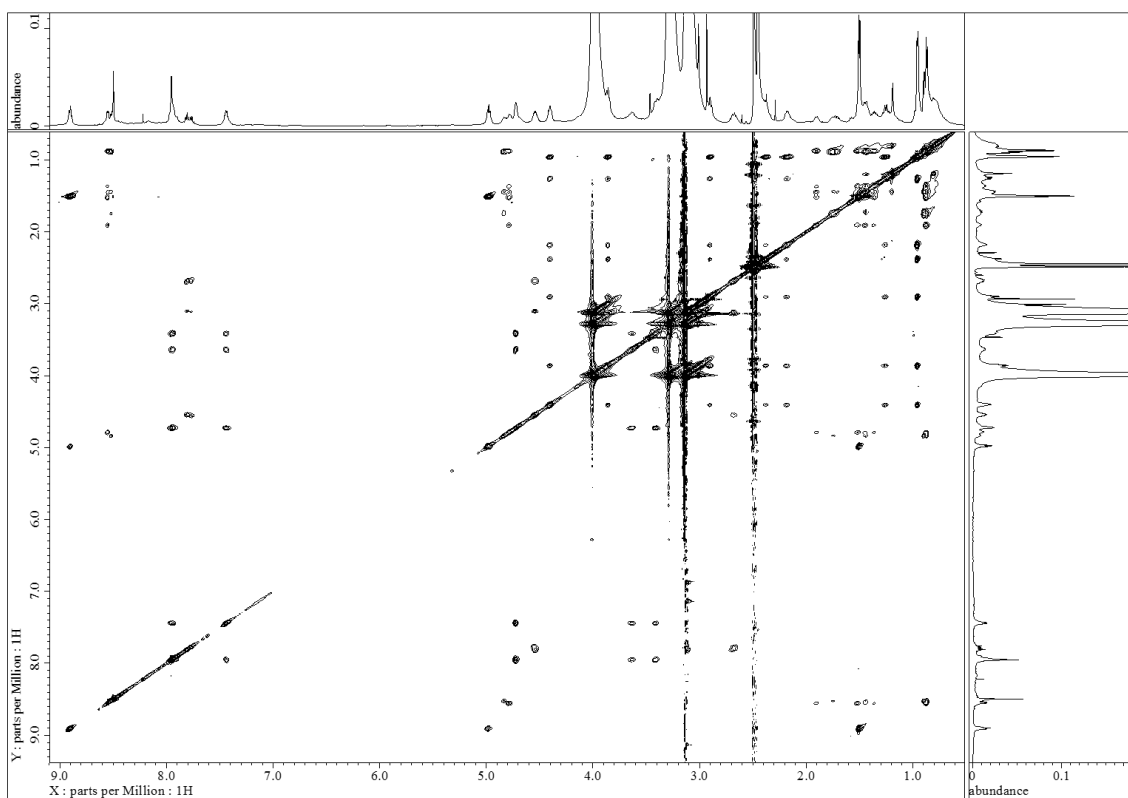


Figure S2-8. TOCSY spectrum of the mixture of **2-1-2-3** in DMSO- d_6 (600 MHz).

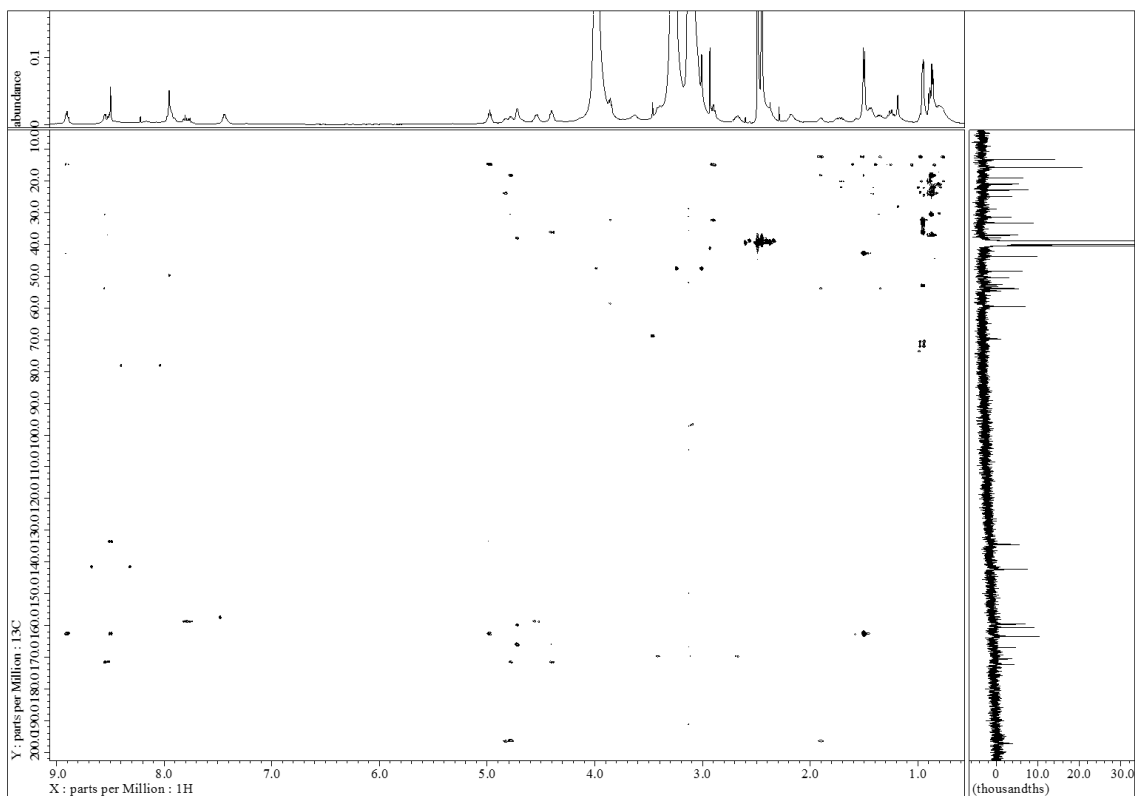


Figure S2-9. HMBC spectrum of the mixture of **2-1-2-3** in DMSO- d_6 (600 MHz).

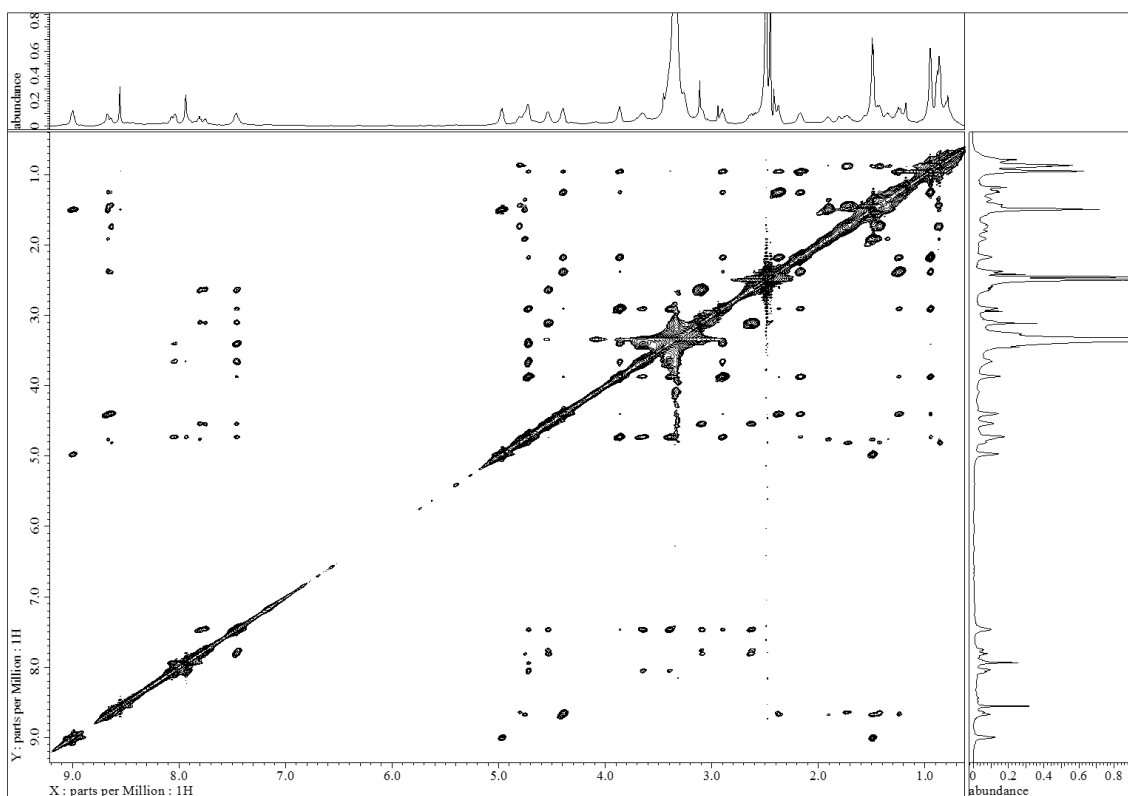


Figure S2-10. NOESY spectrum of the mixture of **2-1-2-3** in DMSO- d_6 (600 MHz).

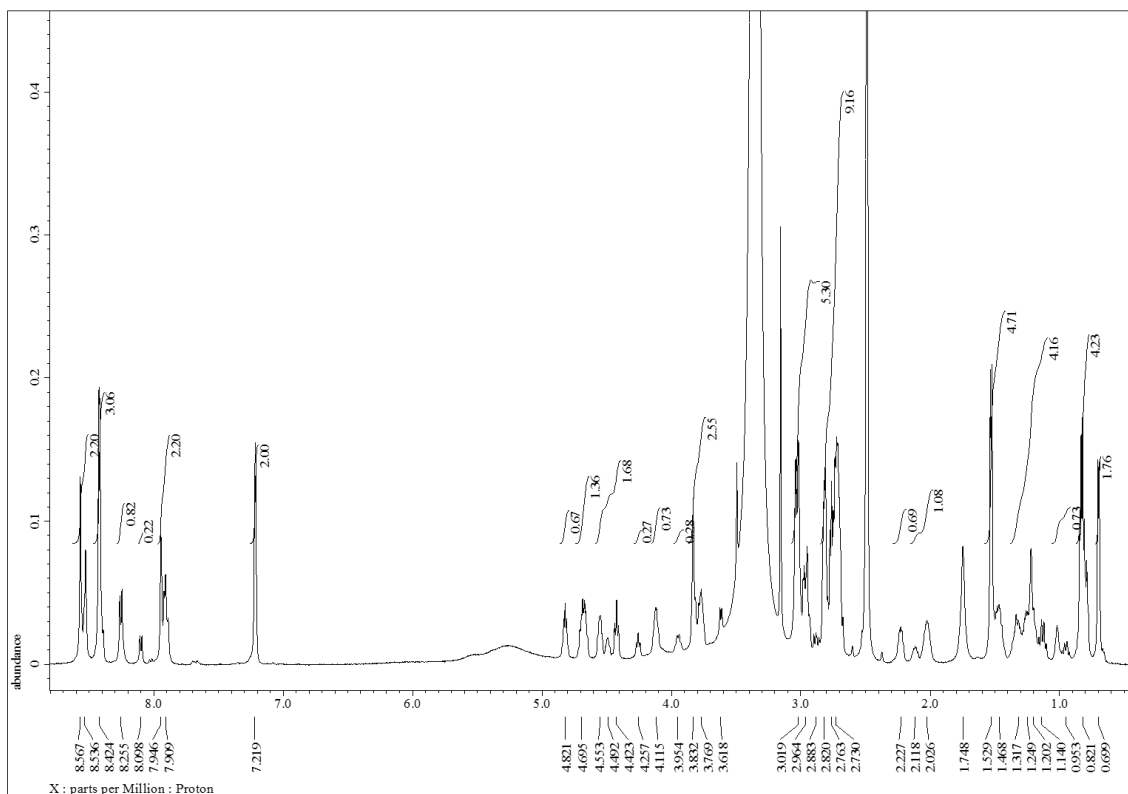


Figure S2-11. ^1H NMR spectrum of the mixture of **2-4a** and **2-4b** in DMSO- d_6 (600 MHz).

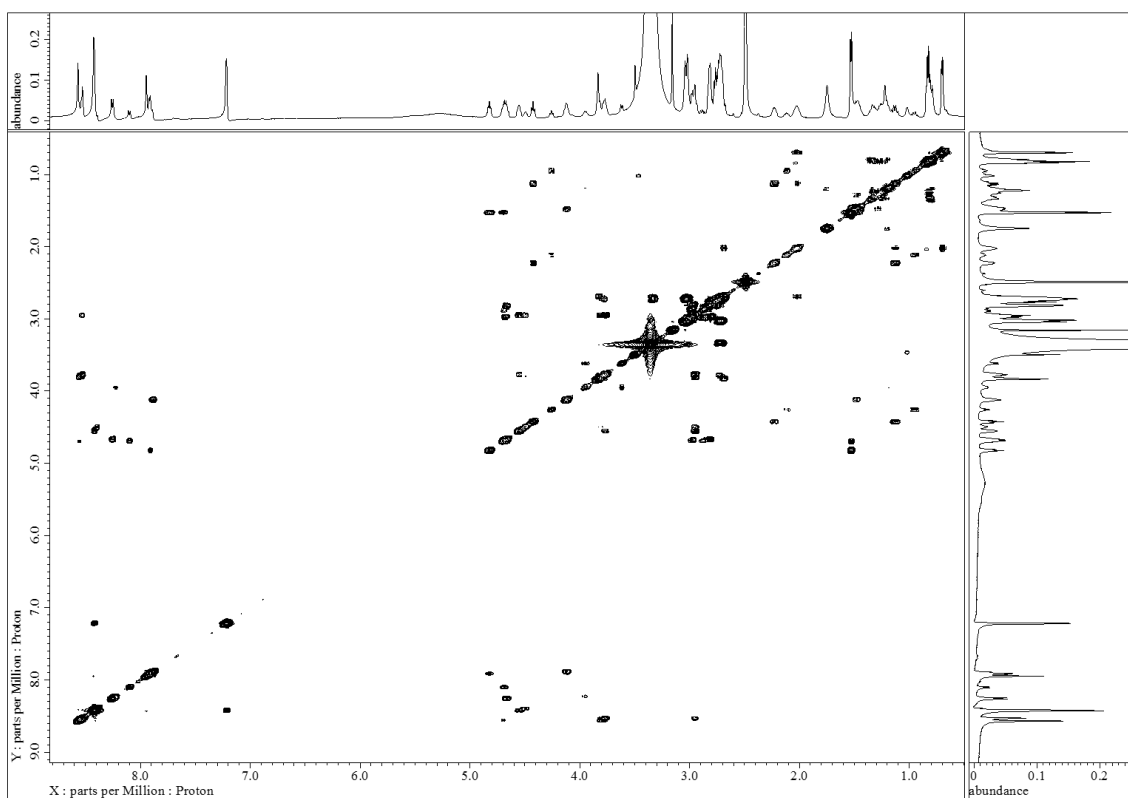


Figure S2-12. COSY spectrum of the mixture of **2-4a** and **2-4b** in DMSO- d_6 (600 MHz).

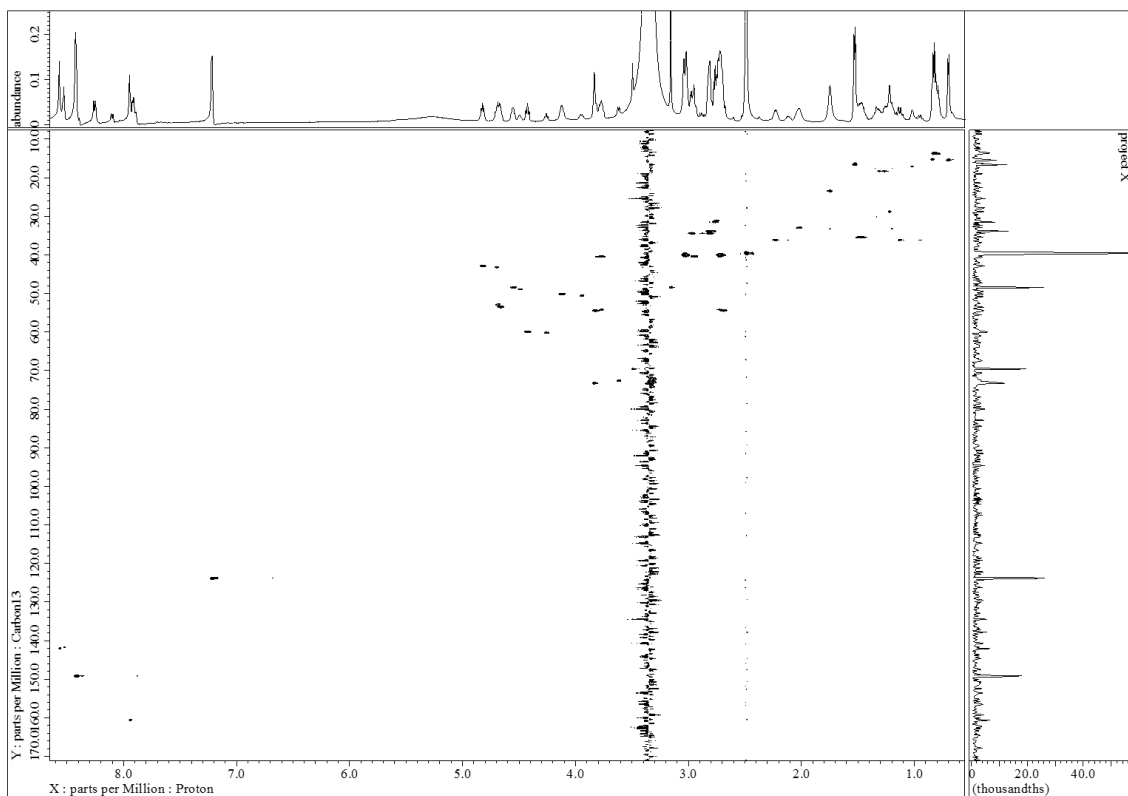


Figure S2-13. HSQC spectrum of the mixture of **2-4a** and **2-4b** in DMSO- d_6 (600 MHz).

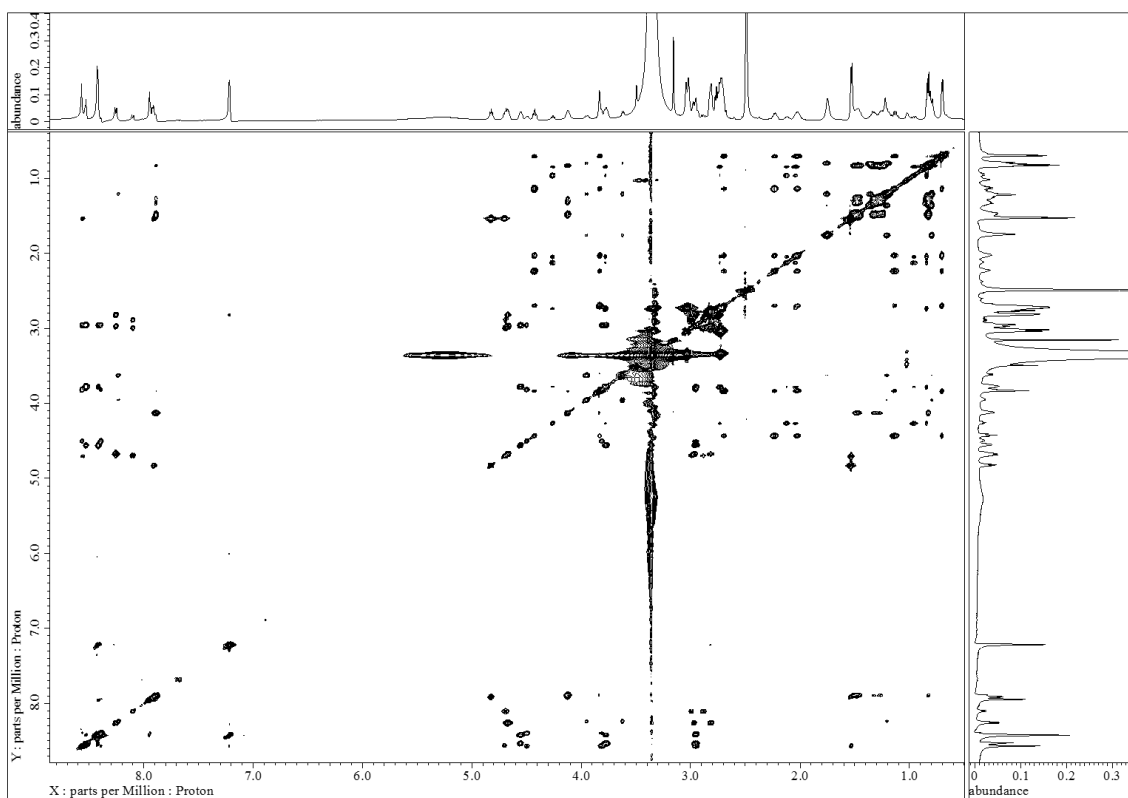


Figure S2-14. TOCSY spectrum of the mixture of **2-4a** and **2-4b** in DMSO- d_6 (600 MHz).

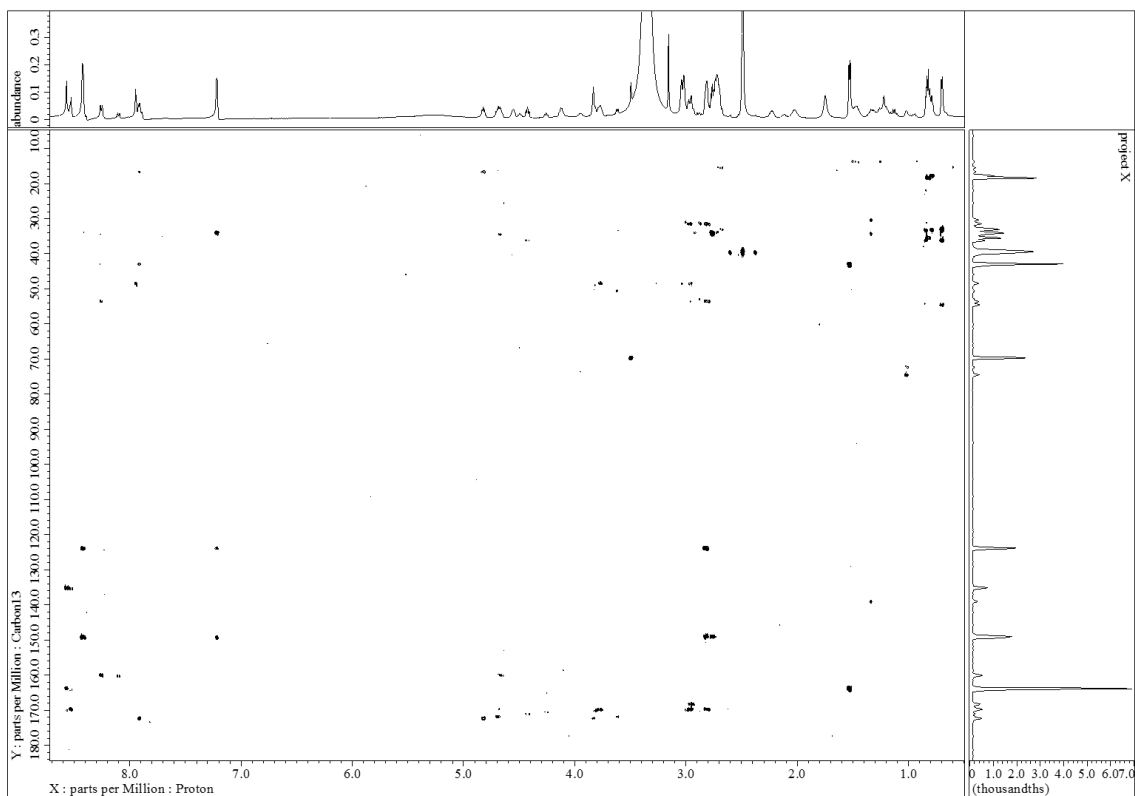


Figure S2-15. HMBC spectrum of the mixture of **2-4a** and **2-4b** in DMSO- d_6 (600 MHz).

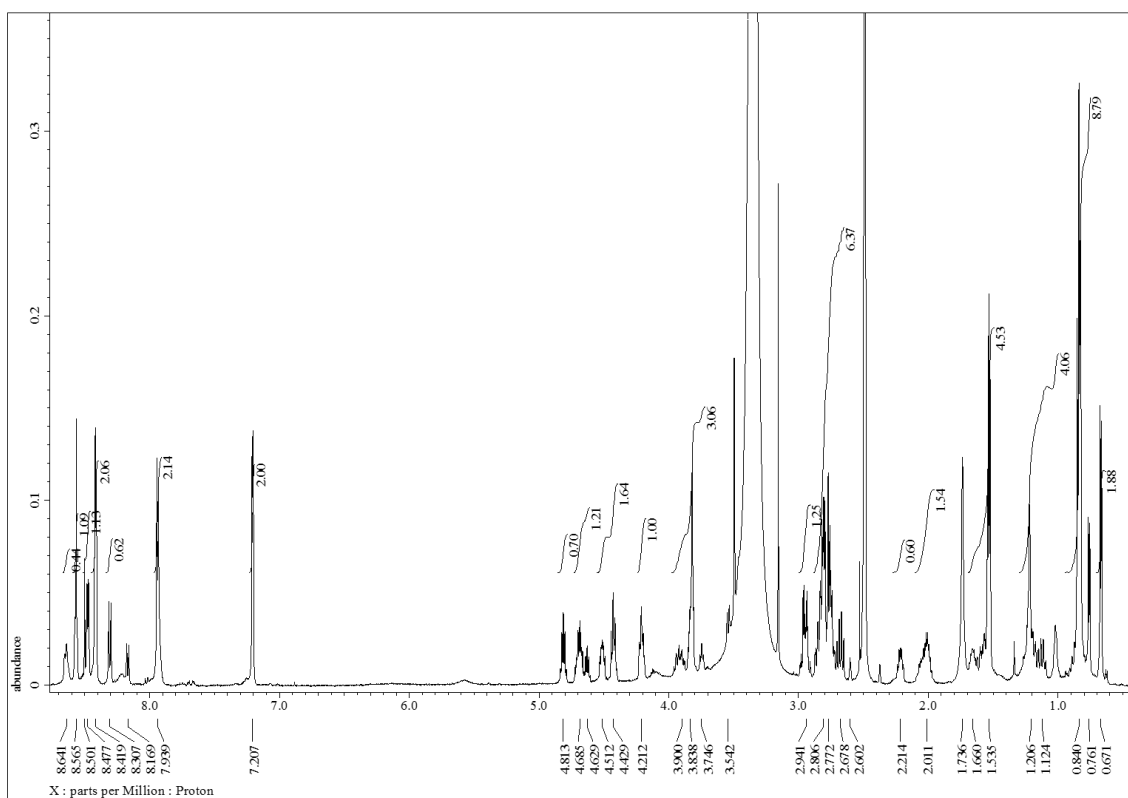


Figure S2-16. ^1H NMR spectrum of the mixture of **2-5a** and **2-5b** in $\text{DMSO-}d_6$ (600 MHz).

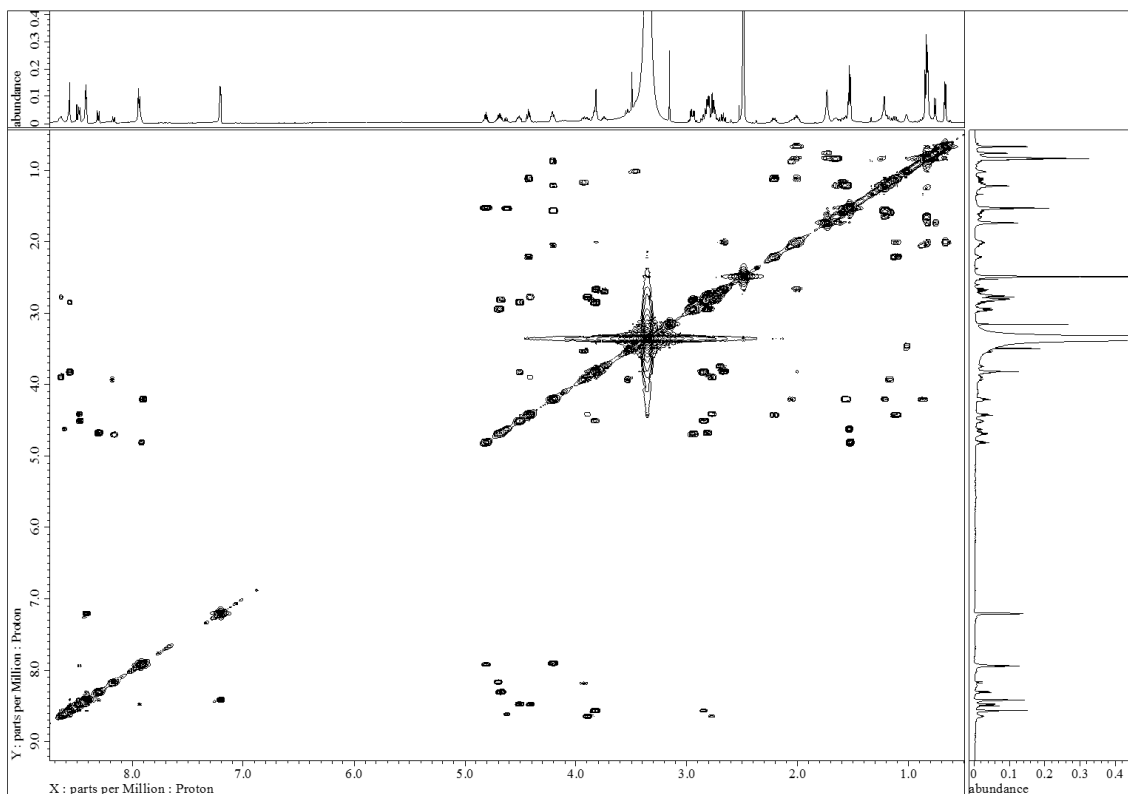


Figure S2-17. COSY spectrum of the mixture of **2-5a** and **2-5b** in $\text{DMSO-}d_6$ (600 MHz).

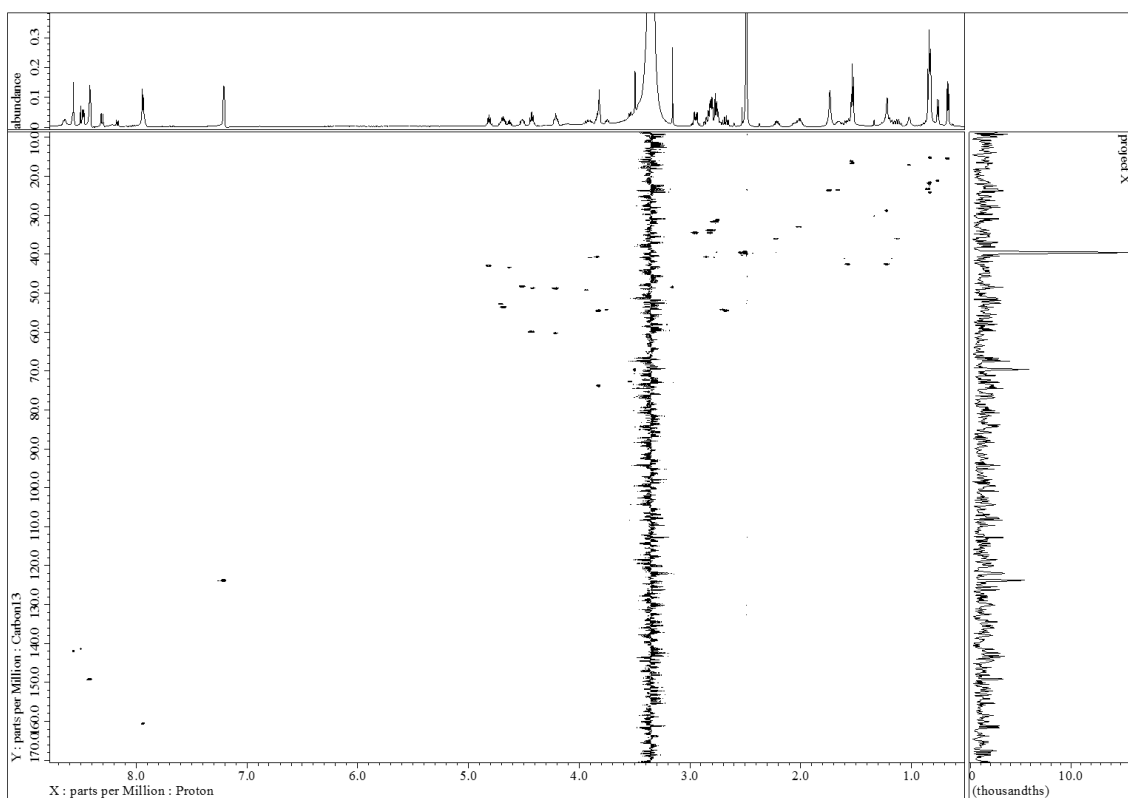


Figure S2-18. HSQC spectrum of the mixture of **2-5a** and **2-5b** in DMSO- d_6 (600 MHz).

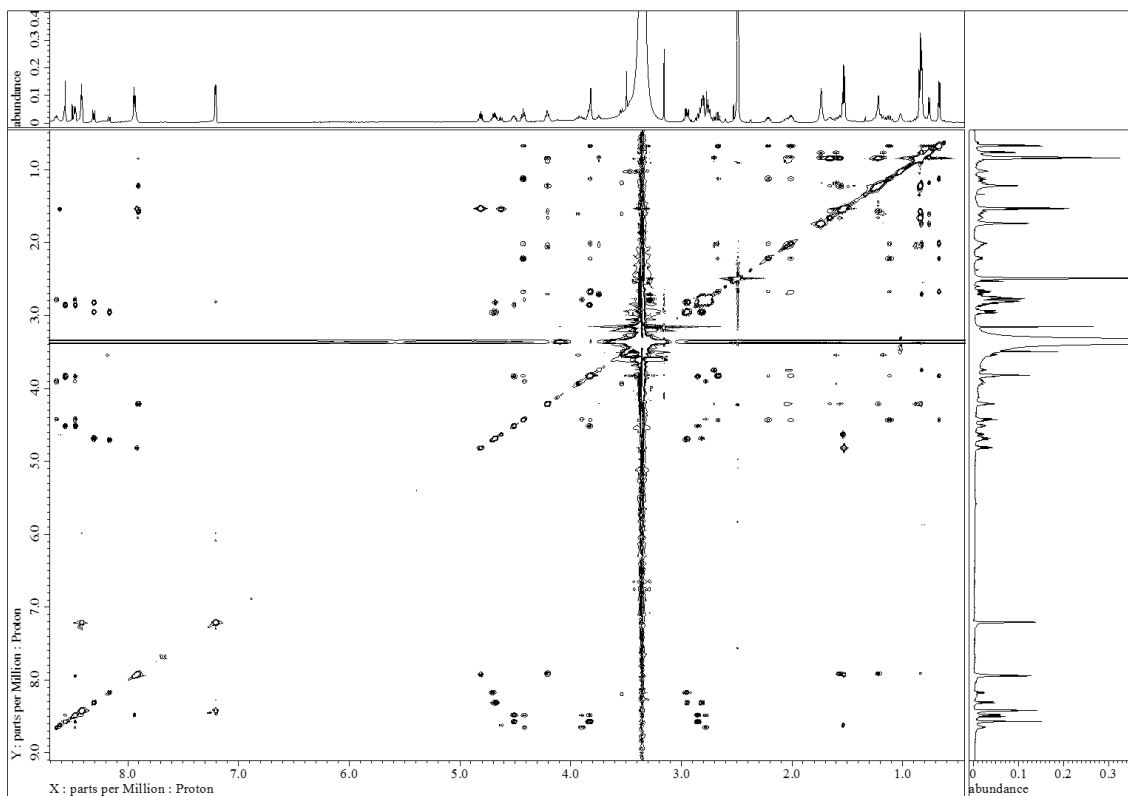


Figure S2-19. TOCSY spectrum of the mixture of **2-5a** and **2-5b** in DMSO- d_6 (600 MHz).

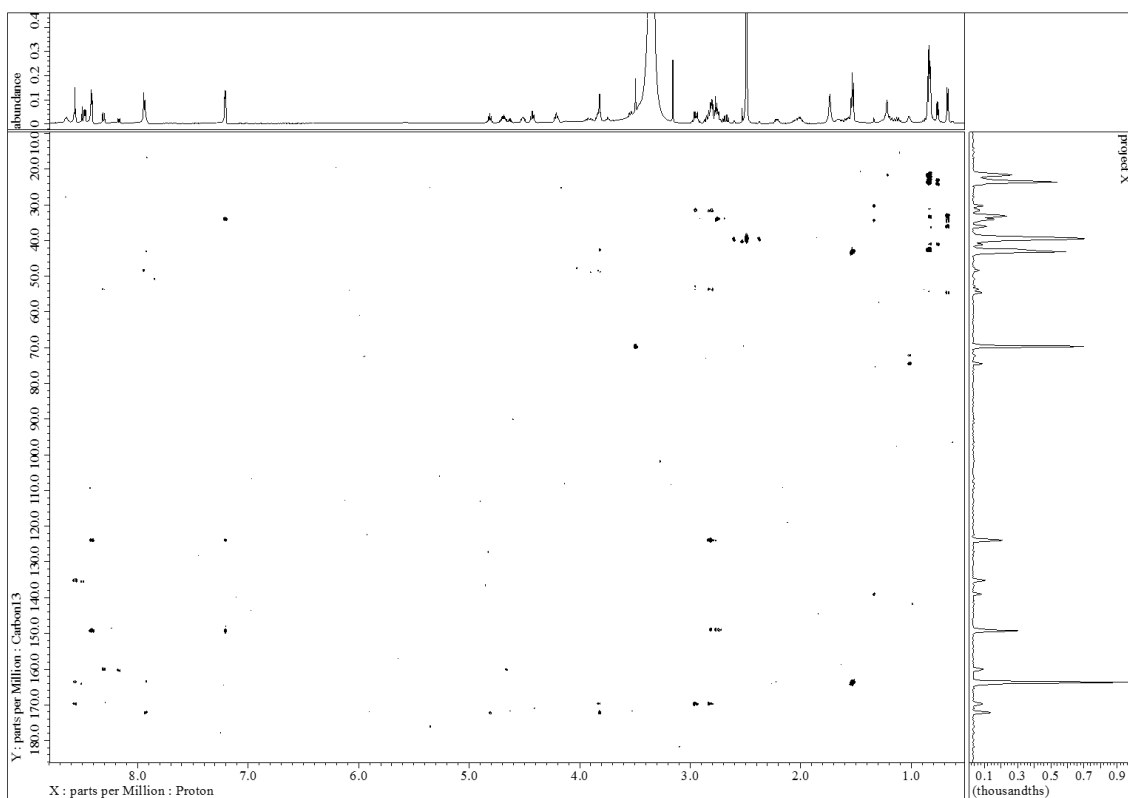


Figure S2-20. HMBC spectrum of the mixture of **2-5a** and **2-5b** in DMSO- d_6 (600 MHz).

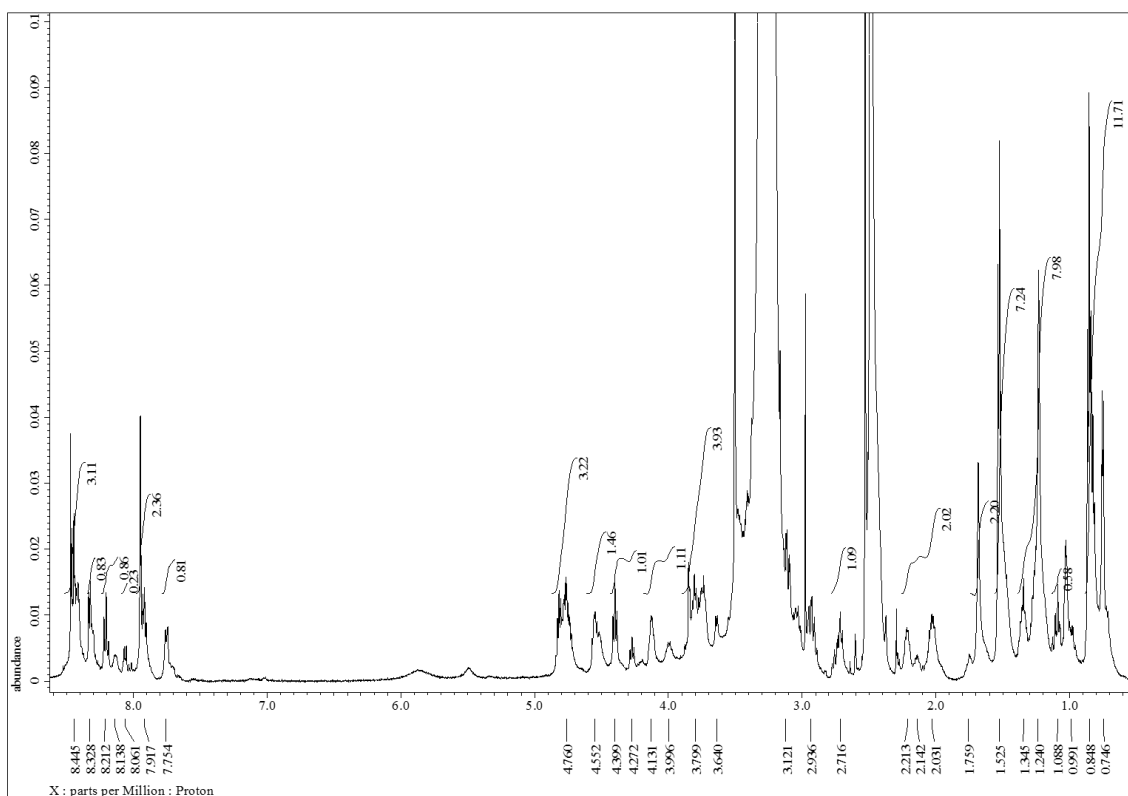


Figure S2-21. ^1H NMR spectrum of the mixture of the reduction products of nazumazole A (**2-6**) in DMSO- d_6 (600 MHz).

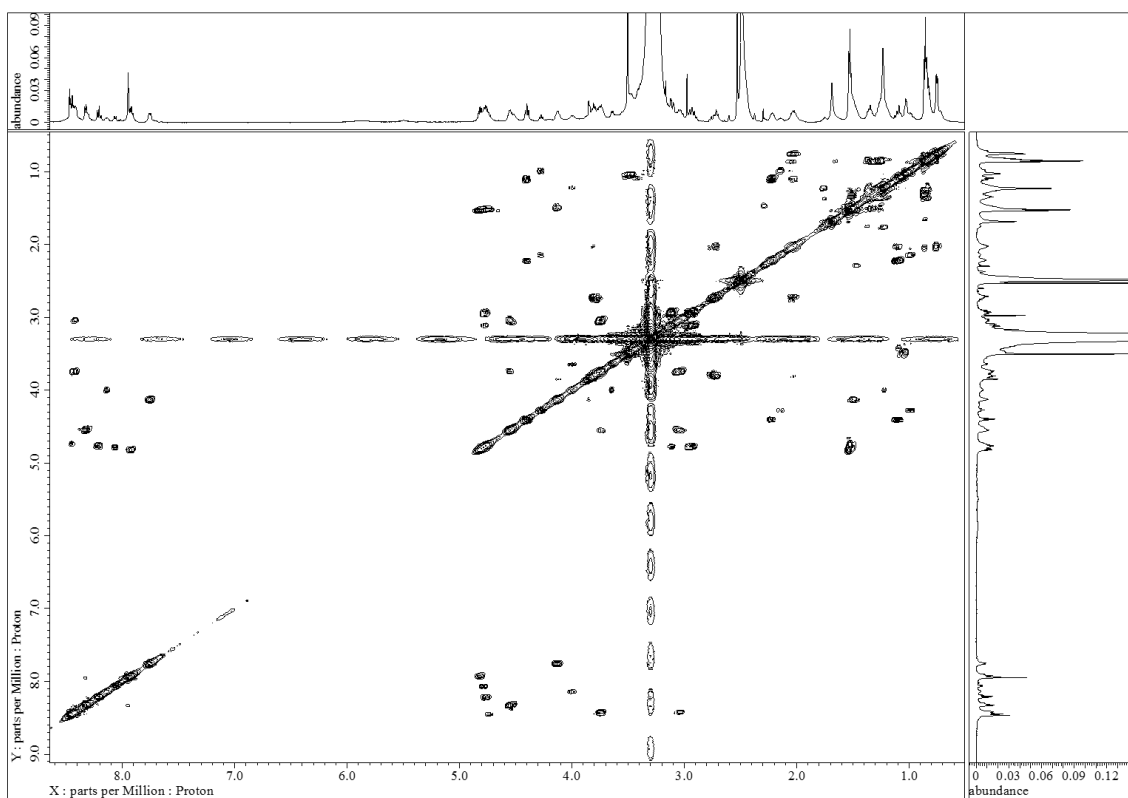


Figure S2-22. COSY spectrum of the mixture of the reduction products of nazumazole A (**2-6**) in DMSO- d_6 (600 MHz).

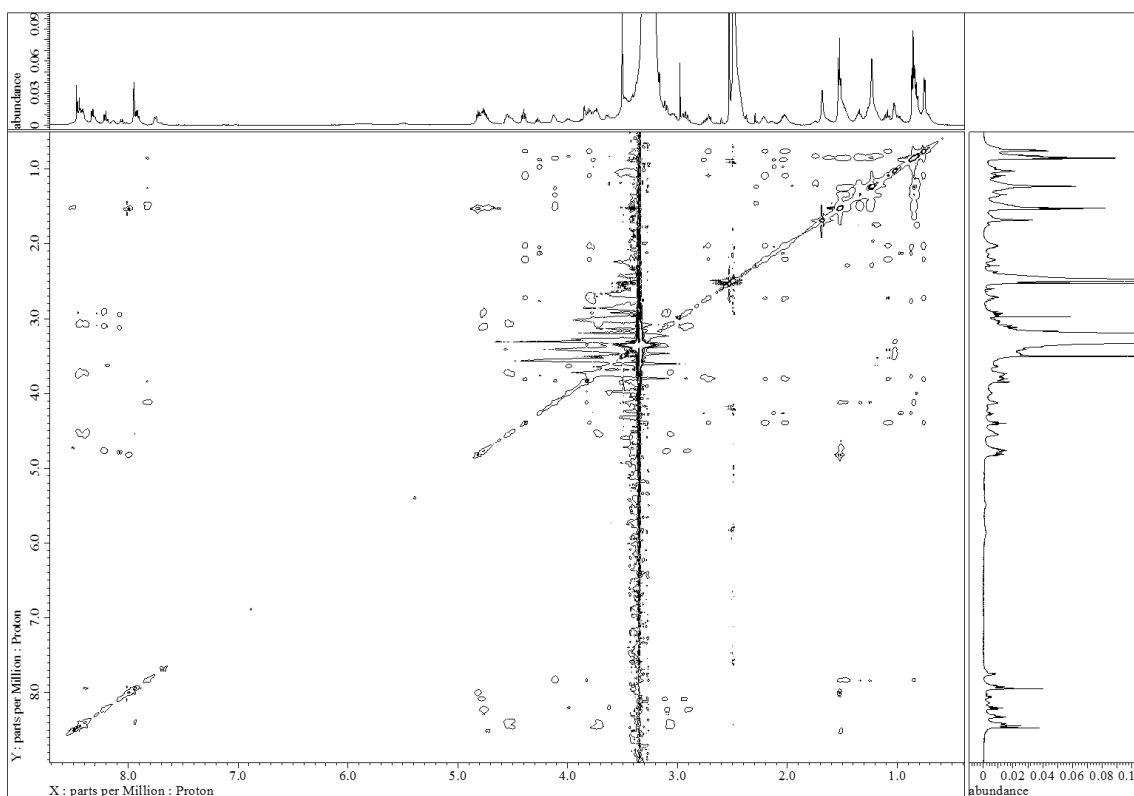


Figure S2-23. TOCSY spectrum of the mixture of the reduction products of nazumazole A (**2-6**) in DMSO- d_6 (600 MHz).

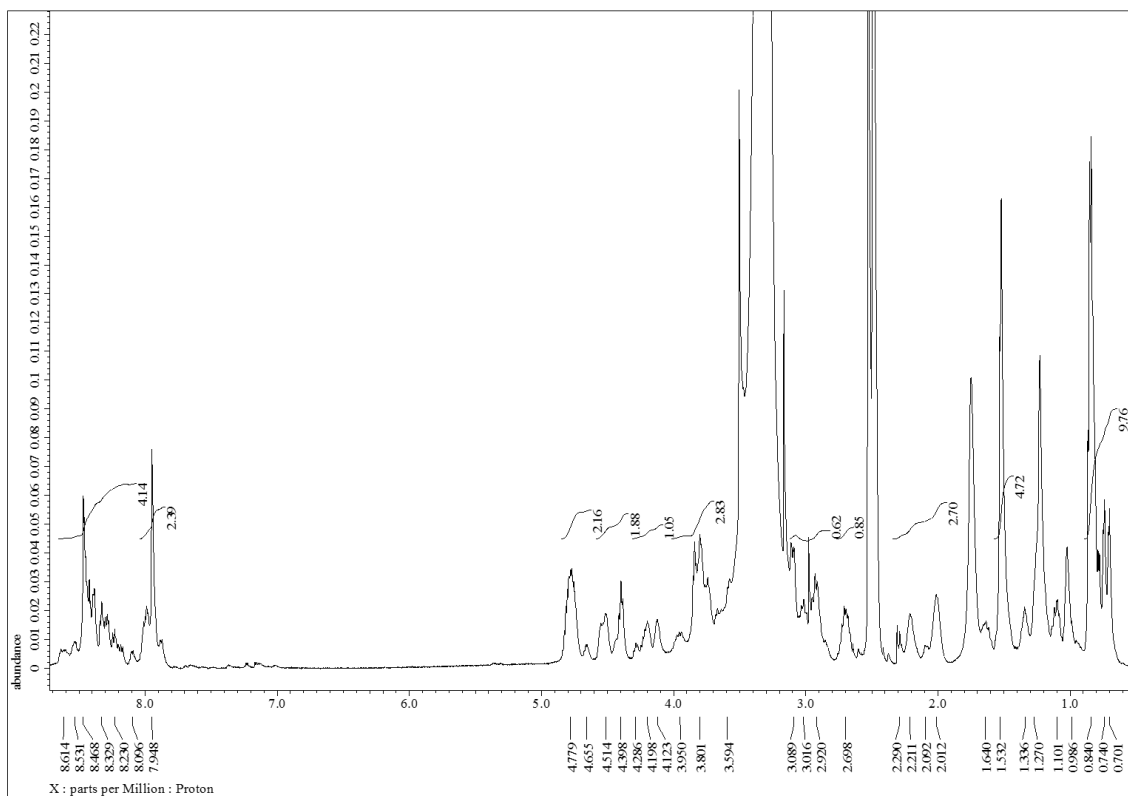


Figure S2-24. ^1H NMR spectrum of the mixture of the reduction products of nazumazole B (**2-7**) in $\text{DMSO-}d_6$ (600 MHz).

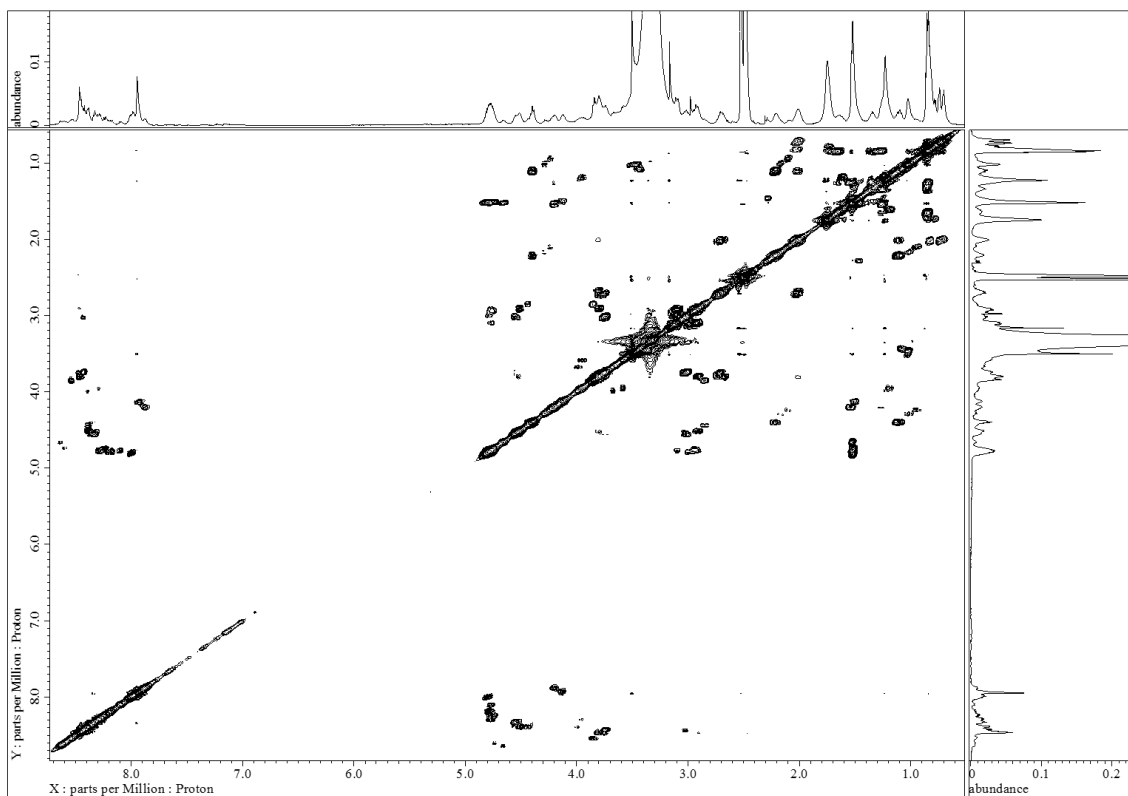


Figure S2-25. COSY spectrum of the mixture of the reduction products of nazumazole B (**2-7**) in $\text{DMSO-}d_6$ (600 MHz).

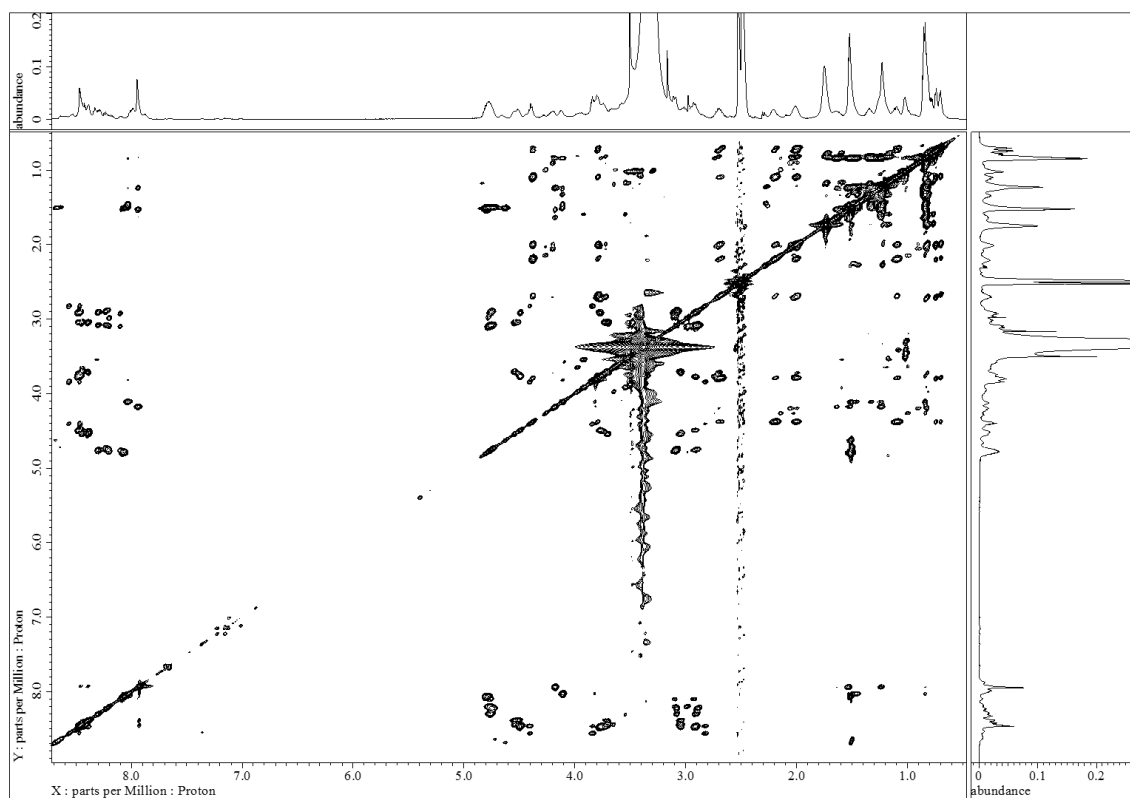


Figure S2-26. TOCSY spectrum of the mixture of the reduction products of nazumazole B (**2-7**) in DMSO- d_6 (600 MHz).

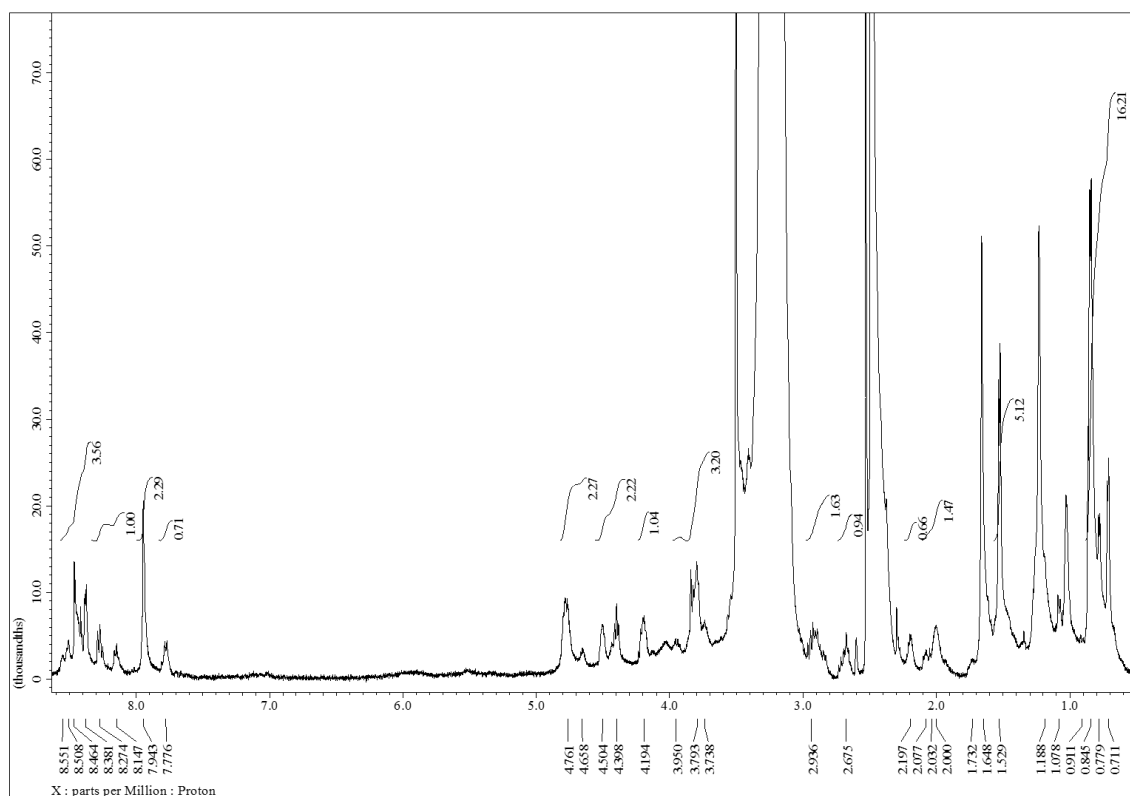


Figure S2-27. ^1H NMR spectrum of the mixture of the reduction products of nazumazole C (**2-8**) in DMSO- d_6 (600 MHz).

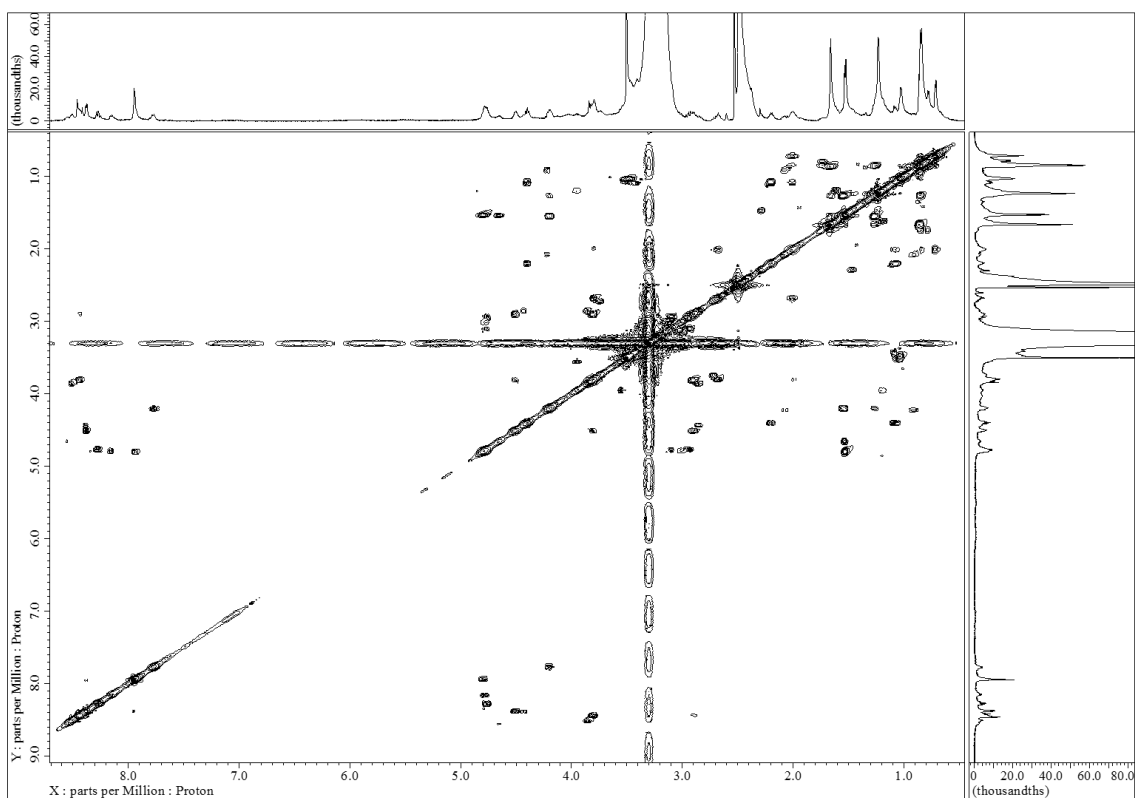


Figure S2-28. COSY spectrum of the mixture of the reduction products of nazumazole C (**2-8**) in DMSO- d_6 (600 MHz).

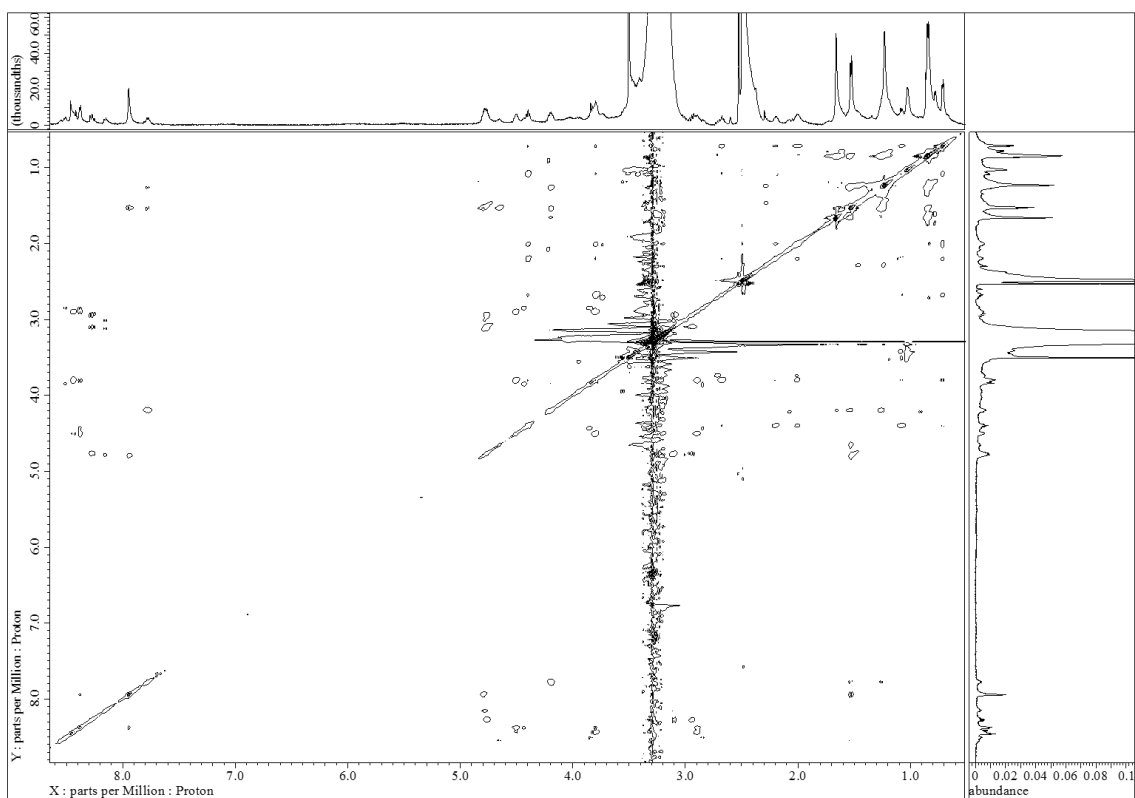


Figure S2-29. TOCSY spectrum of the mixture of the reduction products of nazumazole C (**2-8**) in DMSO- d_6 (600 MHz).

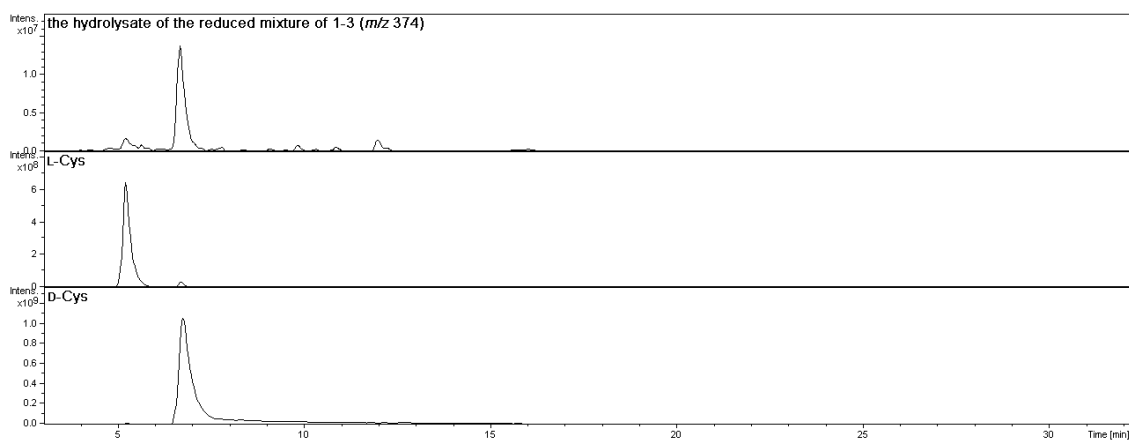


Figure S2-30. LC-MS charts of Marfey's analyses of **2-1-2-3** (Cys).

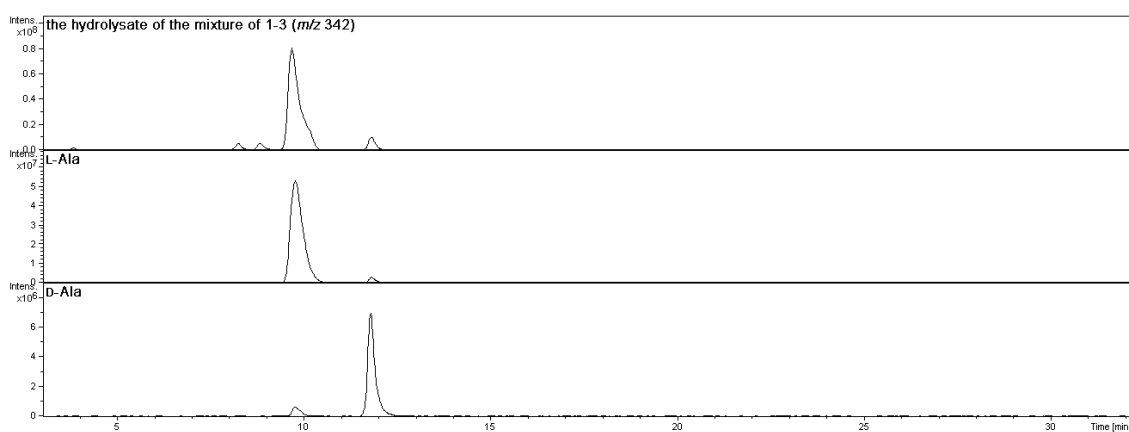


Figure S2-31. LC-MS charts of Marfey's analyses of **2-1-2-3** (Ala).

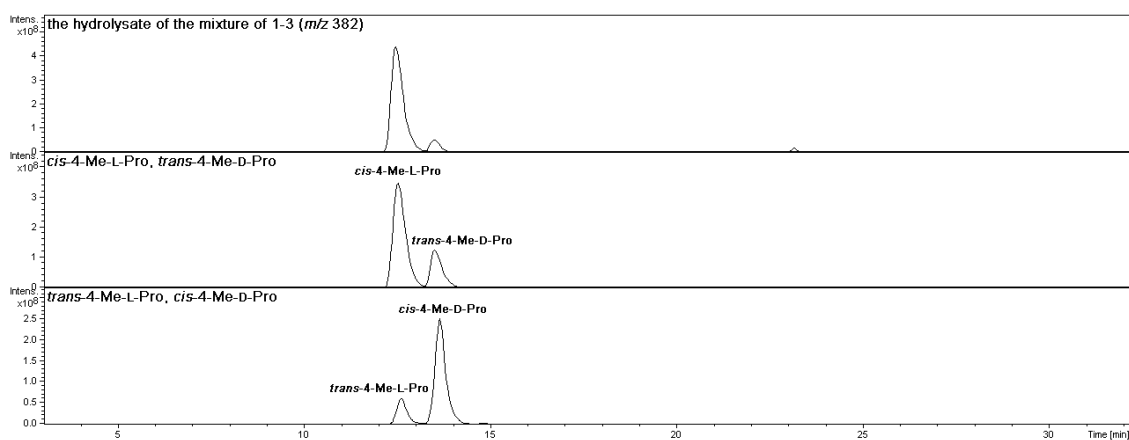


Figure S2-32. LC-MS charts of Marfey's analyses of **2-1-2-3** (Mpr).

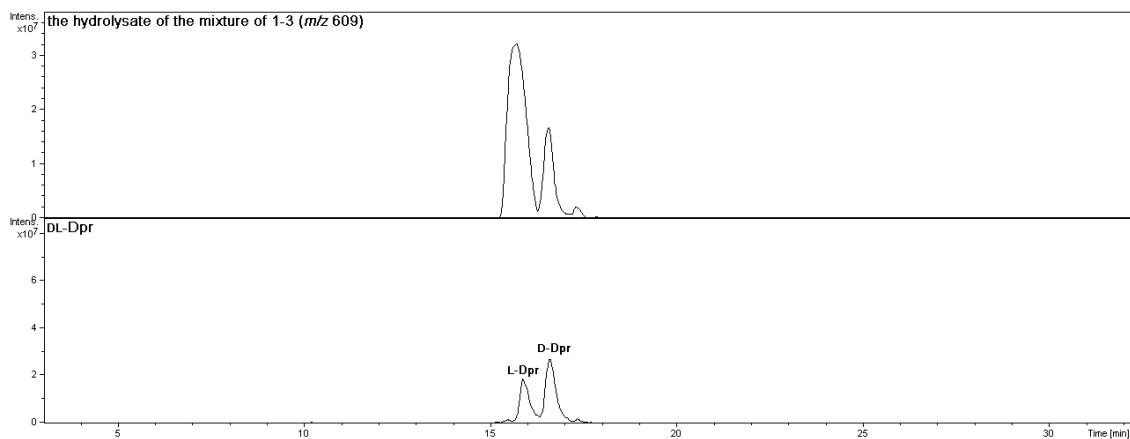


Figure S2-33. LC-MS charts of Marfey's analyses of 2-1-2-3 (Dpr).

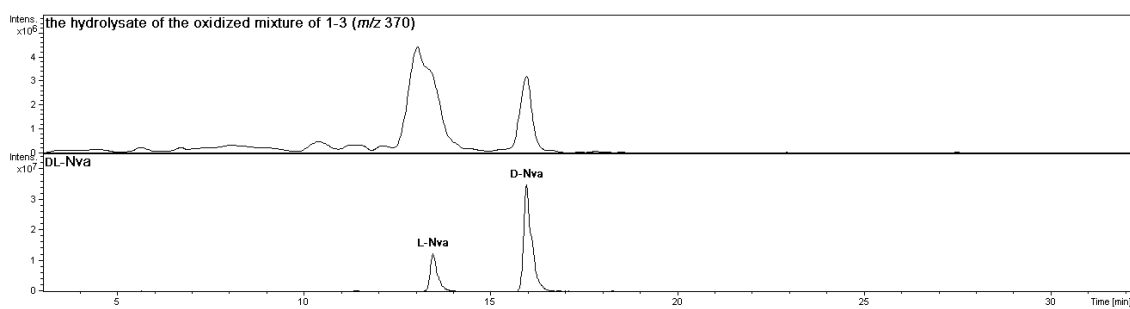


Figure S2-34. LC-MS charts of Marfey's analyses of 2-1-2-3 (Nva).

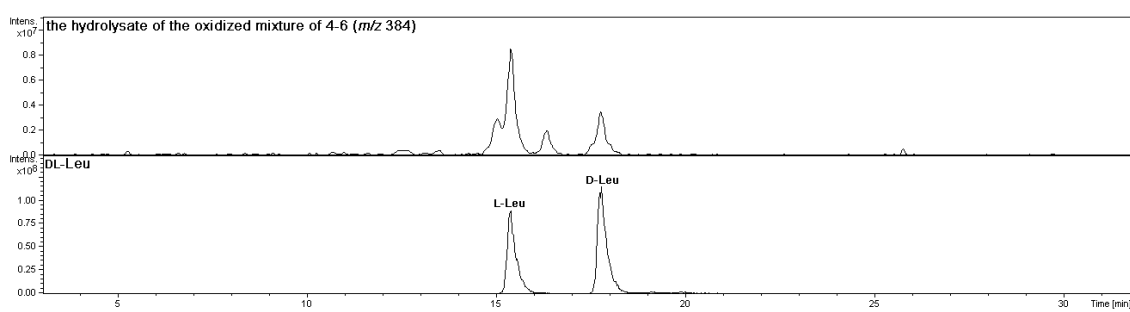


Figure S2-35. LC-MS charts of Marfey's analyses of 2-1-2-3 (Leu)

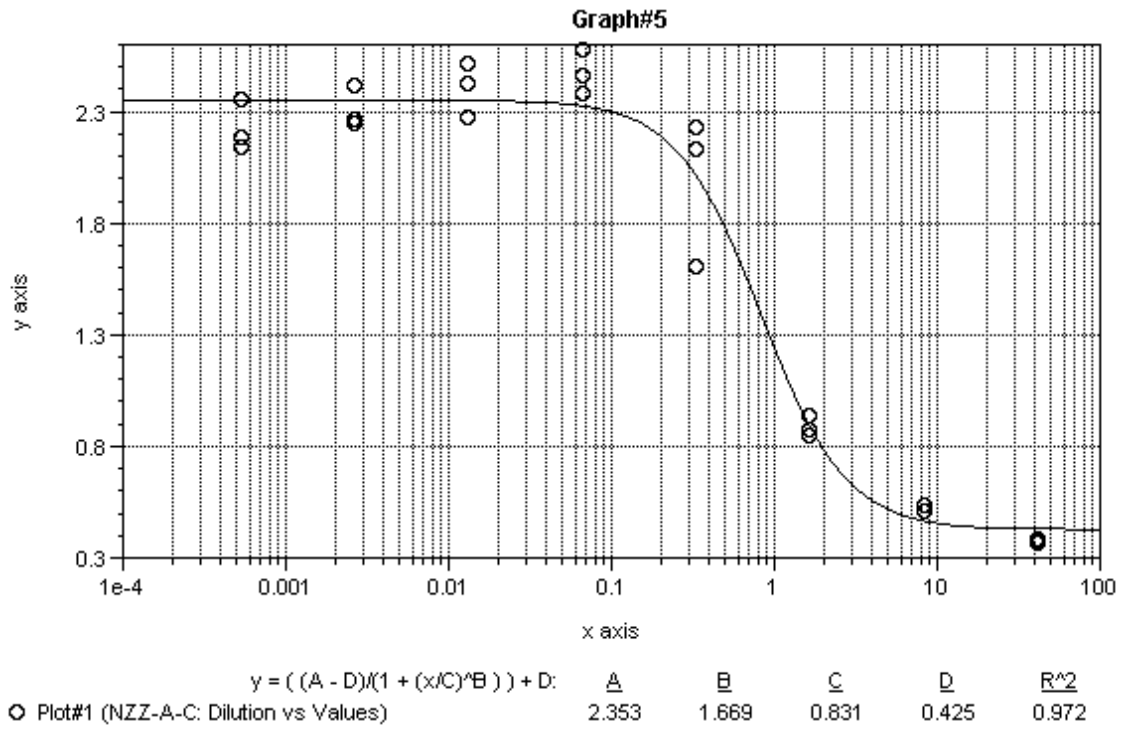


Figure S2-36. The graph of XTT assay of the mixture **2-1-2-3** against P388 murine leukemia cells; x-axis is concentration and y-axis is absorption at 450 nm.

Chapter 3.

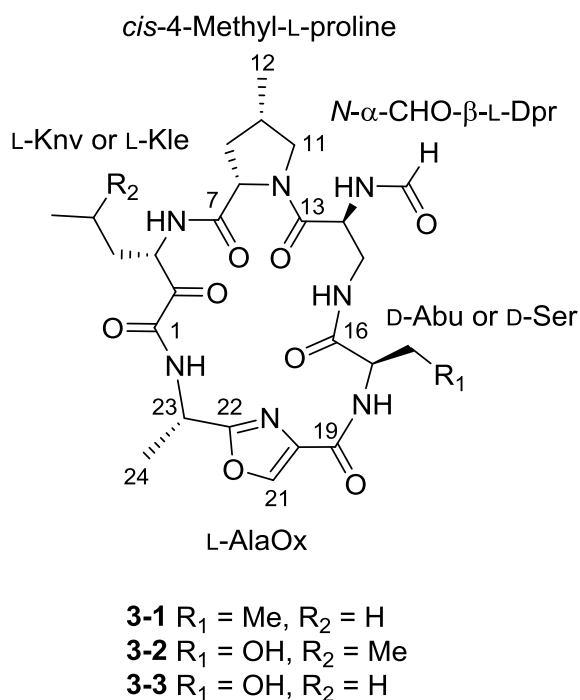
Nazumazoles D–F, cyclic pentapeptides that inhibit chymotrypsin, from the marine sponge *Theonella swinhoei*

3.1. Introduction

In the previous chapter, the structures and bioactivities of dimeric cyclic pentapeptide, nazumazoles A–C (**2-1-2-3**) were described. These peptides were dimerized through disulfide bond, so it was assumed that there were reduced monomeric peptides in the sponge. The disulfide bond was necessary for cytotoxicity, and so, these monomeric peptides might have relatively low activity. To explore the presences and the bioactivities of these peptides, we searched for monomeric analogue of **2-1-2-3**. As a result, we found another broad HPLC peak with the molecular weights of about 500 in the extract of *T. swinhoei* Y. We have purified the peak and further separated into three compounds. The isolation, structure elucidation, and biological activities of these compounds are the subject of this chapter.

3.2. Result and Discussion

The aqueous alcoholic extract of *T. swinhoei* Y was defatted and fractionated by ODS flash chromatography and gel permeation chromatography. We found that nazumazoles D–F (**3-1**–**3-3**) were barely separable by the HPLC on gel permeation column Shodex GS320. Each fraction was further purified by ODS-HPLC followed by another round of gel permeation HPLC to afford nazumazoles D (**3-1**, 1.8 mg), E (**3-2**, 1.0 mg), and F (**3-3**, 0.7 mg) (Figure 3-1).



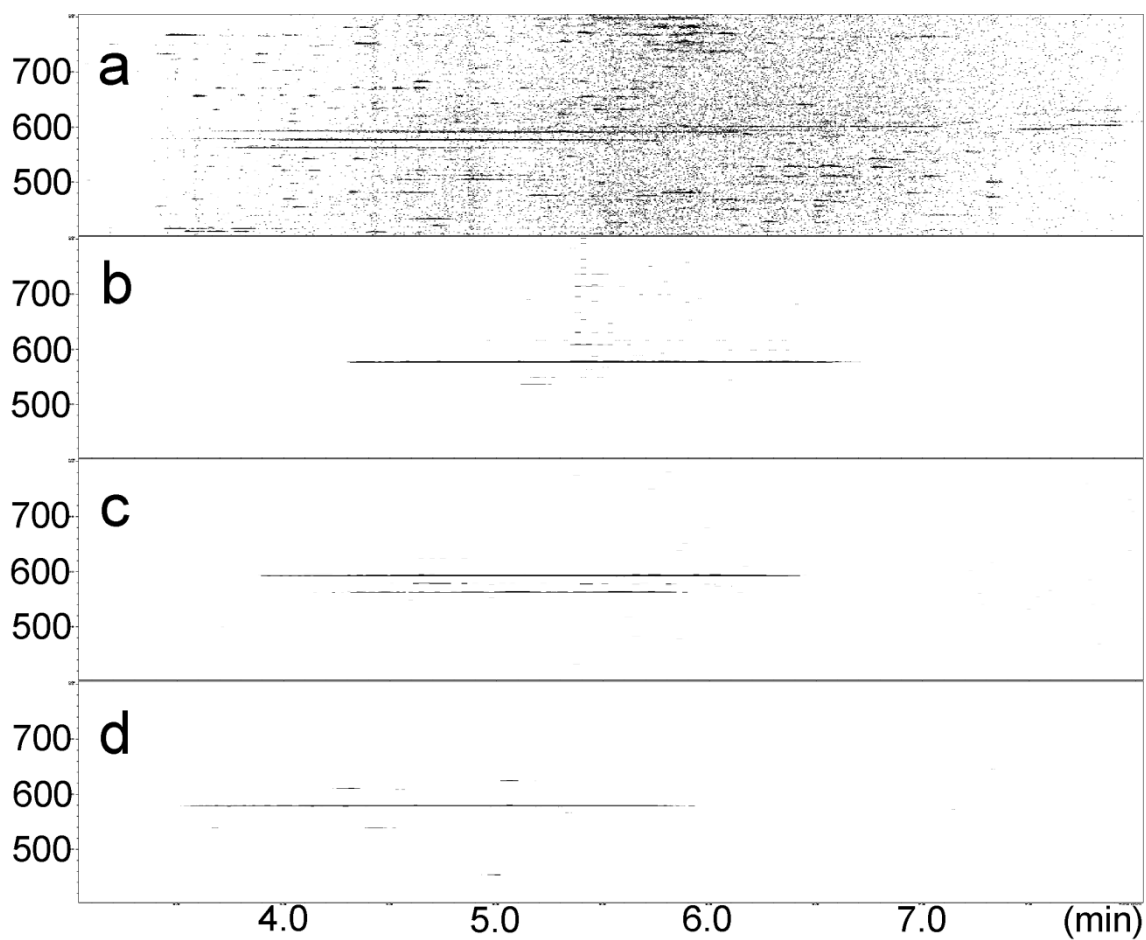


Figure 3-1. 2D LC-MS charts of nazumazoles. (a) the extract of *T. swinhoei* Y, (b) nazumazole D, (c) nazumazole E, and (d) nazumazole F; x-axis is retention time (min) and y-axis is m/z . Peaks of the contaminating lower homologues of nazumazole E were also observed in (c).

The molecular formula of nazumazole D (**3-1**) was determined to be $C_{26}H_{37}N_7O_8$ by HRESIMS. In the 1H NMR spectrum of **3-1** (Table 3-1), there were five amide proton signals and five α -proton signals of amino acid residues, which indicated the peptide nature of **1**. Interpretation of the COSY, TOCSY, and HSQC spectra showed the presence of one each of 1H spin systems ascribable to norvaline (Nva), 4-methylproline (Mpr), 2,3-diaminopropionic acid (Dpr), α -aminobutyric acid (Abu), and Ala. Acid hydrolysis afforded Mpr, Dpr, Abu, and Ala as revealed by Marfey's method.⁵⁴ In the HMBC spectrum, the α -proton of the proposed Nva residue (δ_H 4.83, H-3) was correlated to a shielded ketone carbonyl signal (δ_C 197.6, C-2), which suggested that the keto-carbon was inserted between the α -carbon and the carbonyl carbon of norvaline comprising the α -ketonorvaline (Knv) residue (Figure 3-2). To confirm this assignment, nazumazole D was reduced with $NaBH_4$ followed by acid hydrolysis and derivatization with the Marfey's reagent. The LC-MS analysis of the product afforded two peaks corresponding to the diastereomers of 3-amino-2-hydroxyhexanoic acid (Figure S3-21). An amide carbonyl carbon signal was observed at δ_C 163.8 (C-1) in the HMBC spectrum of **3-1**, in accordance with the presence of the Knv residue. There was a heteroaromatic proton (δ_H 8.60, H-21) and this proton was directly coupled to a carbon signal at δ_C 142.2 (C-21) by $^1J_{CH}$ 214 Hz

and correlated to carbon signals at δ_C 134.8 (C-20) and δ_C 163.6 (C-22), indicating the presence of an oxazole ring.⁵⁰ The carbon signal at δ_C 163.6 (C-22) was also coupled to the α - and β -protons of an alanine-like spin system in the HMBC spectrum, demonstrating that the α -methine was directly connected to the oxazole ring. The remaining unassigned carbon signal was at δ_C 159.5, suggesting that this carbon was connected to C-4 of the oxazole ring to comprise the alanyloxazole (Aox) moiety as found in nazumazoles A–C.

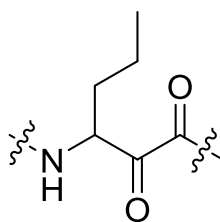


Figure 3-2. The structure of α -ketonorvaline (Knv).

Table 3-1. ^1H (600 MHz) and ^{13}C NMR Data (150 MHz) of Nazumazole D (**1**) in DMSO- d_6 .

amino acid	position	δ_{C} , ^{a, b} type	δ_{H} , ^a (J in Hz)
L-Knv	1	163.8, C	
	2	197.6, C	
	3	54.3, CH	4.83, m
	4	31.1, CH ₂	1.95, m
			1.54, m
	5	18.8, CH ₂	1.50, m
1.38, m			
3-NH	6	12.7, CH ₃	0.90, t (6.9)
			8.78, d (5.5)
L-Mpr	7	172.7, C	
	8	59.2, CH	4.45, dd (8.2, 9.2)
	9	36.7, CH ₂	2.42, m
			1.30, ddd (11.0, 11.5, 12.4)
	10	32.8, CH	2.20, m
	11	53.6, CH ₂	3.90, dd (6.9, 7.3)
2.92, dd (9.6, 10.1)			
<i>N</i> - α -CHO- β -L-Dpr	12	15.6, CH ₃	0.96, d (4.6)
	13	166.9, C	
	14	50.4, CH	4.74, m
	15	38.4, CH ₂	3.72, m
			3.39, m
	14-NH		7.89, d (5.5)
15-NH		7.40, m	
CHO	160.5, CH	7.99, s	
D-Abu	16	172.4, C	
	17	55.3, CH	4.20, m
	18	25.1, CH ₂	1.71, m
			1.50, m
	18-Me	10.0, CH ₃	0.81, t (6.9)
17-NH		7.70, d (9.2)	
L-Aox	19	159.5, C	
	20	134.8, C	
	21	142.2, CH	8.60, s
	22	163.6, C	
	23	43.4, CH	5.03, q (7.3)
	23-NH	15.2, CH ₃	1.54, d (5.5)
9.09, d (7.8)			

^aRecorded at 25 °C. ^b ^{13}C chemical shifts were obtained by HSQC and HMBC experiments.

The amino acid sequence of **3-1** was determined by interpretation of the NOESY and HMBC data (Figure 3-3). NOESY cross-peaks were observed between the NH of the Abu residue (δ_{H} 7.70, 17-NH) and the β -NH of the Dpr residue (δ_{H} 7.40, 15-NH) demonstrating that the β -amino group in the Dpr residue was connected to the carboxyl group of the Abu residue. There was a formyl group (δ_{H} 7.99, CHO) and this proton signal gave NOESY cross-peaks with the α -NH and α -proton of the Dpr residue (δ_{H} 7.89, NH-14; δ_{H} 4.74, H-14), showing that the α -amino group of the Dpr residue was formylated. NOESY correlations between the δ -protons of the Mpr residue (δ_{H} 3.90, H-11a; δ_{H} 2.92, H-11b) and the α -proton of the Dpr residue (δ_{H} 4.74, H-14) showed the connection between the Dpr residue and the Mpr residue, whereas the NOESY cross-peak between the NH of the Knv residue (δ_{H} 8.78, 3-NH) and the α -proton of the Mpr residue (δ_{H} 4.45, H-8) indicated the connection between the Mpr and the Knv residues. The connectivity between the Aox and the Knv residues was shown by an HMBC cross-peak between the NH of the Aox residue (δ_{H} 9.09, 23-NH) and the C-1 carbonyl carbon (δ_{C} 163.8) of the Knv residue. The NH of the Abu residue (δ_{H} 7.70, NH-17) was correlated to the carbonyl carbon of the Aox residue (δ_{C} 159.5, C-19) in the HMBC spectrum, demonstrating that nazumazole D was a cyclic pentapeptide encompassing an oxazole ring.

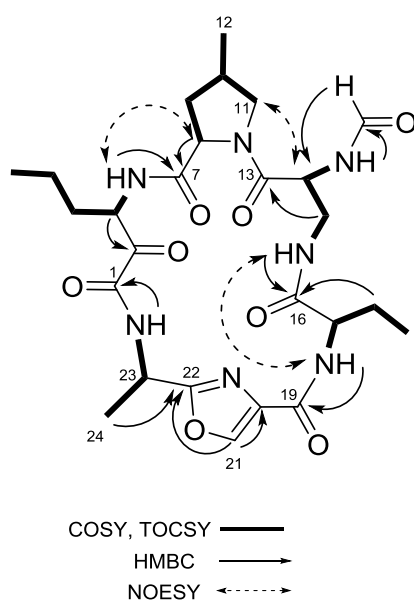


Figure 3-3. Key COSY, TOCSY, HMBC and NOESY correlations in nazumazole D (3-1).

The molecular formula of nazumazole E (3-2) was assigned as $C_{26}H_{37}N_7O_9$ on the basis of HRESIMS. Characteristic structural features of nazumazole D were conserved in 3-2 as inferred from the NMR data (Table S3-1). There were subtle changes: the *n*-propyl side chain of the Knv residue was replaced by an isobutyl group; a Ser residue was substituted for the Abu residue. The NMR signals for the *N*- α -formyl-Dpr, Aox, and Mpr residues were observed in 3-2. The presence of the carbonyl-inserted leucine (Kle, Figure 3-4) was confirmed by the LC-MS analysis of the acid hydrolysate of nazumazole E after reduction with $NaBH_4$ (Figure S3-21). The sequence of the five residues was assigned by interpretation of the ROESY and HMBC data (Figure S3-2a).

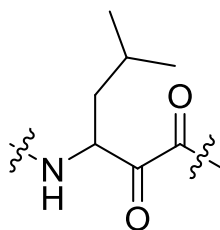


Figure 3-4. The structure of α -ketoleucine (Kle).

Nazumazole F (**3-3**) had the molecular formula of $C_{25}H_{35}N_7O_9$. Comparison of the NMR data of **3-3** (Table S3-2) with those of **3-1** showed that a single amino acid substitution, Abu residue to Ser residue, from nazumazole D occurred in **3-3**. The presence of the Knv residue was confirmed by the LC-MS analysis of the acid hydrolysate of the $NaBH_4$ -reduced nazumazole F. The amino acid sequence of **3-3** was deduced from the ROESY and HMBC data (Figure S3-2b), which showed that the Abu residue in nazumazole D was substituted for a Ser residue in nazumazole F.

The absolute configurations of the α -amino acid residues in **3-1–3-3** were determined by Marfey's method.⁵⁴ Ala, Ser, Abu, Dpr, and Mpr residues were liberated by standard acid hydrolysis (6N HCl, 110 °C, 3 h). The Knv and Kle residues were converted to Nva and Leu residues, respectively, by oxidation with H_2O_2 prior to acid hydrolysis. Authentic samples of the isomers of 4-methylproline were prepared as described in chapter 2. LC-MS analyses revealed the presence of L-Ala, D-Abu, L-Dpr, and L-Nva in **3-1**, L-Ala, D-Ser, L-Dpr, and L-Leu in **3-2**, and L-Ala, D-Ser, L-Dpr, and L-Nva in **3-3** (Figure S3-22–S3-27). In our previous study on the structure elucidation

of nazumazoles A–C, *cis*-4-methyl-L-proline and *trans*-4-methyl-L-proline were only barely separable as were *cis*-4-methyl-D-proline and *trans*-4-methyl-D-proline. We searched for a better separation condition and found that a Phenyl-Hexyl column was most suitable (Figure 3-5). We were able to unambiguously assign the absolute configurations of the Mpr residue in **3-1-3-3** as *cis*-4-methyl-L-proline (Figure S3-28).

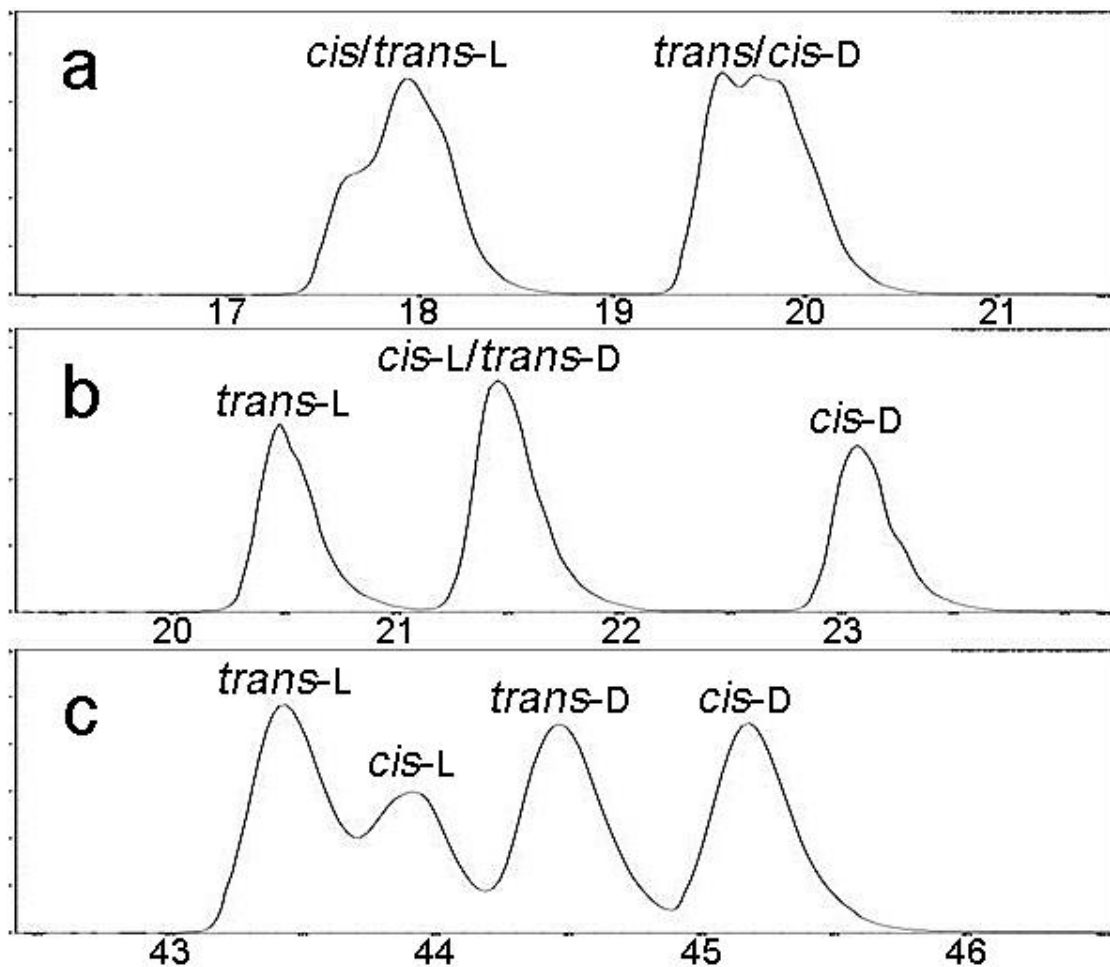


Figure 3-5. LC-MS chart of the four FDAA-derivatives of 4-methylproline using (a) COSMOSIL MS-II, (b) COSMOSIL π -NAP, and (c) Phenyl-Hexyl as the stationary phase (*cis*-L: *cis*-4-methyl-L-proline, *trans*-L: *trans*-4-methyl-L-proline, *cis*-D: *cis*-4-methyl-D-proline, *trans*-D: *trans*-4-methyl-D-proline); x-axis is retention time.

Nazumazoles D–F (**3-1-3-3**) did not show cytotoxicity against P388 murine leukemia cells at a concentration of 50 μM , but a mixture of nazumazoles A–C was cytotoxic. As previously mentioned, cyclotheonamide A from *T. swinhoei* Y is a potent inhibitor of trypsin and thrombin which cleave the carboxyl side of the amide bonds of basic amino acid residues such as Arg.²⁷ The side chain of the ketoarginine (Kar) residue of cyclotheonamide A binds to the specificity pocket of either trypsin or thrombin and the active site hydroxy group of the Ser residue in the enzyme forms a covalent bond with the ketone carboxyl carbon of the Kar residue.²⁹ Against this background we reasoned that nazumazoles might inhibit proteases that cleave the amide bond adjacent to a hydrophobic amino acid residue. We found that nazumazoles D, E, and F inhibited chymotrypsin with IC_{50} values of 2 μM , 3 μM , and 10 μM , respectively (Figure S3-29) and they did not inhibit trypsin or thrombin at a concentration of 50 μM .⁵⁶

3.3. Experimental Section

General Experimental Procedures.

Optical rotations were measured on a Jasco DIP-1000 polarimeter. UV spectra were measured on a Shimadzu BioSpec-1600 spectrophotometer. NMR spectra were measured on a JEOL alpha 600 NMR spectrometer and referenced to the solvent peak: δ_{H} 2.49 and δ_{C} 39.5 for DMSO-*d*₆. ESI mass spectra were recorded on a JEOL JMS-T100LC mass spectrometer. LC-MS experiments were performed on a Shimadzu LC-20AD solvent delivery system and interfaced to a Bruker amaZon SL mass spectrometer. The results of XTT assay and enzyme inhibition assay were recorded with a Molecular Devices SPECTRA max M2.

Extraction and Isolation.

The marine sponge *Theonella swinhoei* was collected at Hachijo Island (September 15, 1998) and kept frozen at -20 °C until processed. The sponge (22 kg, wet weight) was extracted with MeOH and *n*-PrOH-H₂O (3:1). The MeOH extract was partitioned between H₂O and Et₂O. The organic layer was further partitioned between MeOH-H₂O (9:1) and *n*-hexane. The aqueous *n*-PrOH extract was partitioned between

n-PrOH-H₂O-MeOH (3:2:1) and *n*-hexane. The H₂O and aqueous MeOH layers from the MeOH extract and the aqueous alcoholic layer of the *n*-PrOH-H₂O (3:1) extract were combined and subjected to ODS column chromatography by elution with H₂O, MeOH-H₂O (1:1), and CHCl₃-MeOH (1:1). The CHCl₃-MeOH (1:1) fraction was subjected to ODS column chromatography with a step-wise elution with *n*-PrOH-H₂O (2:3) and *n*-PrOH-H₂O (3:1). The former fraction was subjected to gel permeation chromatography (Sephadex LH-20) with CHCl₃-MeOH (1:1). The fraction eluting after cyclotheonamide A²⁷ afforded a brownish oil (5 g). A 550 mg portion of this material was subjected to ODS column chromatography with a step-wise elution with MeCN-H₂O (1:9), MeCN-H₂O (1:3) and MeCN-H₂O (2:3). The first two fractions were combined and subjected to gel permeation HPLC on TSK gel α-2500, eluting with MeCN-H₂O (3:7) containing 0.2% acetic acid to afford twelve fractions (A–L). Fractions E–I were combined and subjected to gel permeation HPLC on Shodex GS320-20FS, eluting with MeOH containing 0.25% acetic acid to afford three fractions (M–O). Fractions N and O were separated by recycle-HPLC on Shodex GS320-20FS, eluting with MeOH containing 0.25% acetic acid to afford four fractions (P–S). Fractions P and R, and Q and S were combined, respectively (fractions T and U). Fractions M, T and U were purified by ODS-HPLC on COSMOSIL 5C₁₈-AR-II with

gradient elution from MeCN-H₂O (1:9) to MeCN-H₂O (1:4) containing 0.5% acetic acid. Finally, each fraction was purified by gel permeation HPLC on Shodex GS320-HQ with gradient elution from MeCN-H₂O (1:9) to MeCN-H₂O (3:7) containing 0.5% acetic acid to afford nazumazole D (**3-1**, 1.8 mg), E (**3-2**, 1.0 mg) and F (**3-3**, 0.7 mg).

Nazumazole D (3-1): yellow powder; $[\alpha]_{\text{D}} -9$ (*c* 0.1, MeOH); UV (MeOH) λ_{max} (log ϵ) 220.0 (3.7); ¹H and ¹³C NMR (DMSO-*d*₆), Table 3-1; HRESIMS *m/z* 598.2580 [M + Na]⁺ (calcd for C₂₆H₃₇N₇NaO₈, 598.2601, Δ -2.1 mmu).

Nazumazole E (3-2): yellow powder; $[\alpha]_{\text{D}} -17$ (*c* 0.1, MeOH); UV (MeOH) λ_{max} (log ϵ) 220.5 (3.7); ¹H and ¹³C NMR (DMSO-*d*₆), Table S3-1; HRESIMS *m/z* 614.2529 [M + Na]⁺ (C₂₆H₃₇N₇NaO₉, 614.2550, Δ -2.1 mmu).

Nazumazole F (3-3): yellow powder; $[\alpha]_{\text{D}} -46$ (*c* 0.05, MeOH); UV (MeOH) λ_{max} (log ϵ) 217.5 (3.4); ¹H and ¹³C NMR (DMSO-*d*₆), Table S3-2; HRESIMS *m/z* 600.2408 [M + Na]⁺ (calcd for C₂₅H₃₅N₇NaO₉, 600.2394, Δ +1.4 mmu).

Marfey's Analyses of Nazumazoles D–F (3-1–3-3).

To a solution of **3-1** (50 μg) in MeOH (1.0 mL) was added NaBH_4 (1.0 mg) and left at rt for 10 min. 5% Acetic acid in H_2O (1.0 mL) was added to the mixture and the solution was applied to an ODS column and eluted with H_2O and MeCN- H_2O (3:2). The aqueous MeCN fraction was dried in vacuo to afford a diastereomeric mixture of dihydronazumazole D. In the same manner, dihydronazumazoles E and F were prepared. Reduced peptides were hydrolyzed in 6 N HCl at 110 $^\circ\text{C}$ for 3 h. The reaction mixtures were dried by a stream of N_2 and redissolved in H_2O (100 μL). 1% L-FDAA solution in acetone (100 μL) and 1 M NaHCO_3 in H_2O (20 μL) were added to the solution, and kept at 55 $^\circ\text{C}$ for 30 min. After neutralization with 2 N HCl (10 μL), the reaction mixtures were analyzed by LC-MS on COSMOSIL 2.5 C_{18} -MS-II with gradient elution from MeCN- H_2O (1:9) to MeCN- H_2O (7:3) containing 0.5% acetic acid for 32 min. Standard amino acids were derivatized with L-FDAA and analyzed by LC-MS in the same manner. Retention times of amino acids and LC-MS charts are shown in Table S3-3 and Figures S3-22–S3-25.

LC-MS Analyses of the Four FDAA-derivatives of 4-methylproline.

The synthetic procedures of *cis*-4-methyl-L-proline and *trans*-4-methyl-L-proline were described in the previous chapter. Solutions of *cis*-4-methyl-L-proline (0.7 mg) and *trans*-4-methyl-L-proline (0.9 mg) in H₂O (100 μL) were derivatized with D-/L-FDAA in the same manner as Marfey's analyses of nazumazoles D-F, respectively. *cis*-/*trans*-4-Methyl-L-proline derivatized with D-FDAA were used as the standards of enantiomers of *cis*-/*trans*-4-methyl-D-proline. The four FDAA-derivatized 4-methylproline were analyzed by LC-MS on COSMOSIL 2.5C₁₈-MS-II, COSMOSIL 2.5 π-NAP, or phenomenex Phenyl-Hexyl with gradient elution from 10% to 50% aqueous MeCN containing 0.5% acetic acid for 57 min (Figure S3-28).

Oxidation of Knv and Kle Residues.

To the solutions of **3-1**, **3-2**, and **3-3** (100 μg, each) in 5% NaOH in H₂O (200 μL) was added 30% H₂O₂ (50 μL) and the mixture was kept at 65 °C for 20 min. The reaction products were dried and subjected to acid hydrolysis, derivatization, and LC-MS analysis as described above (Table S3-3, and Figure S3-26 and S3-27).

Enzyme Inhibition Assay.

Enzyme inhibitory assays were performed in triplicate in 96-well micro plates. Bovine α -chymotrypsin (25 ng; Sigma-Aldrich C4129) in a buffer (70 μ L of a 20 mM Tris-HCl solution, pH 7.8) was preincubated for 15 min at 37 $^{\circ}$ C in the presence of 1 μ L of a sample solution or DMSO as negative control. After preincubation, chymotrypsin substrate {Suc-Leu-Leu-Val-Tyr 4-methylcoumaryl-7-amide (MCA), 5 μ L of 2 mM solution in DMSO) was added, and the solution was incubated for 1 h at 37 $^{\circ}$ C. The reaction was stopped by adding a solution of sodium acetate (80 μ L, 1 M, pH 4.0). Formation of MCA was measured by fluorometry (the excitation and emission wavelengths were 355 and 460 nm, respectively). 4-(2-Aminoethyl) benzenesulfonyl fluoride hydrochloride (AEBSF; 1 μ L of a 4 mM solution in H₂O) was used as a positive control. Trypsin and thrombin inhibition assays were performed in the same manner using either bovine trypsin (1 μ g/ μ L solution; Wako 208-13954) or bovine thrombin (0.5 μ g/ μ L solution; Sigma-Aldrich); trypsin substrate (Bz-L-Arg-*p*NA•HCl, 5 mM solution prepared in DMSO) or thrombin substrate (Bz-Phe-Val-Arg-*p*NA•HCl, 1.3 mM solution in H₂O). Formation of *p*NA was measured by UV absorption (405 nm).

3.4. Supporting Information

Table S3-1. ^1H (600 MHz) and ^{13}C NMR Data (150 MHz) of Nazumazole E (**3-2**) in $\text{DMSO-}d_6$.

amino acid	position	δ_{C} , ^{a, b} type	δ_{H} , ^a (J in Hz)	ROESY	HMBC
L-Kle	1	164.1, C			
	2	unassigned ^c			
	3	53.1, CH	4.92, m		
	4	37.8, CH ₂	1.71, m		
			1.46, m		
	5	24.6, CH	1.78, m		
	6	23.2, CH ₃	0.92, d (6.4)		
<i>cis</i> -4-methyl-L-proline	5-Me	20.9, CH ₃	0.89, d (6.4)		
	3-NH		8.67, d (6.9)	8	7
	7	172.0, C			
<i>N</i> - α -CHO-L- β -Dpr	8	59.4, CH	4.39, m	3-NH	13
	9	36.8, CH ₂	2.36, m		
			1.19, m		7
	10	33.2, CH	2.18, m		
	11	53.8, CH ₂	3.87, dd (7.3, 9.2)	14	
			2.90, t (10.5)		
	12	15.9, CH ₃	0.95, d (6.0)		
	13	170.8, C			
	14	50.5, CH	4.69, m	11a	
	15	39.2, CH ₂	3.53, m		
14-NH		8.08, d (6.9)	COH	COH	
15-NH		7.43 dd, (6.0, 6.4)	17-NH	16	
COH	160.8, CH	7.97, s		14	
D-Ser	16	170.9, C			
	17	56.1, CH	4.38, m		19
	18	61.8, CH ₂	3.58, m		
3.53, m					16
17-NH		7.82, d (9.2)	15-NH	19	
L-Aox	19	159.8, C			
	20	135.0, C			
	21	142.1, CH	8.60, s		20, 22
	22	163.6, C			
	23	43.5, CH	5.02, m		22
	24	15.6, CH ₃	1.55, d (7.3)		22
23-NH		9.12, d (8.2)		1	

^aRecorded at 25 °C. ^b ^{13}C chemical shifts were obtained by HSQC and HMBC experiments.

^cNo HMBC correlation to amide carbonyl carbon was observed.

Table S3-2. ^1H (600 MHz) and ^{13}C NMR Data (150 MHz) of Nazumazole F (**3-3**) in $\text{DMSO-}d_6$.

amino acid	position	δ_{C} , ^{a, b} type	δ_{H} , ^a (J in Hz)	ROESY	HMBC
L-Knv	1	164.3, C			
	2	unassigned ^c			
	3	54.3, CH	4.86, m	17-NH	
	4	31.1, CH ₂	1.90, m 1.53, m		
	5	18.4, CH ₂	1.45, m 1.38, m		
	6	13.1, CH ₃	0.89, t (7.3)		
<i>cis</i> -4-methyl-L-proline	3-NH		8.78, d (6.4)	8	
	7	unassigned ^c			
	8	59.2, CH	4.39, m	3-NH	
	9	36.5, CH ₂	2.35, m 1.18, m		
	10	32.8, CH	2.17, m		
	11	53.6, CH ₂	3.87, dd (7.3, 9.2) 2.89, t (10.5)	14	
<i>N</i> - α -CHO-L- β -Dpr	12	15.6, CH ₃	0.94, d (6.4)		
	13	unassigned ^c			
	14	50.1, CH	4.69, m	11a, COH	
	15	38.8, CH ₂	3.53, m		
	14-NH		8.07, d (6.9)	COH	COH
	15-NH		7.46, t (6.0)		16
D-Ser	COH	160.5, CH	7.97, s	14	14
	16	170.9, C			
	17	56.0, CH	4.38, m		
	18	61.5, CH ₂	3.56, m 3.53, m		
	17-NH		7.80, d (9.2)	3	19
	L-Aox	19	159.7, C		
20		135.0, C			
21		141.8, CH	8.60, s	12, 24	20, 22
22		163.5, C			
23		43.0, CH	5.02, m		22
24		15.2, CH ₃	1.54, d (7.3)		22
	23-NH		9.20, d (8.2)		1

^aRecorded at 25 °C. ^b ^{13}C chemical shifts were obtained by HSQC and HMBC experiments.

^cNo HMBC correlation to amide carbonyl carbon was observed.

Table S3-3. Results of Marfey's Analyses of Nazumazoles D–F (**3-1-3-3**).

amino acid	retention time (min)		
	L	D	sample
Ser	7.2	7.9	7.9 (3-2, 3-3)
Ala	9.8	11.8	9.7 (3-1-3-3)
Abu	11.2	13.6	13.7 (3-1)
Dpr	15.9	16.9	15.9 (3-1-3-3)
Nva	13.5	15.9	13.3 (3-1), 13.5 (3-3)
Leu	15.4	17.6	15.4 (3-2)

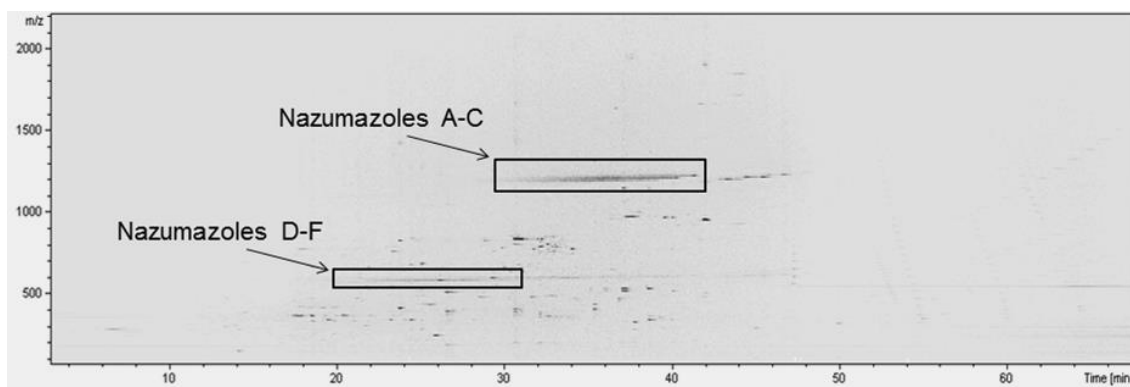


Figure S3-1. Two-dimensional LC-MS chart of nazumazoles D–F (**3-1-3-3**) and nazumazoles A–C (**2-1-2-3**) in crude sample; x-axis is retention time and y-axis is m/z .

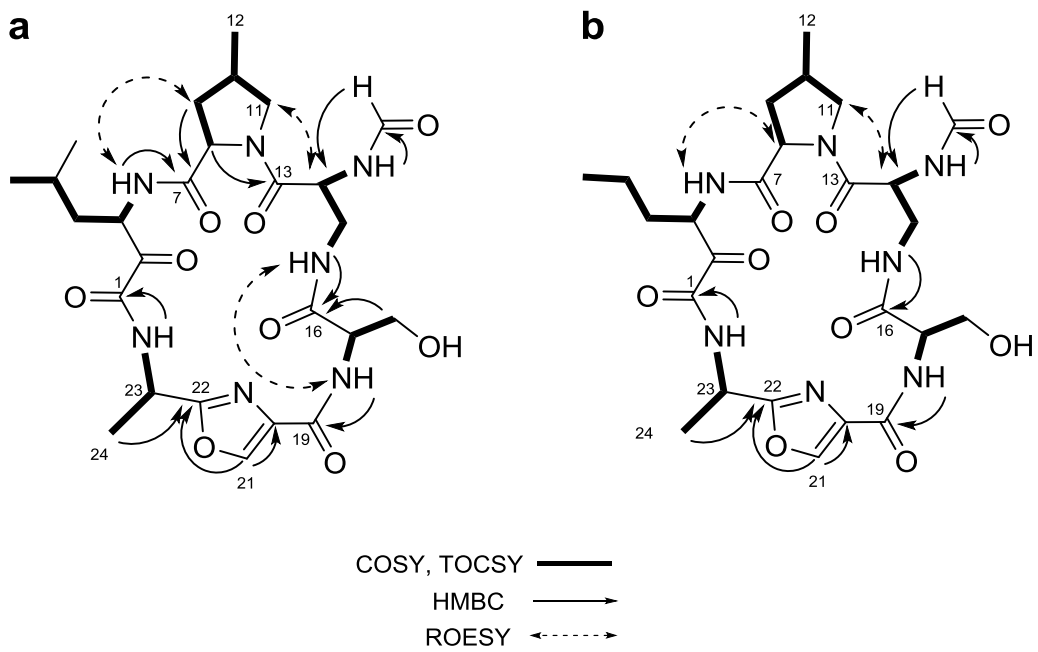


Figure S3-2. Key COSY, TOCSY, HMBC and ROESY correlations in (a) nazumazoles E and (b) F.

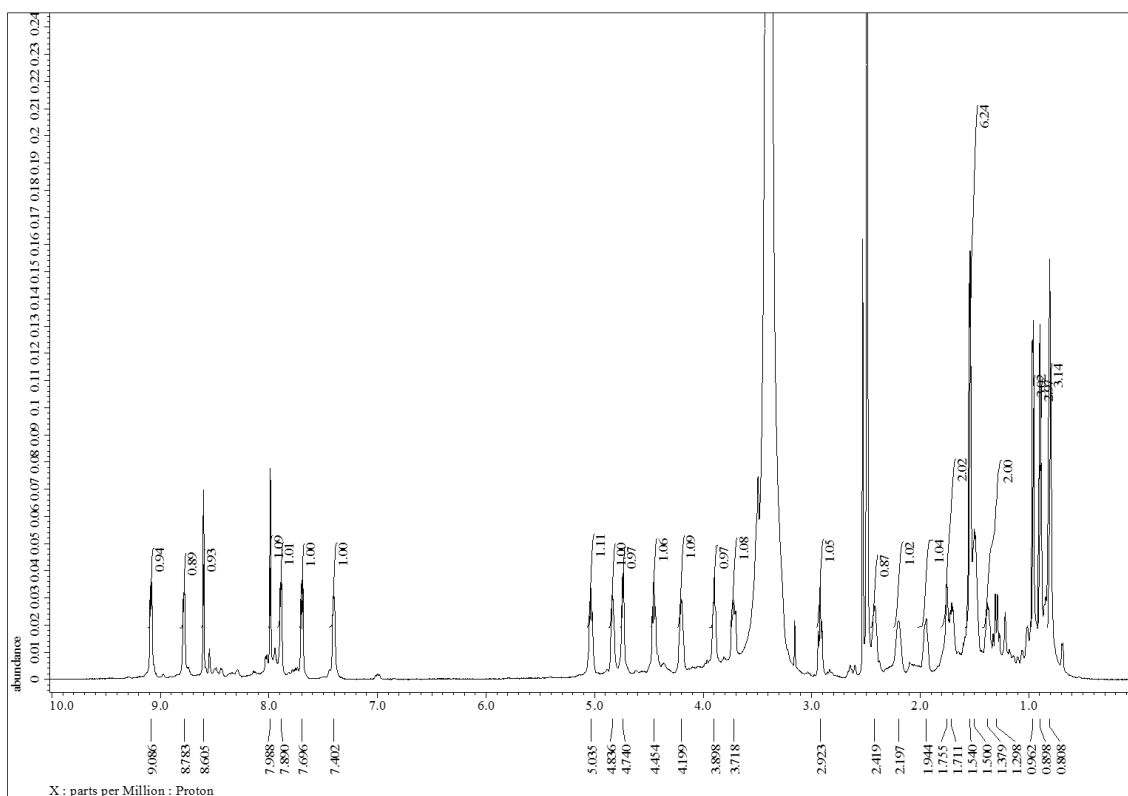


Figure S3-3. ^1H NMR spectrum of nazumazole D (**3-1**) in $\text{DMSO-}d_6$ (600 MHz).

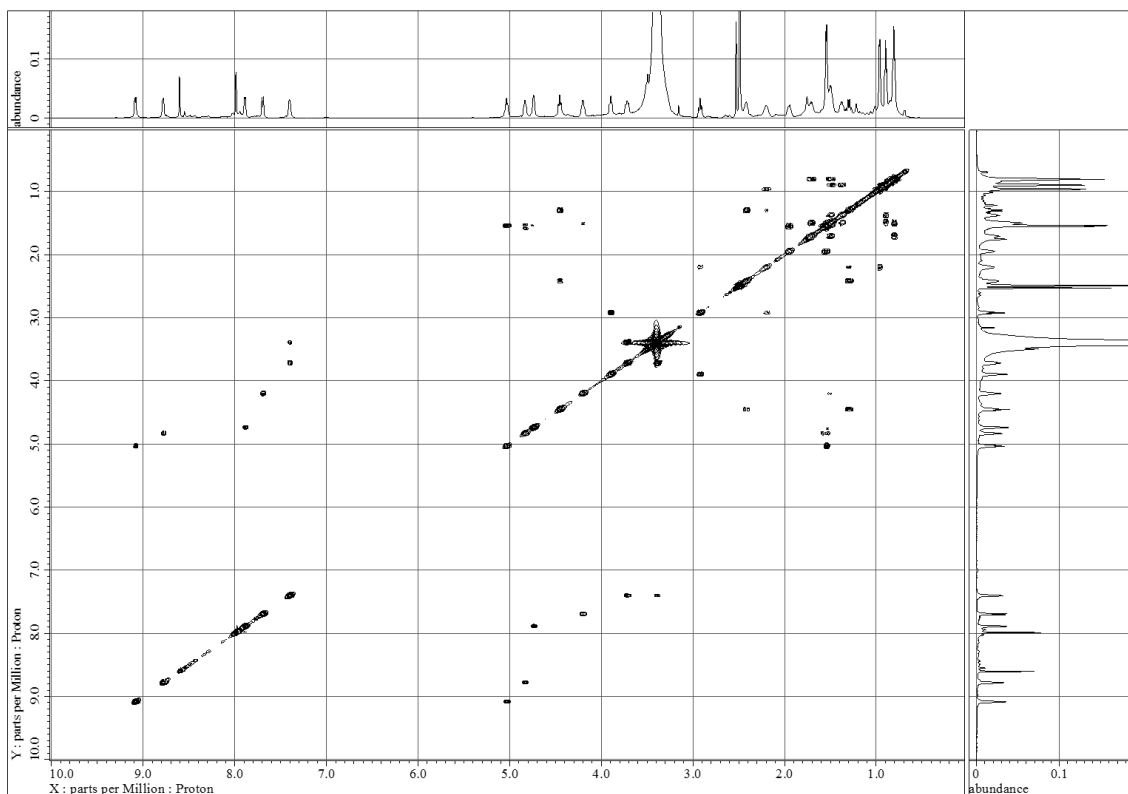


Figure S3-4. COSY spectrum of nazumazole D (**3-1**) in $\text{DMSO-}d_6$ (600 MHz).

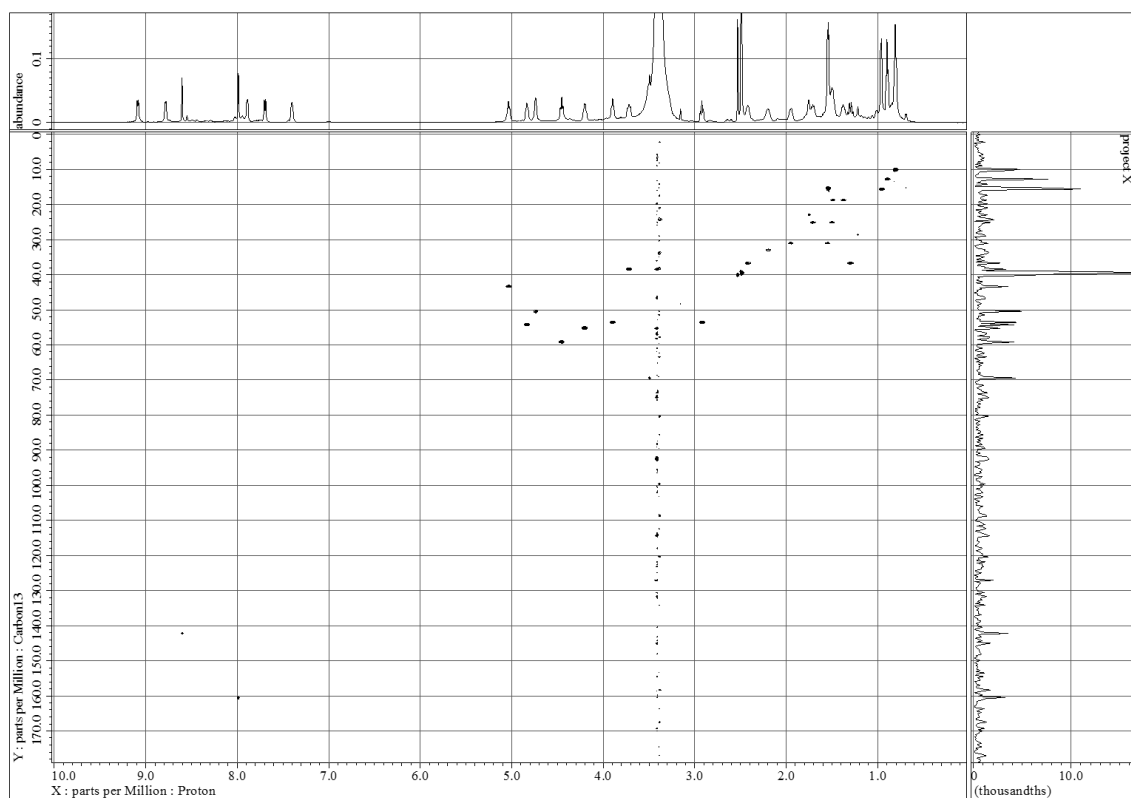


Figure S3-5. HSQC spectrum of nazumazole D (**3-1**) in DMSO- d_6 (600 MHz).

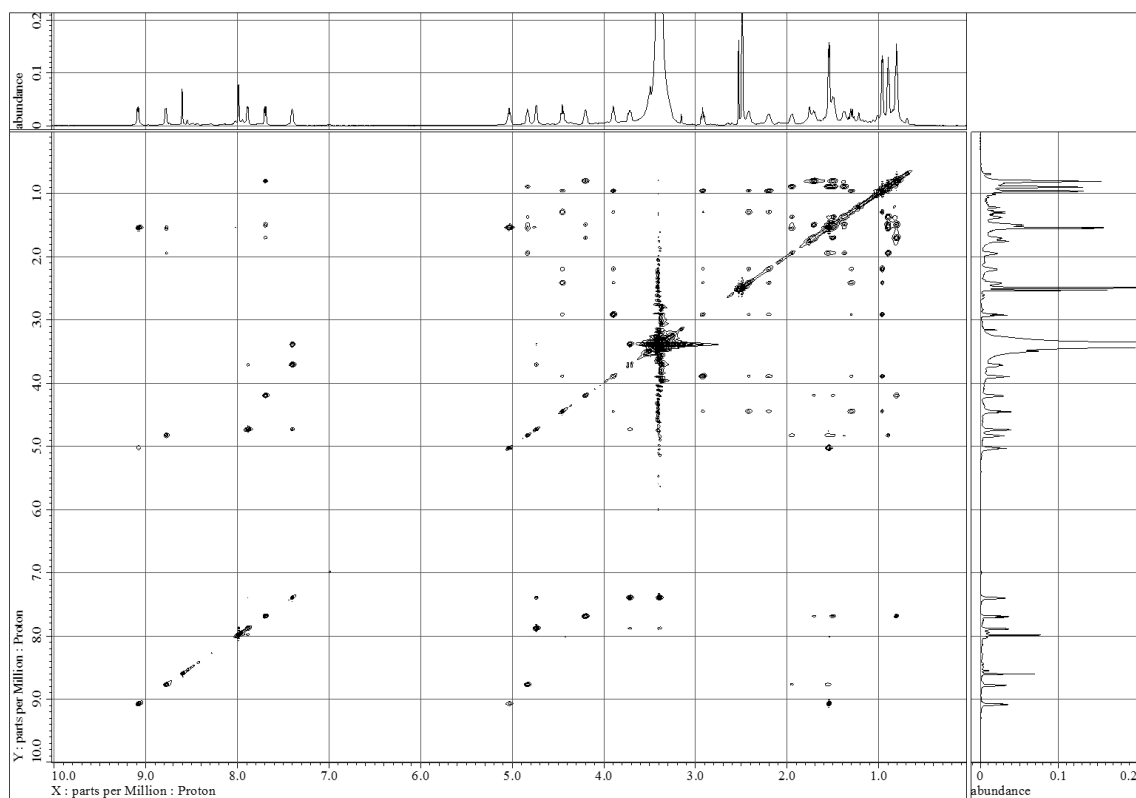


Figure S3-6. TOCSY spectrum of nazumazole D (**3-1**) in DMSO- d_6 (600 MHz).

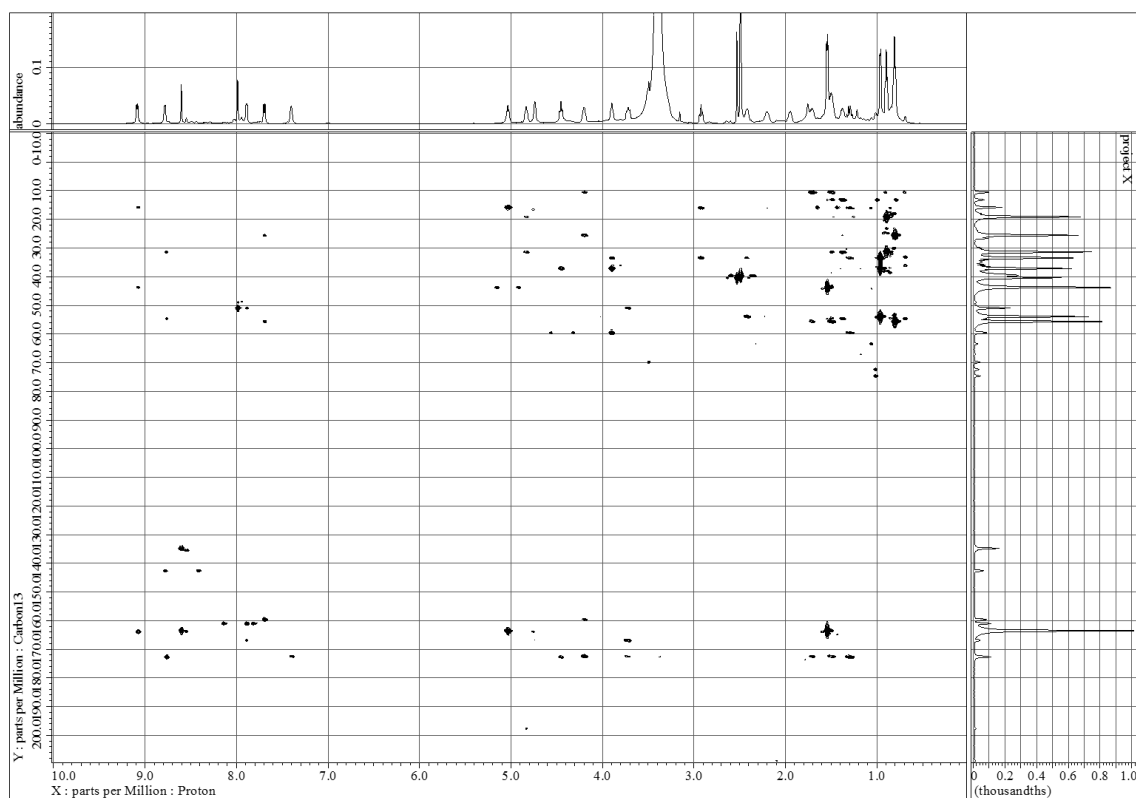


Figure S3-7. HMBC spectrum of nazumazole D (**3-1**) in DMSO- d_6 (600 MHz).

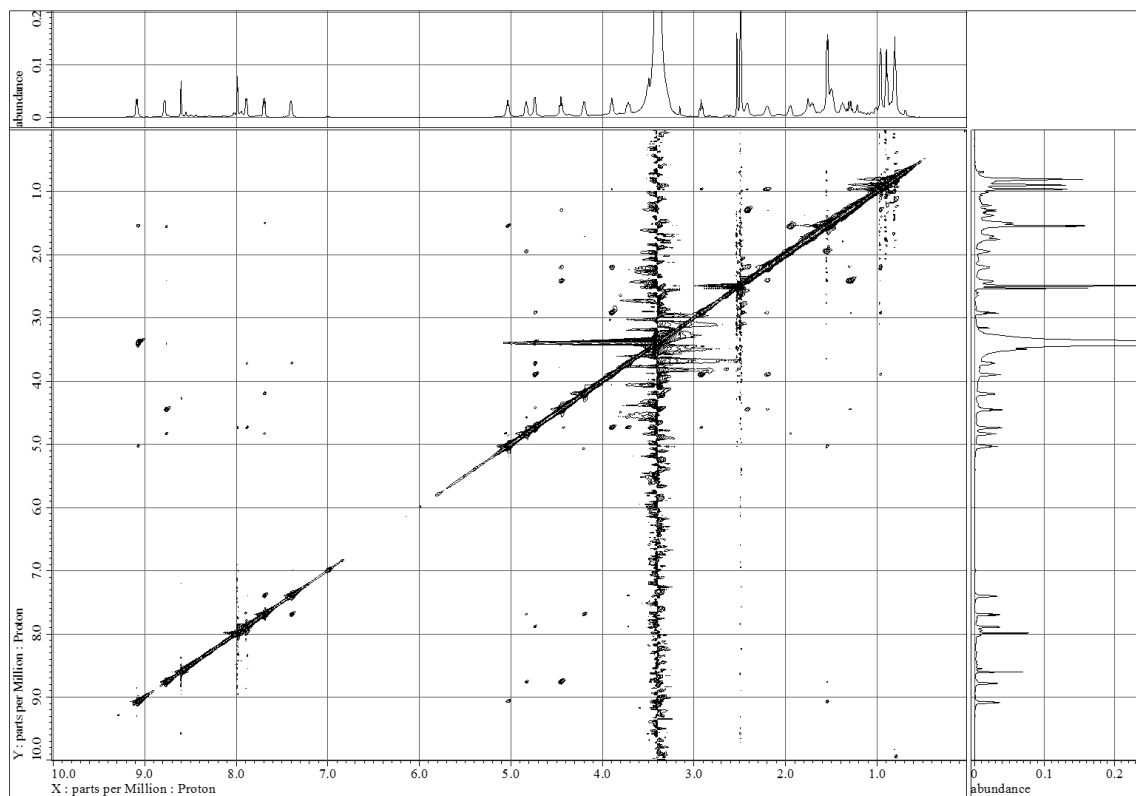


Figure S3-8. NOESY spectrum of nazumazole D (**3-1**) in DMSO- d_6 (600 MHz).

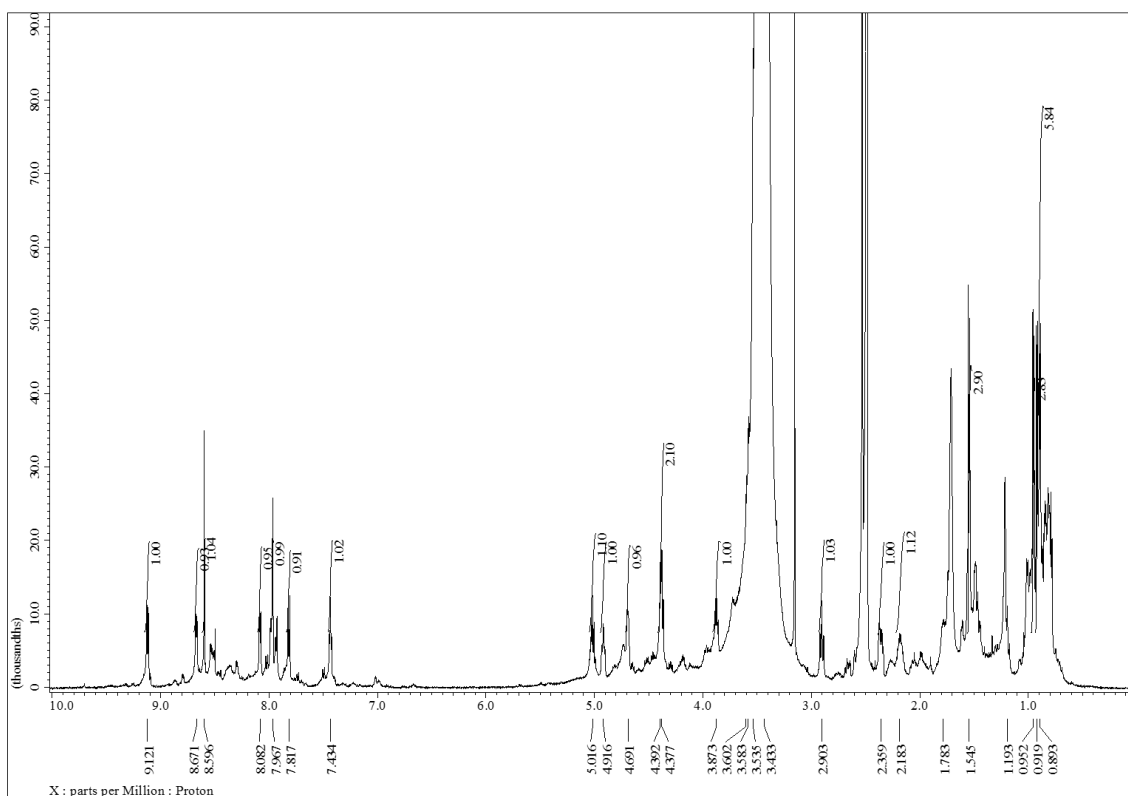


Figure S3-9. ^1H NMR spectrum of nazumazole E (3-2) in $\text{DMSO-}d_6$ (600 MHz).

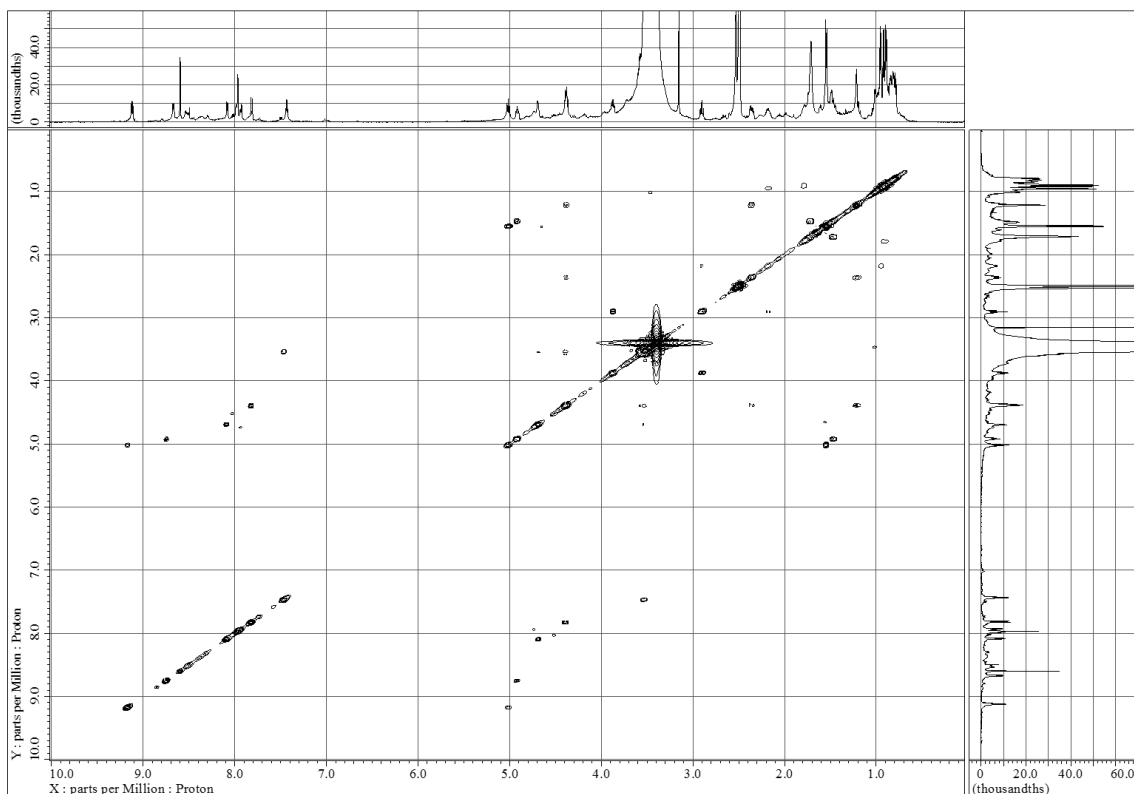


Figure S3-10. COSY spectrum of nazumazole E (3-2) in $\text{DMSO-}d_6$ (600 MHz).

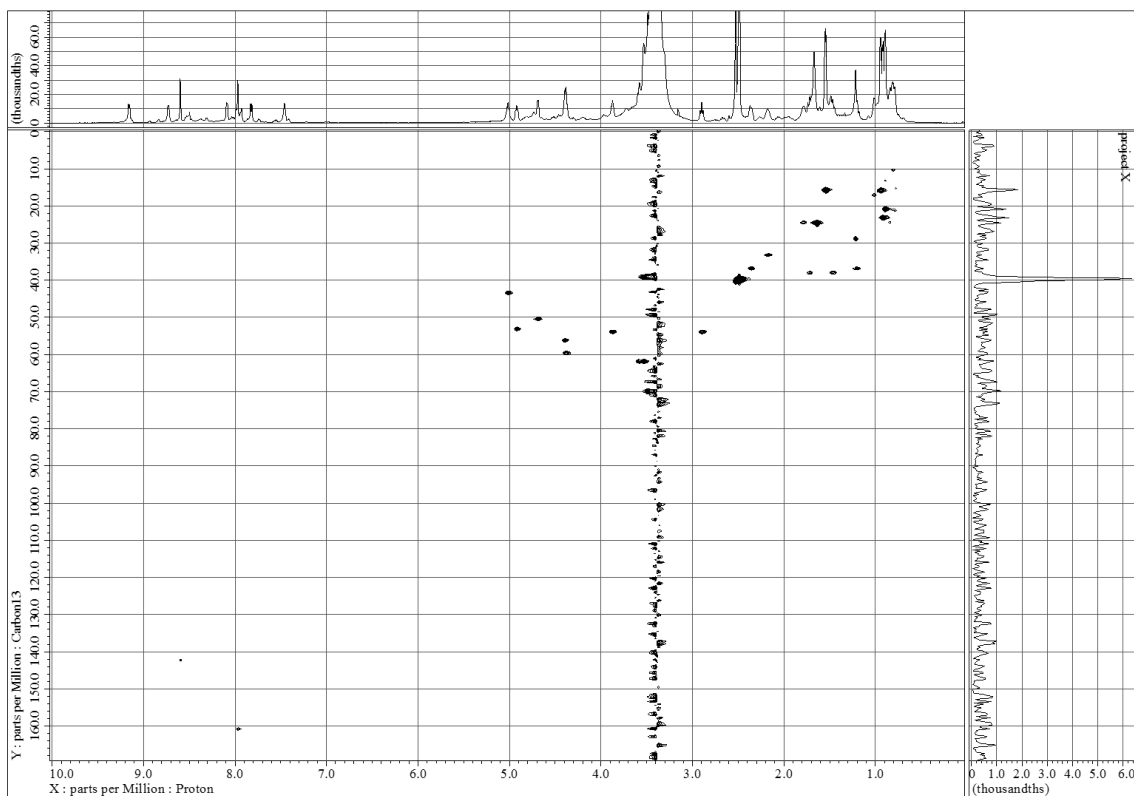


Figure S3-11. HSQC spectrum of nazumazole E (**3-2**) in DMSO- d_6 (600 MHz).

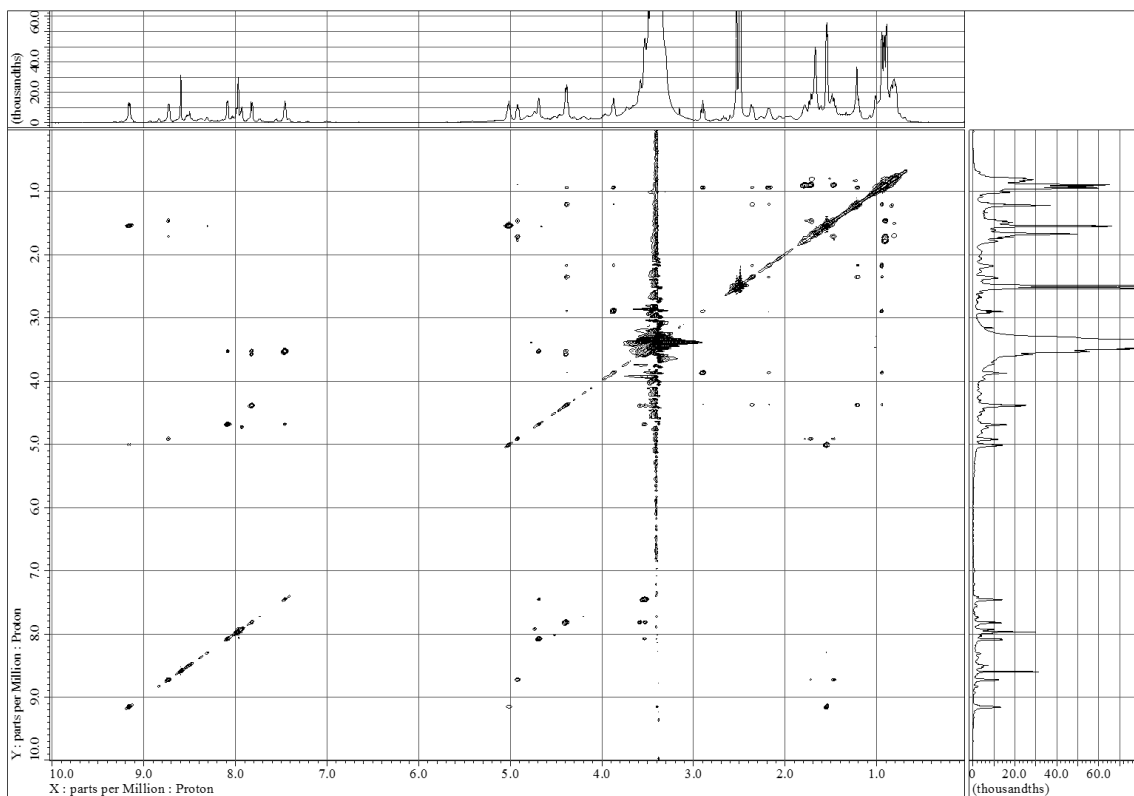


Figure S3-12. TOCSY spectrum of nazumazole E (**3-2**) in DMSO- d_6 (600 MHz).

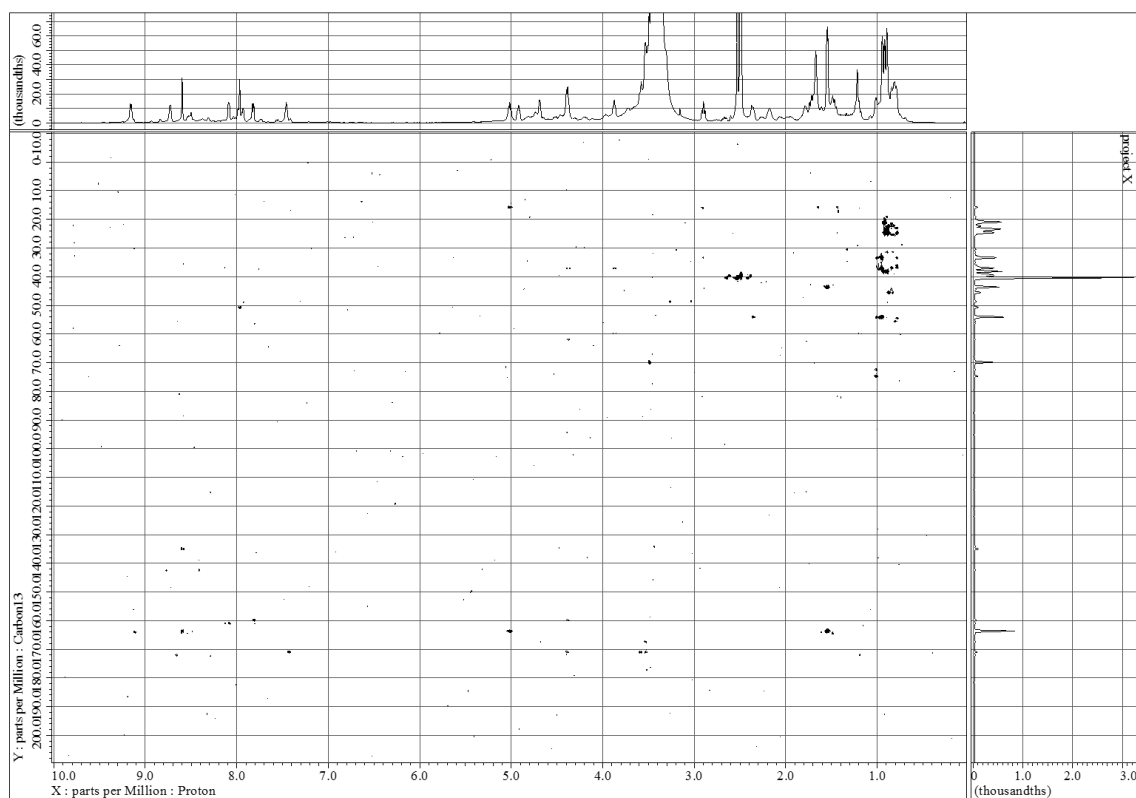


Figure S3-13. HMBC spectrum of nazumazole E (**3-2**) in DMSO- d_6 (600 MHz).

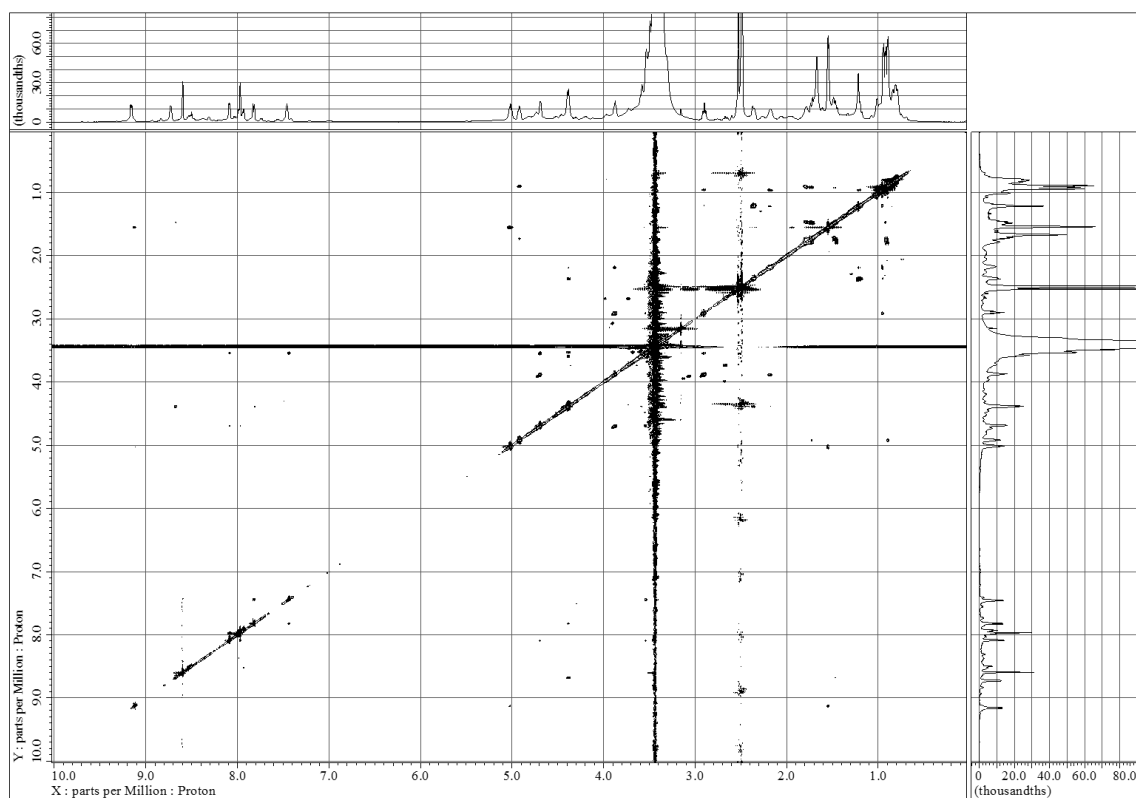


Figure S3-14. ROESY spectrum of nazumazole E (**3-2**) in DMSO- d_6 (600 MHz).

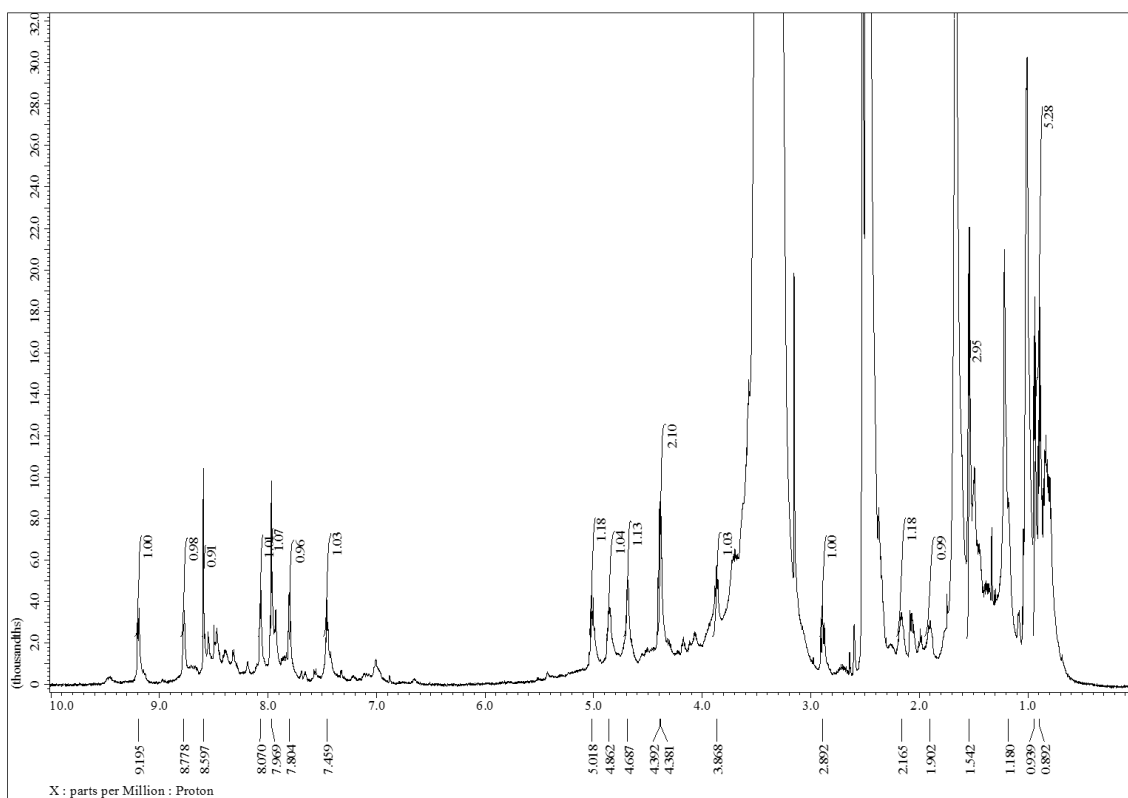


Figure S3-15. ¹H NMR spectrum of nazumazole F (3-3) in DMSO-d₆ (600 MHz).

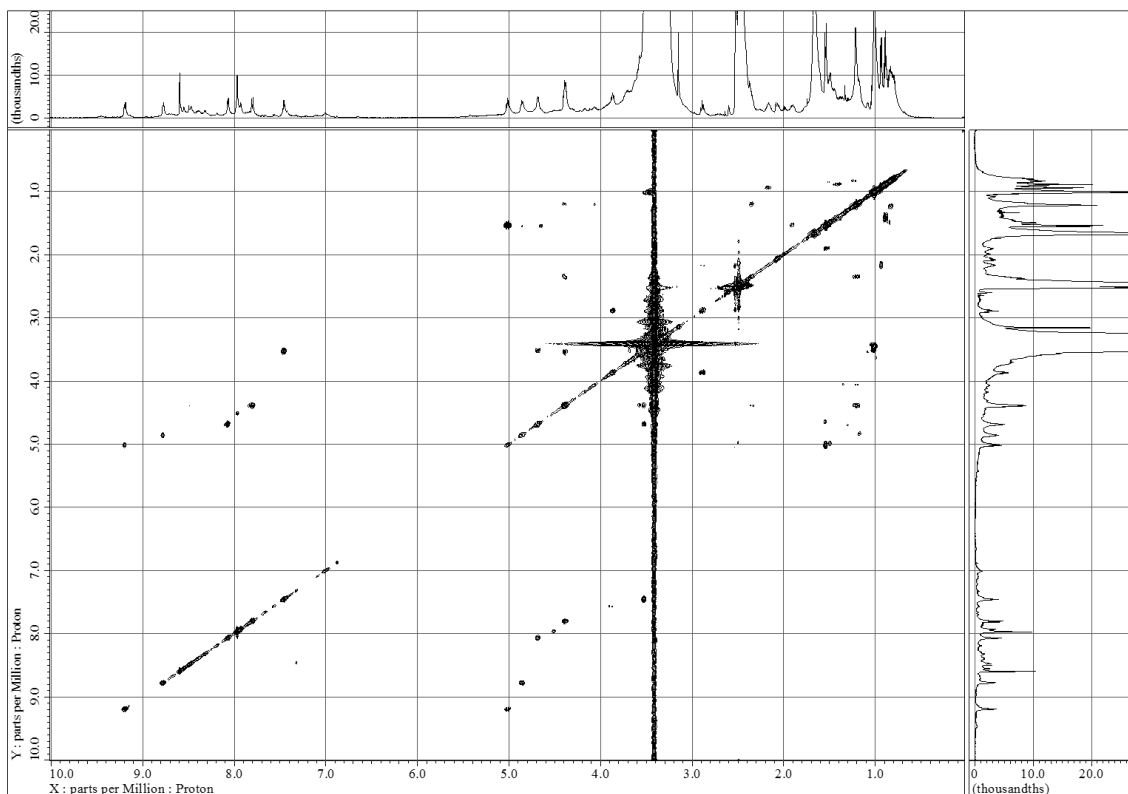


Figure S3-16. COSY spectrum of nazumazole F (3-3) in DMSO-d₆ (600 MHz).

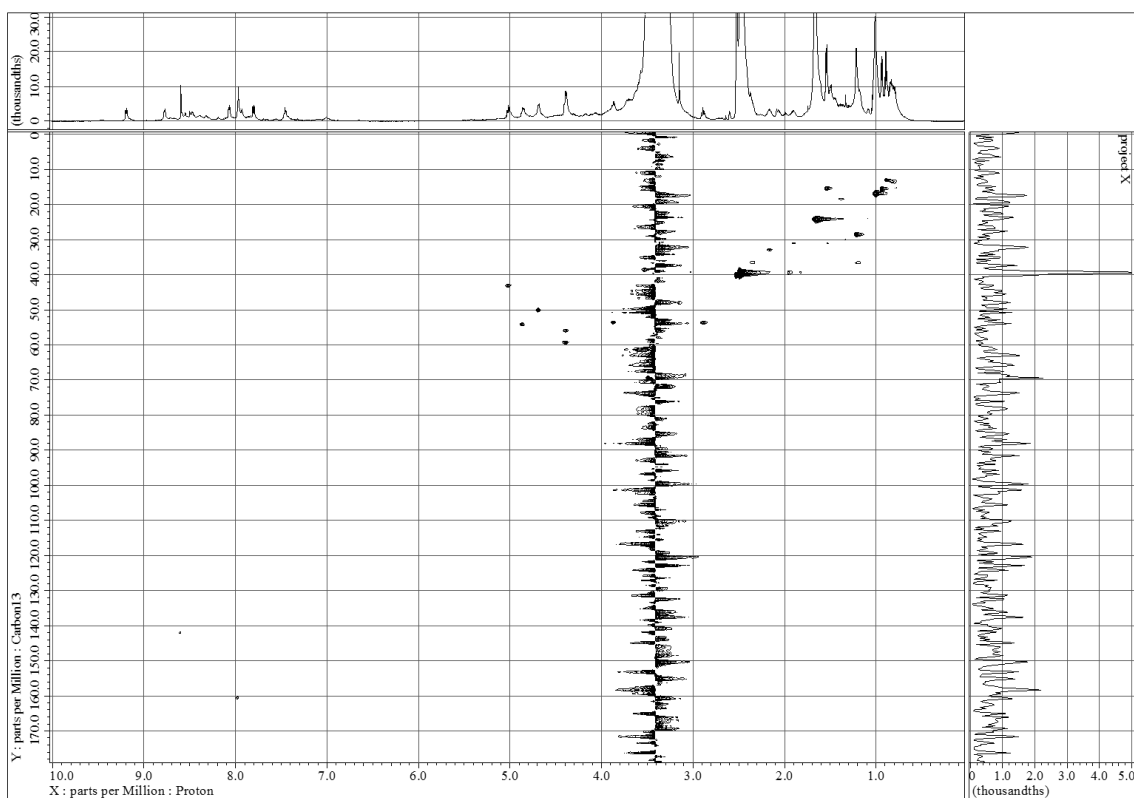


Figure S3-17. HSQC spectrum of nazumazole F (**3-3**) in DMSO-*d*₆ (600 MHz).

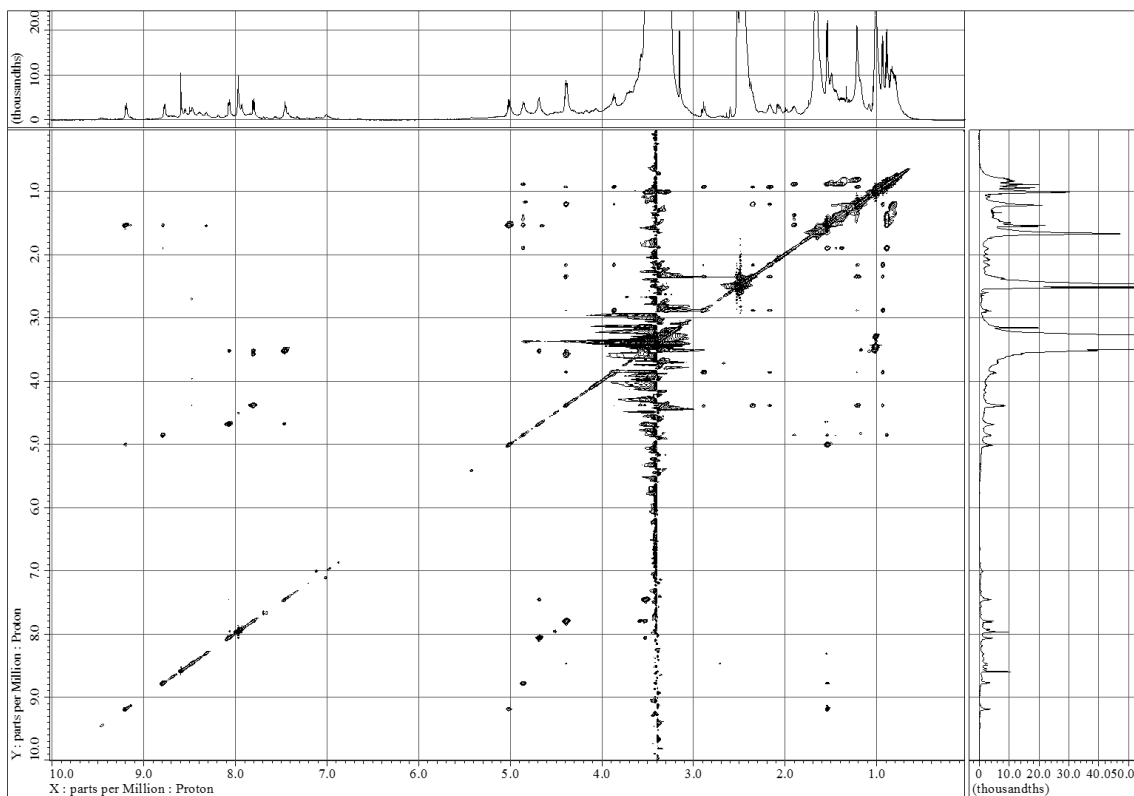


Figure S3-18. TOCSY spectrum of nazumazole F (**3-3**) in DMSO-*d*₆ (600 MHz).

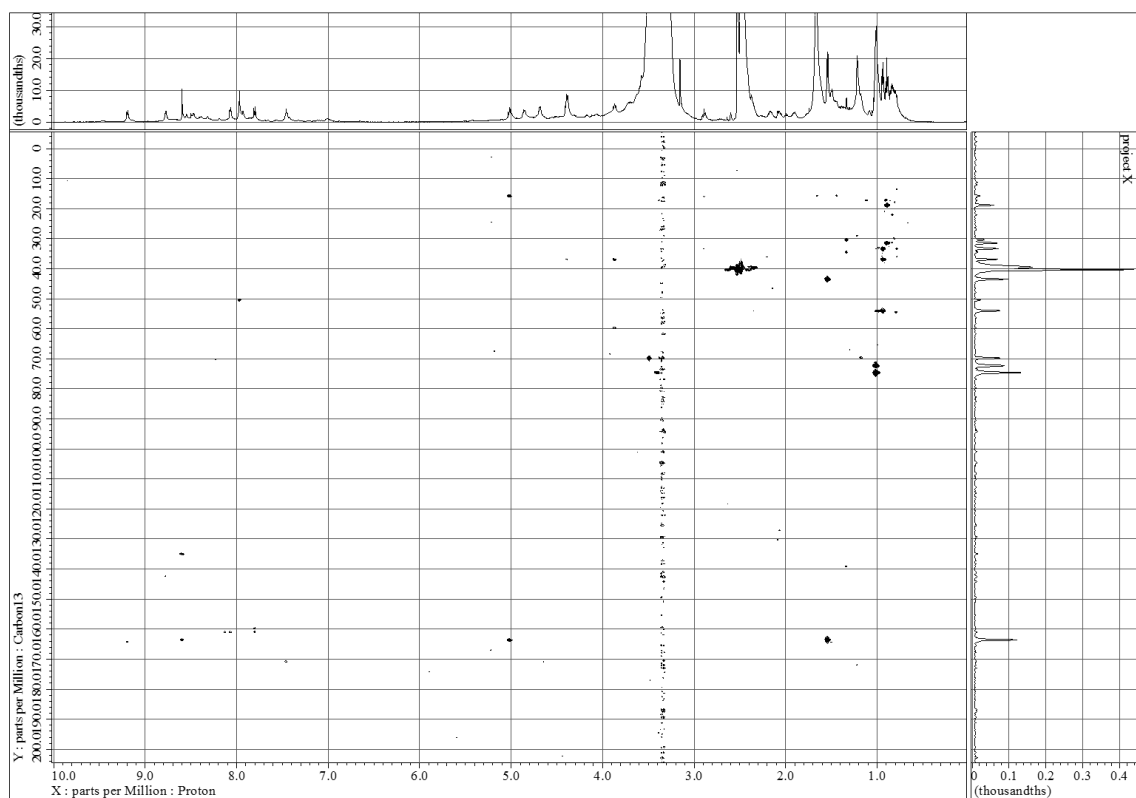


Figure S3-19. HMBC spectrum of nazumazole F (**3-3**) in DMSO- d_6 (600 MHz).

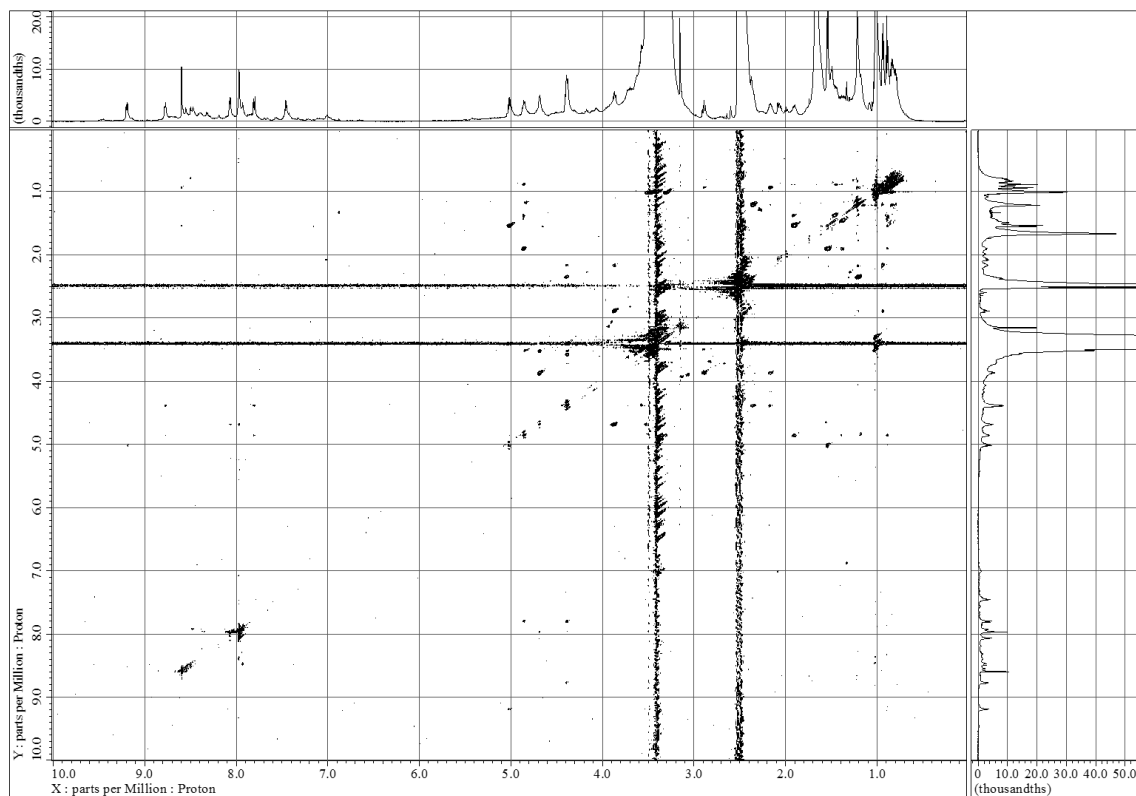


Figure S3-20. ROESY spectrum of nazumazole F (**3-3**) in DMSO- d_6 (600 MHz).

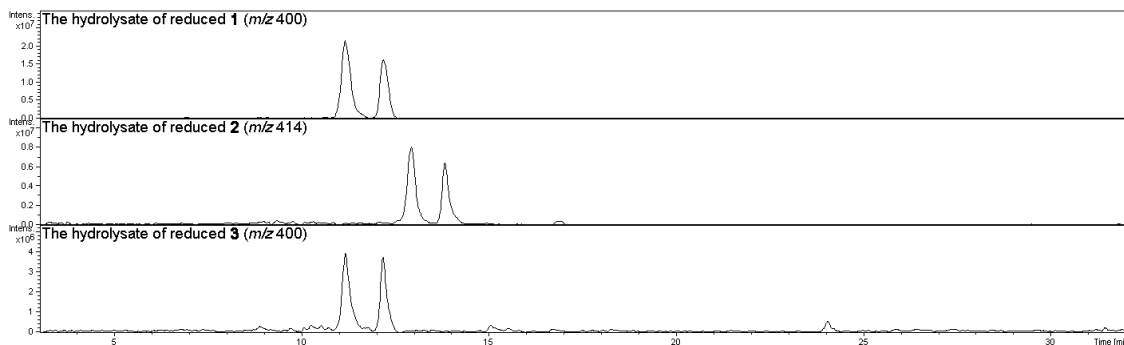


Figure S3-21. LC-MS charts of the DAA-derivatives of reduced Knv (m/z 400) and Kle (m/z 414).

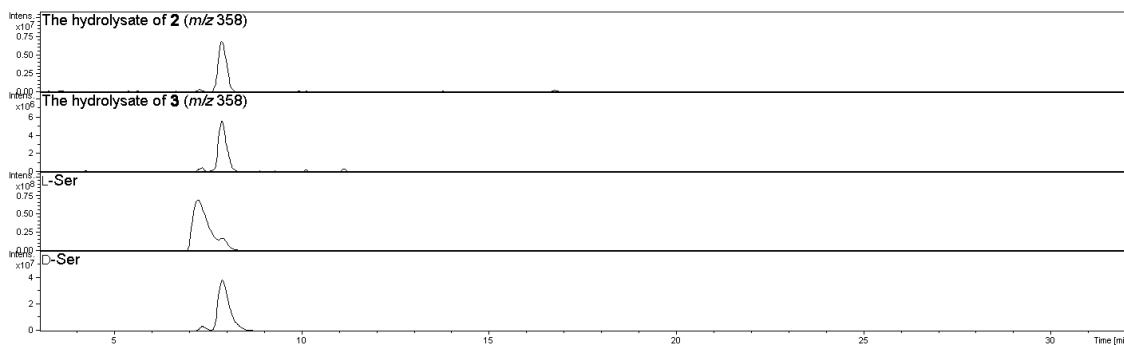


Figure S3-22. LC-MS charts of Marfey's analyses of nazumazoles D-F (3-1-3-3) (Ser).

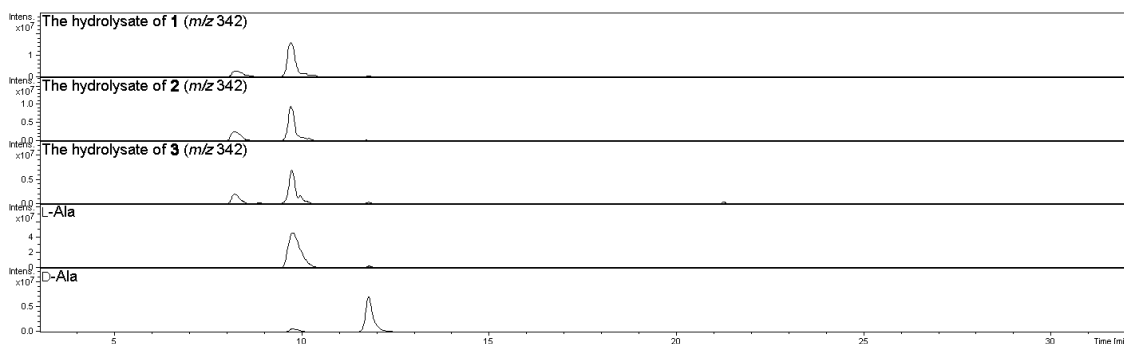


Figure S3-23. LC-MS charts of Marfey's analyses of nazumazoles D-F (3-1-3-3) (Ala).

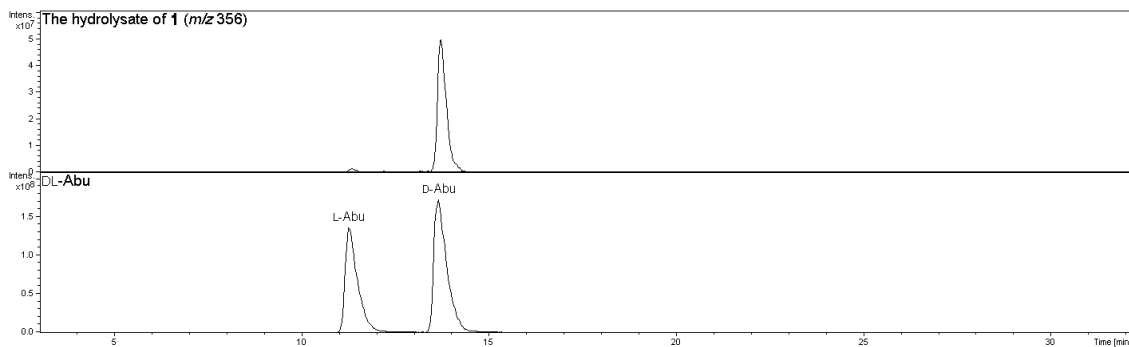


Figure S3-24. LC-MS charts of Marfey's analyses of nazumazoles D–F (3-1–3-3) (Abu).

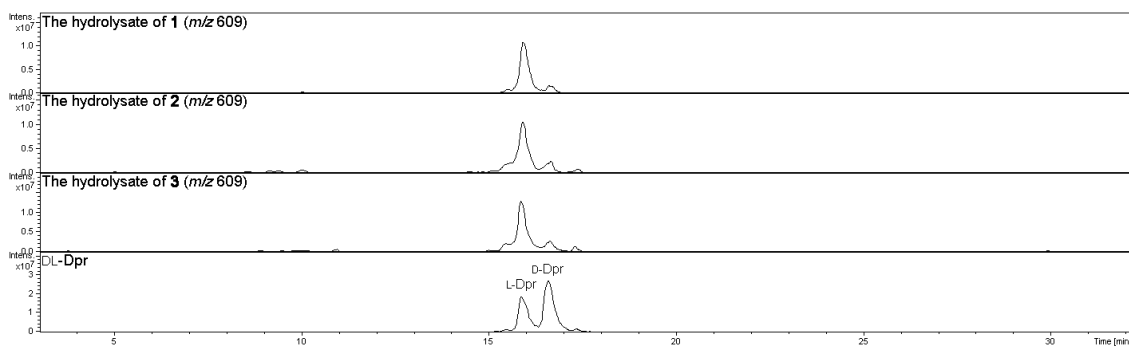


Figure S3-25. LC-MS charts of Marfey's analyses of nazumazoles D–F (3-1–3-3) (Dpr).

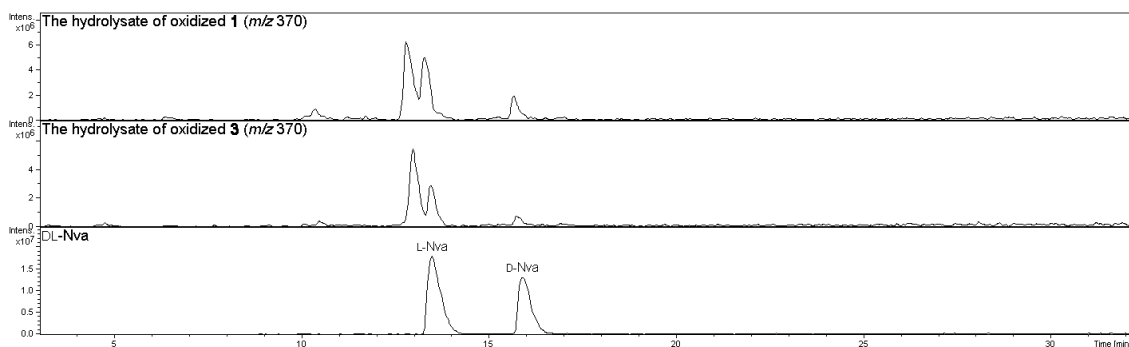


Figure S3-26. LC-MS charts of Marfey's analyses of nazumazoles D–F (3-1–3-3) (Nva).

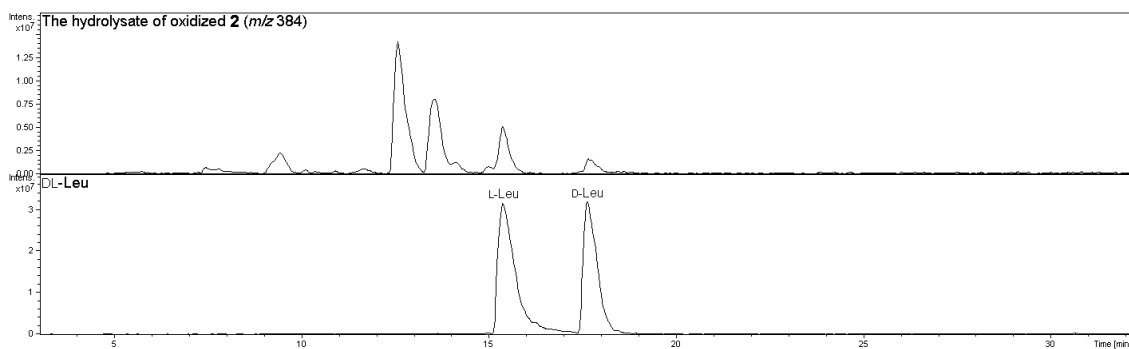


Figure S3-27. LC-MS charts of Marfey's analyses of nazumazoles D-F (1-3) (Leu).

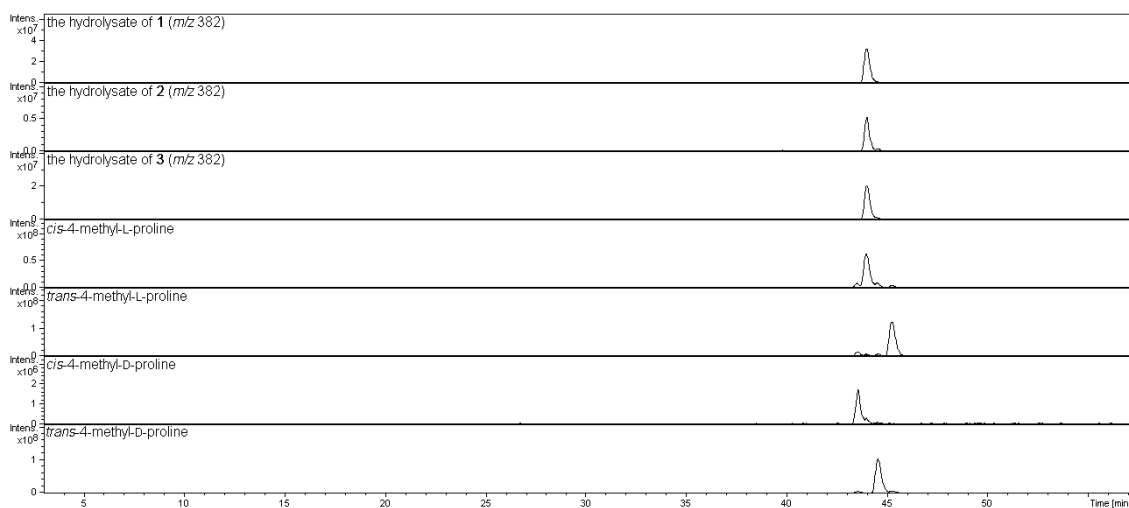


Figure S3-28. LC-MS charts of Marfey's analyses of nazumazoles D-F (3-1-3-3) (Mpr).

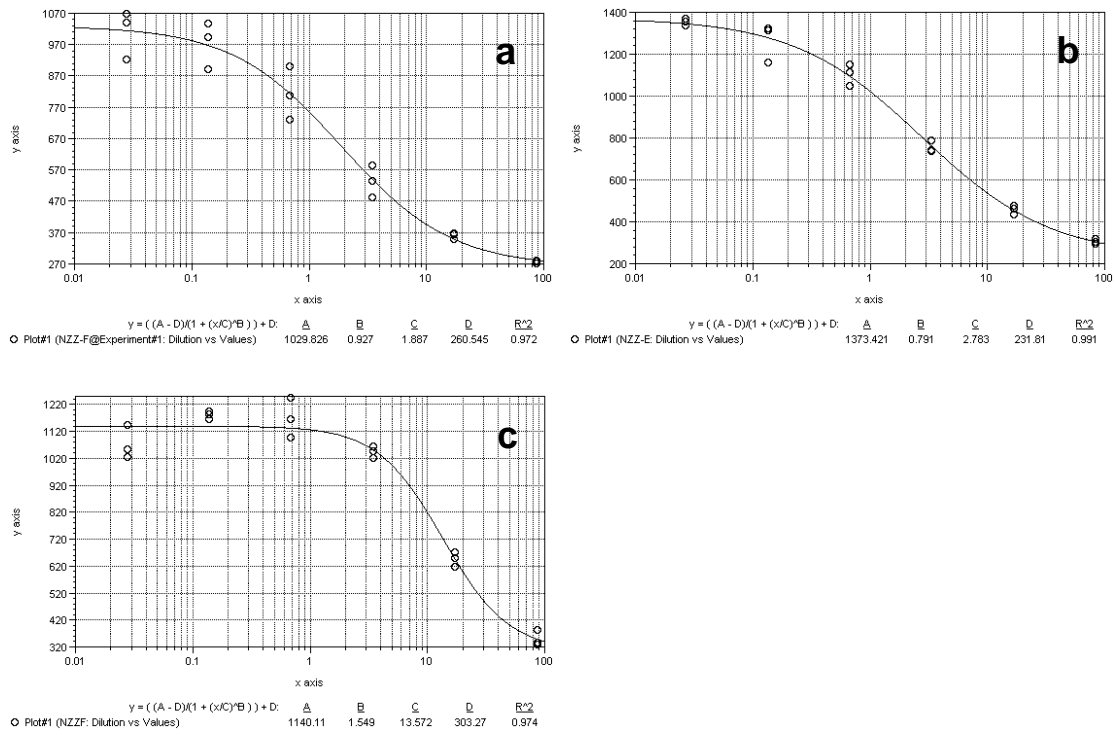


Figure S3-29. The graphs of chymotrypsin inhibitory assay of nazumazoles D (a), E (b) and F (c).

Chapter 4.

Theonellamide H, a cytotoxic peptide with colony dependent distribution from the marine sponge *Theonella swinhoei*

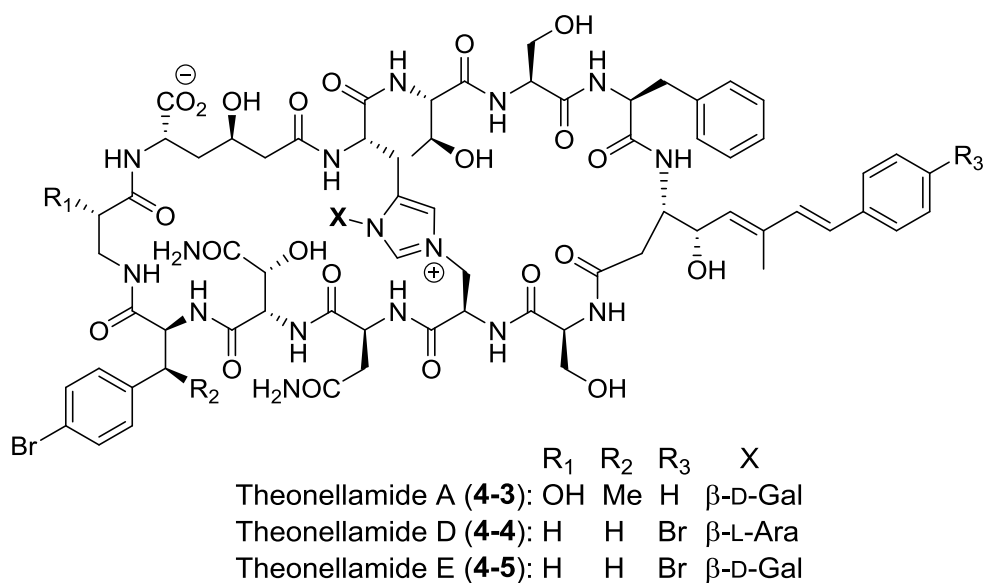
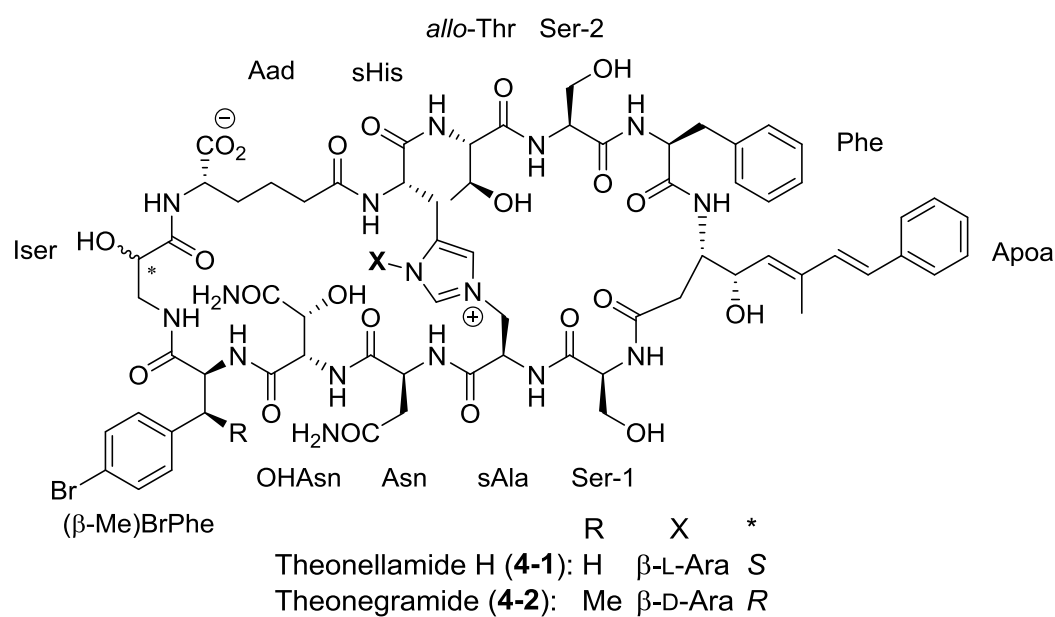
4.1. Introduction

In several reports describing the origins of natural products from marine invertebrates, differences of chemical contents among individual contents were reported, e. g., patellamides⁵⁷ in the ascidian *Lissoclinum patella*⁵⁸ and dysiherbaine⁵⁹ in the sponge *Lendenfeldia chondrodes*.⁶⁰ The presence of these compounds was attributed to the presence of the biosynthetic genes of these compounds in the producing cyanobacteria. Considering these reports, we hypothesized that the metabolic profiles of marine invertebrates are different from colony to colony owing to the diversity of bacterial composition. In most previous research on the isolation of secondary metabolites, conspecifics collected at the same region were extracted together and no attention was paid to their individual differences. To utilize bacterial resources in marine invertebrates more efficiently, we compared metabolic profiles by individual sponge colonies and searched for the compound which was contained in only selected colonies.

4.2. Result and Discussion

We collected colonies of the marine sponge *Theonella swinhoei* with yellow interior (*T. swinhoei* Y) at Hachijo Island, Tokyo, Japan. We selected 15 colonies (YT-1–YT-15) and extracted them separately. First, we examined the homogeneity of chemical profile within one specimen. To test this, we obtained two pieces (YT-11-1 and YT-11-2) from different parts of a large colony (YT-11), extracted them with MeOH, and analyzed their chemical profiles by LC-MS. The compositions of secondary metabolites were compared by analyzing the total ion chromatograms. YT-11-1 and YT-11-2 exhibited an identical chemical profile (Figure S4-3). Then, a 10–20 g piece was taken from each colony, extracted, and the extract was analyzed by LC-MS (Figure S4-1–S4-4). The contents of the major compounds, such as onnamide A (and its analogues)²², aurantoside A and B²⁶, and nazumamide A⁶¹, were conserved among all colonies. However, we found that the quantity of several metabolites was variable among colonies. Notably, 7 out of 15 colonies contained the compound with molecular ions at m/z 1703 and 1705. Therefore, we intended to isolate this compound, and conduct structure determination and evaluation of biological activity.

The colony (YT-11) which contained the compound was extracted with EtOH and partitioned between H₂O and CHCl₃. The BuOH extract of the aqueous layer was sequentially subjected to ODS column chromatography and two rounds of RP-HPLC to obtain theonellamide H (**4-1**, 1.2 mg).⁶²



The molecular formula of **4-1** was determined by HRESIMS as $C_{74}H_{95}BrN_{16}O_{26}$, which was smaller than that of theonegramide (**4-2**)⁶³ by one methylene unit. Theonegramide has been isolated from *T. swinhoei* collected at the Philippines, and this compound is a congener of theonellamide D.^{64a} The peptide nature of **4-1** was indicated by the NH signals between δ_H 7.43 and 8.67 in the ¹H NMR spectrum. In addition, an anomeric carbon signal (δ_C 88.2, δ_H 4.98) was observed in the HSQC spectrum of **4-1**, suggesting the presence of a sugar portion. Interpretation of the COSY, HSQC, TOCSY, HMBC, and NOESY spectra in DMSO-*d*₆/H₂O (4:1) at 50 °C revealed the presence of one residue each of 3-amino-4-hydroxy- 6-methyl-8-phenyl- 5,7-octadienoic acid (Apoa), Phe, Ser (Ser-2), Thr, histidinoalanine, α -aminoadipic acid (Aad), isoserine (Iser), *p*-bromophenylalanine (BrPhe), β -hydroxyasparagine (OHAsn), and Asn in **4-1**. In order to observe signals buried under the huge water signal, NMR spectra were also measured at 30 °C. By this experiment, the signals of one additive Ser residue (Ser-1) appeared (see Table 4-1).

Table 4-1. ^1H and ^{13}C NMR data (600 MHz) of theonellamide H (4-1) in $\text{DMSO-}d_6/\text{H}_2\text{O}$ (4:1).

amino acid	position	δ_{C} , ^{a, b, c} type	δ_{H} , ^a (J in Hz)	amino acid	position	δ_{C} , ^{a, b, c} type	δ_{H} , ^a (J in Hz)
Ser-1 ^d	α	56.4, CH	3.72, m	Arabinose	1	88.2, CH	4.98, d (8.8)
	β	60.8, CH ₂	3.63, m		2	69.1, CH	3.67, m
	NH		7.92, m		3	72.6, CH	3.43, m
Apoa	α	36.9, CH ₂	2.38, m	4,5 ^e	unassigned	unassigned	
			2.11, dd (12.6, 3.3)	Aad	α	54.2, CH	3.93, m
	β	52.4, CH	4.10, m		β	31.7, CH ₂	1.77, m
	γ	67.9, CH	4.25, dd (8.8, 3.9)			1.53, m	
	δ	132.4, CH	5.20, d (8.8)	γ	21.9, CH ₂	1.40, m	
	ϵ	135.7, C		δ	35.4, CH ₂	2.23, m	
	ϵ -Me	12.8, CH ₃	1.66, s			1.98, m	
	ζ	133.3, CH	6.63, d (16.5)		NH		7.63, m
	η	127.7, CH	6.50, d (16.5)	Iser	α	69.7, CH	4.11, m
	1	137.6, C			β	43.0, CH ₂	3.90, m
	2, 6	126.2, CH	7.40, d (7.7)			7.45, m	
	3, 5	128.9, CH	7.30, dd (7.7, 7.7)	BrPhe	α	55.0, CH	4.31, ddd (8.1, 8.1, 4.0)
	4	127.7, CH	7.19, m		β	36.6, CH ₂	3.03, m
Phe	NH		7.79, m				
	α	54.2, CH	4.55, ddd (8.8, 8.0, 8.0)	1''''	137.6, C		
	β	38.6, CH ₂	2.82, dd (13.4, 8.0)		2''', 6'''	131.2, CH	7.04, d (8.3)
			2.65, m	3''', 5'''	131.2, CH	7.27, d (8.3)	
	1'	137.0, C		6'''	120.0, CH		
	2', 6'	129.2, CH	7.16, m		NH		8.67, m
	3', 5'	128.3, CH	7.22, m	OHAsn	α	54.2, CH	5.30, dd (8.3, 8.3)
	4'	126.8, CH	7.17, m		β	72.0, CH	4.03, d (7.2)
	NH		8.02, d (8.8)				6.77, brs
	Ser-2	α	56.2, CH	4.48, m		NH	
β		61.5, CH ₂	3.66, m	Asn	a	51.5, CH	4.47, m
		3.59, m	b		36.6, CH ₂	2.56, m	2.24, m
Thr	NH		8.66, m				unassigned
	α	58.0, CH	4.22, m	sAla	α	50.6, CH	5.05, m
	β	68.2, CH	3.56, m		β	49.8, CH ₂	4.89, d (13.7)
γ	21.0, CH ₃	0.90, d (6.1)				8.22, d (9.3)	
sHis	α	53.9, CH	4.82, m				
	β	26.0, CH ₂	3.23, m				
			2.99, m				
	2''	136.5, CH	8.90, s				
	4''	131.4, C					
	5''	123.6, CH	7.24, s				
	NH		8.35, m				

^a Recorded at 50 °C. ^b ^{13}C chemical shifts were obtained by HSQC and HMBC experiments.

^c ^{13}C chemical shifts of amide carbonyl carbons were not assigned.

^d ^1H and ^{13}C chemical shifts of Ser-1 residues were obtained from NMR spectra at 30 °C.

^e Overlapped by the signal of water.

The amino acid sequence of **4-1** was determined by NOESY spectrum measured at 30 °C and 50 °C (Figure 4-1). The NOESY correlations between the amide proton and the α -proton were observed between residues: Ser-1 (δ_{H} 7.92) and APOA (δ_{H} 2.37 and δ_{H} 2.09) at 30 °C; APOA (δ_{H} 7.90) and Phe (δ_{H} 4.54) at 30 °C; Phe (δ_{H} 8.02) and Ser-2 (δ_{H} 4.48) at 50 °C; Ser-2 (δ_{H} 8.76) and Thr (δ_{H} 4.23) at 30 °C; Thr (δ_{H} 7.43) and sHis (δ_{H} 4.82) at 50 °C; Iser (δ_{H} 7.52) and BrPhe (δ_{H} 4.27) at 30 °C; BrPhe (δ_{H} 8.72) and OHAsn (δ_{H} 5.29) at 30 °C; OHAsn (δ_{H} 8.44) and Asn (δ_{H} 4.45) at 30 °C; Asn (δ_{H} 7.78) and sAla (δ_{H} 5.05) at 50 °C; sAla (δ_{H} 8.27) and Ser-1 (δ_{H} 3.72) at 30 °C. In addition, NOESY correlations between the signal of amide NH proton of sHis residue (δ_{H} 8.46) and the signal of δ -protons of Aad residue (δ_{H} 2.23 and δ_{H} 1.99) at 30 °C were observed, which indicated the amide bond between δ -carbonyl carbon of Aad residue and sHis residue. No NOESY signal was observed from the signal of NH proton of Aad residue. However, taking the molecular formula and the number of unsaturation into account, compound **4-1** should construct macrocyclic structure. Therefore, Iser and Aad should form the last amide bond⁶⁵, and the amino acid sequence of **4-1** was determined as almost identical to that of **4-2**. β -Methyl-*p*-bromophenylalanine residue in **4-2** was substituted for BrPhe in **4-1**. HMBC cross-peaks between the anomeric proton signal (δ_{H} 4.98) and carbon signals in the imidazole ring (δ_{C} 131.4 and δ_{C} 136.5) indicated that

the sugar portion was attached at C-1 to the remaining nitrogen on the imidazole ring of histidinoalanine residue.

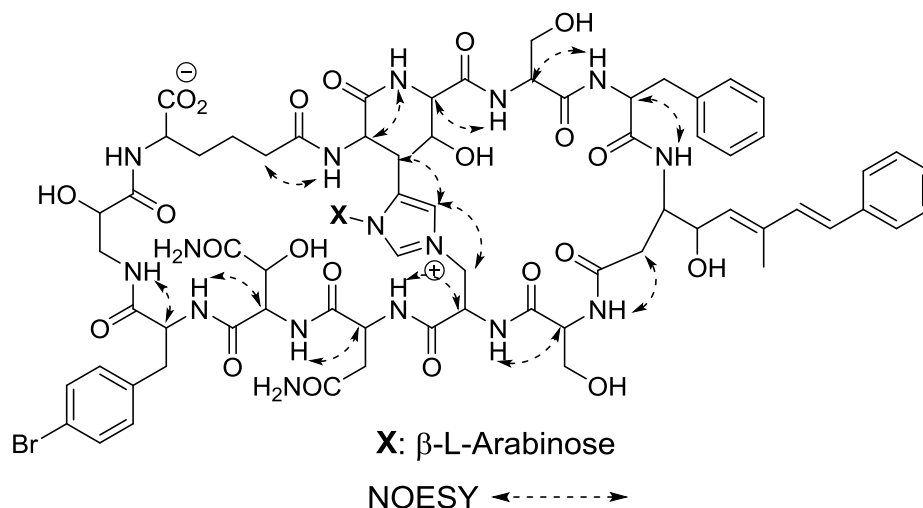


Figure 4-1. Key NOESY correlations in 4-1.

The (*5E*, *7E*) geometry of the Apoa moiety was elucidated from the ^{13}C NMR chemical shift of the ϵ -methyl signal at δ_c 12.8 and the proton coupling constant ($^3J_{\text{H}-\zeta/\text{H}-\eta} = 16.5$ Hz) associated with the *trans*-disubstituted olefin. The absolute configuration of each amino acid residue in 4-1 was determined by Marfey's method.⁵⁴ Phe, Ser, Thr, histidinoalanine, Aad, Iser, and BrPhe were liberated by standard acid hydrolysis. OHAsn and Asn were obtained as β -hydroxyasparatic acid (OHAsp) and Asp, respectively. With hydrogenation before acid hydrolysis, Apoa was obtained as 3-amino-4-hydroxy-6-methyl-8-phenyl-octanoic acid (H_4 -Apoa). Standards of histidinoalanine, BrPhe, OHAsp, and H_4 -Apoa were obtained from the hydrolysate of

the mixture of theonellamide A, D, and E (**4-3-4-5**).^{64a} Marfey's analysis with detection by ESI-MS revealed the presence of L-Phe, L-Ser, L-*allo*-Thr, L-histidino-D-alanine, L-Aad, L-Iser, L-BrPhe, (2*S*, 3*R*)-OHAsn, L-Asn, and (3*S*, 4*S*)-Apoa (Figure S4-17–S4-25).⁶⁶ Although the absolute configuration of Iser residue in **4-2** was assigned as *R*, L-Iser was detected by Mafey's analysis of **4-1**.

The ¹H NMR data suggested that the sugar portion was arabinose. To identify the sugar, acid hydrolysate of **4-1** was subjected to 3-phenylthiocarbamoylthiazoline-4(*R*)-carboxylate derivatization.^{67,68} The derivative was analyzed by LC-MS and its retention time was compared with those of authentic samples of both D- and L-arabinose (Figure S4-16). From this result, the sugar portion was established as L-arabinose.

Theonellamide H exhibited moderate cytotoxicity against HeLa cells with an IC₅₀ value of 1.9 μM (Figure S4-26). This cytotoxicity was almost same as that of theonellamides A–E against P388 murine leukemia cells.^{64a}

As described above, there are several morphologically distinct types in the marine sponge *T. swinhoei*, and they have different chemical profiles. Theonellamides^{20,64} and their analogues, theonegramide⁶³ and theopalauamide³⁷, had been isolated from *T. swinhoei* W. To the best of our knowledge, theonellamide H is the first analogue of theonellamides which was isolated from *T. swinhoei* Y.

4.3. Experimental Section

General Experimental Procedures.

Optical rotations were measured on a Jasco DIP-1000 polarimeter. UV spectra were measured on a Shimadzu BioSpec-1600 spectrophotometer. NMR spectra were measured on a JEOL alpha 600 NMR spectrometer and referenced to the solvent peak: δ_{H} 2.49 and δ_{C} 39.5 for DMSO- d_6 . ESI mass spectra were recorded on a JEOL JMS-T100LC mass spectrometer. LC-MS experiments were performed on a Shimadzu LC-20AD solvent delivery system and interfaced to a Bruker amaZon SL mass spectrometer. The result of XTT assay was recorded with a Molecular Devices SPECTRA max M2.

Comparing the Chemical Profiles in *T. swinhoei* Y by Colonies.

The marine sponges *T. swinhoei* with yellow interior (*T. swinhoei* Y) were collected at Hachijo Island and kept frozen at -20 °C until processed. The small amounts (10–20 g) taken from 15 sponge colonies (YT-1–YT-15) were extracted with MeOH and the extracts were dried in vacuo. The extracts were separately applied to a column of ODS (ϕ 5 mm \times 10 mm) and eluted with MeOH. The MeOH eluates were analyzed by

LC-MS on COSMOSIL 2.5C₁₈-MS-II with gradient elution from H₂O to MeCN containing 0.5% acetic acid for 70 minutes.

Extraction and Isolation.

The sponge YT-11 (850 g, wet weight) was extracted with EtOH. The extract was partitioned between H₂O and CHCl₃. The water layer was extracted with BuOH. The BuOH layer was subjected to ODS column chromatography with a stepwise elution with MeCN-H₂O (1:4), MeCN-H₂O (3:7), MeCN-H₂O (2:3), and MeCN-H₂O (1:1). The fraction eluted with MeCN-H₂O (2:3) was subjected to ODS-HPLC on COSMOSIL 5C₁₈-MS-II. Gradient elution was performed using solvent A (50 mM KH₂PO₄ aqueous solution) and solvent B (*n*-PrOH); from A:B (4:1) to A:B (1:1). The fraction that contained the compound exhibiting ions at *m/z* 1703 and 1705 in ESIMS was further purified by ODS-HPLC on COSMOSIL 5C₁₈-AR-II with gradient elution from MeCN-H₂O (3:7) to MeCN-H₂O (1:1) containing 0.5% acetic acid to afford theonellamide H (1.2 mg).

To increase the amount of theonellamide H, we isolated the compound from the extract of *T. swinhoei* Y made in 1999. The marine sponge *T. swinhoei* Y was collected at Hachijo Island (22 kg, wet weight) was extracted with MeOH and *n*-PrOH-H₂O (3:1).

The MeOH extract was partitioned between H₂O and Et₂O. The organic layer was further partitioned between MeOH-H₂O (9:1) and *n*-hexane. The aqueous *n*-PrOH extract was partitioned between *n*-PrOH-H₂O-MeOH (3:2:1) and *n*-hexane. The H₂O and aqueous MeOH layers from the MeOH extract and the aqueous alcoholic layer of the *n*-PrOH-H₂O (3:1) extract were combined and subjected to ODS column chromatography by elution with H₂O, MeOH-H₂O (1:1), and CHCl₃-MeOH (1:1). The CHCl₃-MeOH (1:1) fraction was subjected to ODS column chromatography with a step-wise elution with H₂O, *n*-PrOH-H₂O (2:3), and *n*-PrOH-H₂O (3:1). The fraction eluted with H₂O was extracted with BuOH. The BuOH extract (24 g) was dissolved in CHCl₃-MeOH (1:1) and kept in freezer. 1 g portion of this material was subjected to ODS column chromatography with a stepwise elution with MeCN-H₂O (1:3), MeCN-H₂O (9:11), and MeCN-H₂O (3:2). The fraction eluted with MeCN-H₂O (9:11) was subjected to ODS-HPLC on COSMOSIL 5C₁₈-AR-II with gradient elution from MeCN-H₂O (3:7) to MeCN containing 0.5% acetic acid. The compound was further purified by RP-HPLC on COSMOSIL π -Nap with gradient elution from MeCN-H₂O (1:3) to MeCN-H₂O (1:1) containing 0.5% acetic acid to afford theonellamide H (2.2 mg).

Theonellamide H (4-1): pale yellow powder; $[\alpha]_D -19$ [*c* 0.05, *n*-PrOH-H₂O (2:1)]; UV [*n*-PrOH-H₂O (2:1)] λ_{\max} (log ϵ) 210.5 (4.62) 278.0 (4.20); ¹H and ¹³C NMR {DMSO-*d*₆/H₂O (4:1)}, Table 4-1 and Table S4-1; HRESIMS *m/z* 1725.5701 (calcd for C₇₄H₉₅⁷⁹BrN₁₆O₂₆, 1725.5685, Δ +1.7 mmu)

Marfey's Analysis of Theonellamide H (4-1).

Compound **4-1** (100 μ g) was dissolved in 6N HCl (200 μ L) and heated at 110 °C for 3 h. The mixture of theonellamides A, D, and E was hydrolyzed in the same manner. The solvent was evaporated with a stream of N₂ gas, and then redissolved in 0.6 M NaHCO₃ (100 μ L). To the solution was added 3% FDNP-L-Val in EtOH (80 μ L) and the mixture was kept at 55 °C for 1 h. After neutralization with 3 N HCl (20 μ L), the reaction mixture was analyzed by LC-MS on COSMOCORE 2.6PBr with gradient elution from MeCN-H₂O (1:9) to MeCN-H₂O (7:3) containing 0.5% acetic acid for 32 min. Standard amino acids were derivatized with FDNP-D/L-Val, and then analyzed by LC-MS in the same manner. Standard amino acids of L-BrPhe and (2*S*, 3*R*)- β -OHAsp were obtained from the hydrolysate of the mixture of theonellamides A, D, and E. Retention times of amino acids and LC-MS charts are shown in Table S4-2 and S4-3, and Figure S4-17–S4-23.

Determination of the Absolute Configuration of Histidinoalanine Residue.

The mixture of theonellamide A, D, and E (500 μg) was dissolved in 6 N HCl (250 μL) and subjected to acid hydrolysis for relatively long time (110 $^{\circ}\text{C}$, 16 h). A half portion of the hydrolysate was derivatized with FDNP-L-Val and then analyzed by LC-MS in the same manner as Marfey's analysis of **4-1**. In addition to L-histidino-D-alanine, L-histidino-L-alanine was detected. The ratio of LD-isomer and LL-isomer was 3:1. Another half portion of the hydrolysate was derivatized with FDNP-D-Val, which was used as the standards of enantiomers of D-histidino-L-alanine and D-histidino-D-alanine. Retention times and LC-MS charts are shown in Table S4-4 and Figure S4-24.

Determination of the Absolute Configuration of 3-Amino-4-Hydroxy-6-Methyl-8-phenyl-5,7-octadienoic acid (Apoa) Residue.

To a solution of compound **4-1** (100 μg) in MeCN-H₂O (1:1, 1 mL) was added 10% Pd/C (2 mg), and the mixture was stirred under the atmosphere of H₂ for 18 h. The mixture was filtered on Celite and the solvent was dried in vacuo to afford a diastereomeric mixture of tetrahydrotheonellamide H. The reduced peptide was subjected to acid hydrolysis, derivatization with FDNP-L-Val, and LC-MS analysis as

described above. The standard amino acid of a diastereomeric mixture of 3-amino-6-methyl-8-phenyl-octanoic acid (H₄-Apoa) was obtained from the hydrolysate of the reduced mixture of Theonellamide A, D, and E and derivatized with FDNP-D/L-Val, and then analyzed by LC-MS in the same manner (Table S4-5 and Figure S4-25).

Identification, and Determination of the Absolute Configuration of the Sugar portion in Theonellamide H (4-1).

Compound **4-1** (60 µg) was dissolved in 6 N HCl (200 µL) and heated at 110 °C for 3 h. The solvent was evaporated with a stream of N₂ gas, and then dissolved in 10% HCl in MeOH (200 µL). The reaction mixture was heated at 100 °C for 1h. After evaporation of the solvent, to the hydrolysate of **1** was added a solution of L-cysteine methyl ester hydrochloride in pyridine (2 mg/mL; 100 µL) and then heated at 60 °C for 1 h. Then, 5 µL of phenylisothiocyanate was added and the solution was heated for a further hour at 60 °C. The solvent was evaporated, and the product was dissolved in MeOH (100 µL). The reaction product was analyzed by LC-MS on COSMOSIL 2.5C₁₈-MS-II with gradient elution from MeCN-H₂O (1:9) to MeCN-H₂O (3:17) containing 0.5% acetic acid for 60 minutes. L- and D-Arabinose were treated in the same manner. The retention times are shown in Table S4-2. The LC-MS chart is shown in Figure S4-16.

XTT Assay against HeLa Cells.

HeLa human cervical cancer cells were cultured in Dulbecco's modified Eagle's medium (Wako Chemical) medium, supplemented with 100 U/mL of penicillin G (Wako Chemical), 100 mg/mL of streptomycin sulfate (Wako Chemical), and 10% fetal bovine serum (Gibco), at 37 °C under a 5% CO₂ atmosphere. To each well of a 96-well microplate containing 200 μL of tumor cell suspension (1×10^4 cells/mL) was added a sample after 24 h preincubation, and the plate was incubated for 72 h. After the addition of 50 μL of 3'-[1-(phenylaminocarbonyl)-3,4-tetrazolium]-bis(4-methoxy-6-nitro)benzenesulfonic acid hydrate (XTT) solution (1 mg/mL) containing 4% of phenazine methosulfate (PMS) solution (0.153 mg/mL) to each well, the plates were further incubated for 4 h. The absorbance at 450 nm was measured with a microplate reader.

2.4. Supporting Information

Table S4-1. ^1H and ^{13}C NMR data (600 MHz) of theonellamide H (4-1) in $\text{DMSO-}d_6/\text{H}_2\text{O}$ (4:1) at 30 °C.

amino acid	position	δ_{C} , ^{a, b, c} type	δ_{H} , ^a (J in Hz)	amino acid	position	δ_{C} , ^{a, b, c} type	δ_{H} , ^a (J in Hz)
Ser-1	α	56.4, CH	3.72, m	Arabinose	1	88.7, CH	4.97, d (7.7)
	β	60.8, CH ₂	3.63, m		2	69.4, CH	3.64, m
	NH		7.92, m		3	72.7, CH	3.39, m
Apoa	α	37.2, CH ₂	2.37, m		4,5 ^d	unassigned	unassigned
			2.09, m	Aad	α^{d}	unassigned	unassigned
	β	unassigned ^d	4.08, m		β	32.5, CH ₂	1.76, m
	γ	unassigned ^d	4.25, m				1.52, m
	δ	132.8, CH	5.17, d (8.3)		γ	22.6, CH ₂	1.39, m
	ϵ	unassigned ^e			δ	35.5, CH ₂	2.23, m
	ϵ -Me	13.5, CH ₃	1.65, s				1.99, m
	ζ	133.5, CH	6.63, (15.9)		NH		7.64, m
	η	128.2, CH	6.50, d (15.9)	Iser	α^{e}	unassigned	unassigned
	1	unassigned ^e			β	43.5, CH ₂	unassigned ^d
2, 6	126.5, CH	7.41, d (7.7)				2.93, m	
3, 5	128.9, CH	7.31, dd (7.7, 7.7)		NH		7.52, brd (6.6)	
4	127.9, CH	7.19, m	BrPhe	α	55.4, CH	4.27, m	
NH		7.90, m		β	36.8, CH ₂	3.02, m	
Phe	α	54.4, CH	4.54, m				2.64, m
	β	39.0, CH ₂	2.81, m		1'''	unassigned ^e	
			2.63, m		2''', 6'''	131.5, CH	7.05, d (8.3)
	1'	unassigned ^e			3''', 5'''	131.5, CH	7.27, d (8.3)
	2', 6'	129.5, CH	7.16, m		6'''	unassigned ^e	
	3', 5'	128.9, CH	7.23, m		NH		8.72, brs
	4'	127.2, CH	7.18, m	OHAsn	α	54.4, CH	5.29, m
	NH		8.06, d (8.8)		β^{d}	unassigned	unassigned
Ser-2	α	56.4, CH	4.49, m		NH ₂		7.23, m
	β	61.8, CH ₂	3.66, m				6.87, brs
			3.57, m		NH		8.44, m
Thr	NH		8.76, d (7.7)	Asn	α	51.8, CH	4.45, m
	α	unassigned ^d	4.23, m		β	36.8, CH ₂	2.54, m
	β	68.7, CH	3.54, m				2.20, m
sHis	γ	21.2, CH ₃	0.89, d (5.5)		NH ₂		unassigned
	α	54.1, CH	4.81, m		NH		7.83, m
	β	26.2, CH ₂	3.22, m	sAla	α	50.8, CH	5.04, m
			2.98, m		β	50.1, CH ₂	4.89, m
	2''	136.8, CH	8.91, s				4.16, m
	4''	unassigned ^e			NH		8.27, m
	5''	123.9, CH	7.23, s				
NH		8.46, d (9.3)					

^a Recorded at 50 °C. ^b ^{13}C chemical shifts were obtained by HSQC experiments.

^c ^{13}C chemical shifts of amide carbonyl carbons were not assigned.

^d Overlapped by the signal of water.

^e HMBC spectrum was not obtained at 30 °C, so these signals could not be assigned.

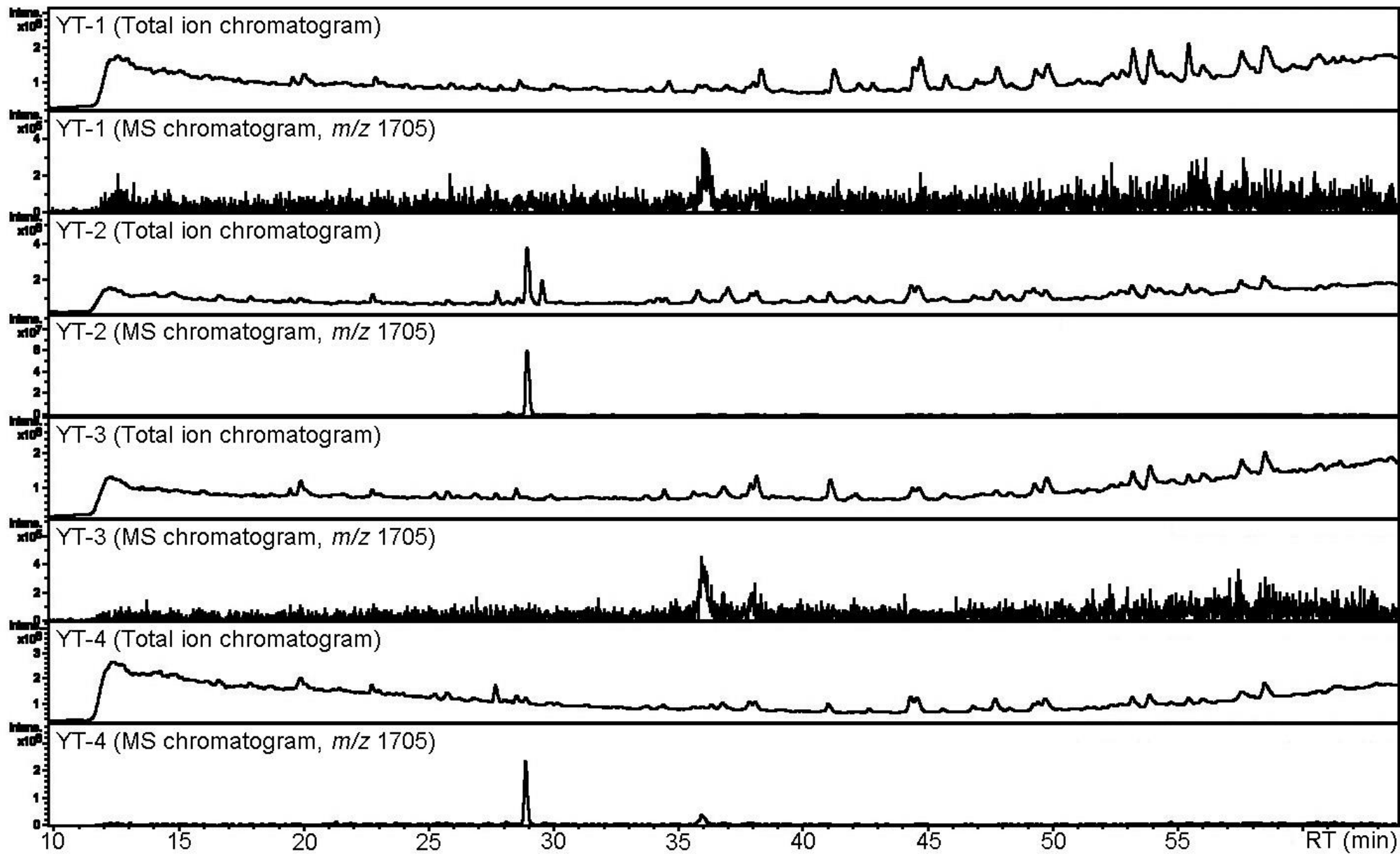


Figure S4-1. LC-MS charts of the extracts of YT-1–YT-4 (total ion chromatograms and MS chromatograms of the ion at m/z 1705).

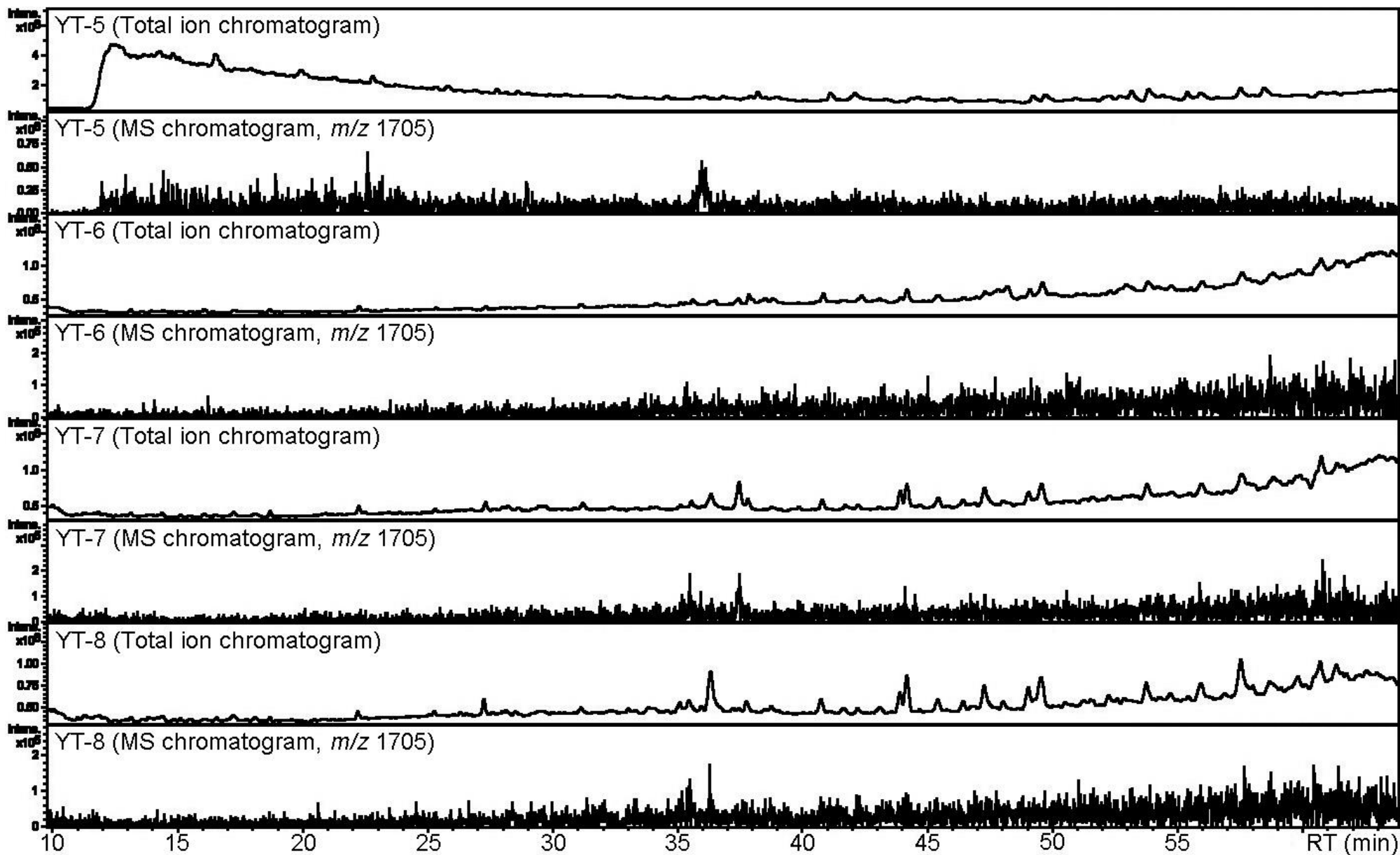


Figure S4-2. LC-MS charts of the extracts of YT-5–YT-8 (total ion chromatograms and MS chromatograms of the ion at m/z 1705).

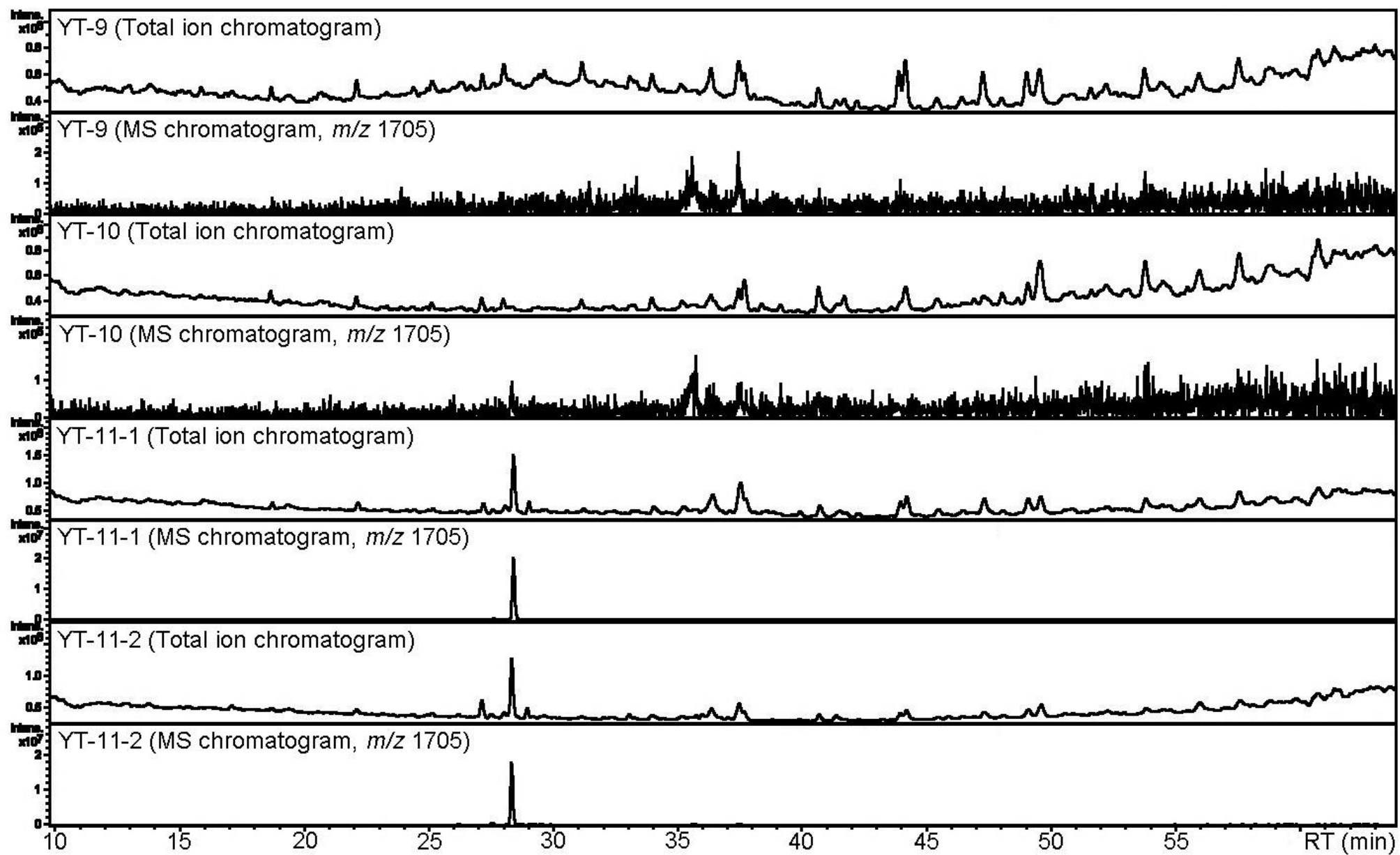


Figure S4-3. LC-MS charts of the extracts of YT-9–YT-11 (total ion chromatograms and MS chromatograms of the ion at m/z 1705).

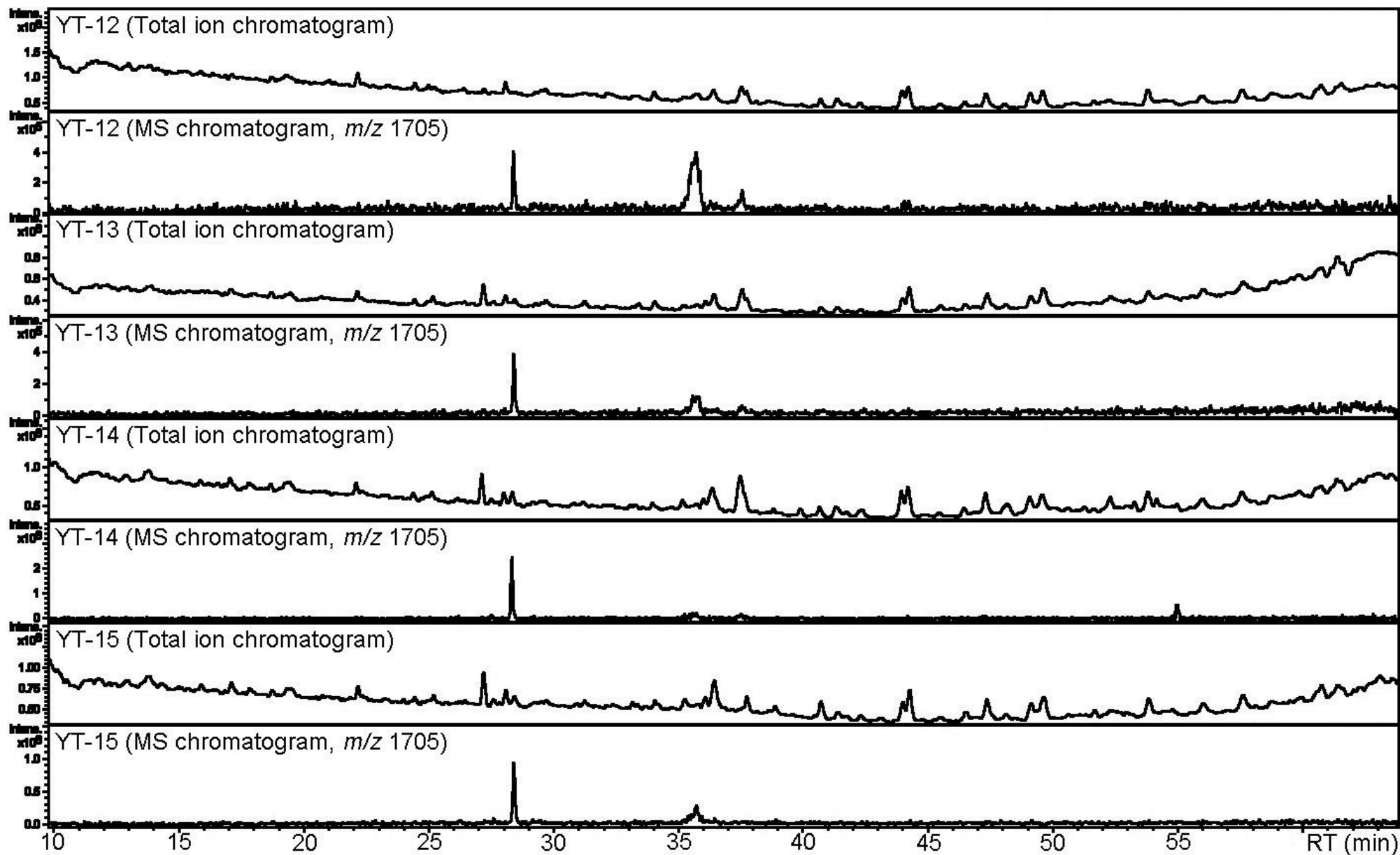


Figure S4-4. LC-MS charts of the extracts of YT-12–YT-15 (total ion chromatograms and MS chromatograms of the ion at m/z 1705).

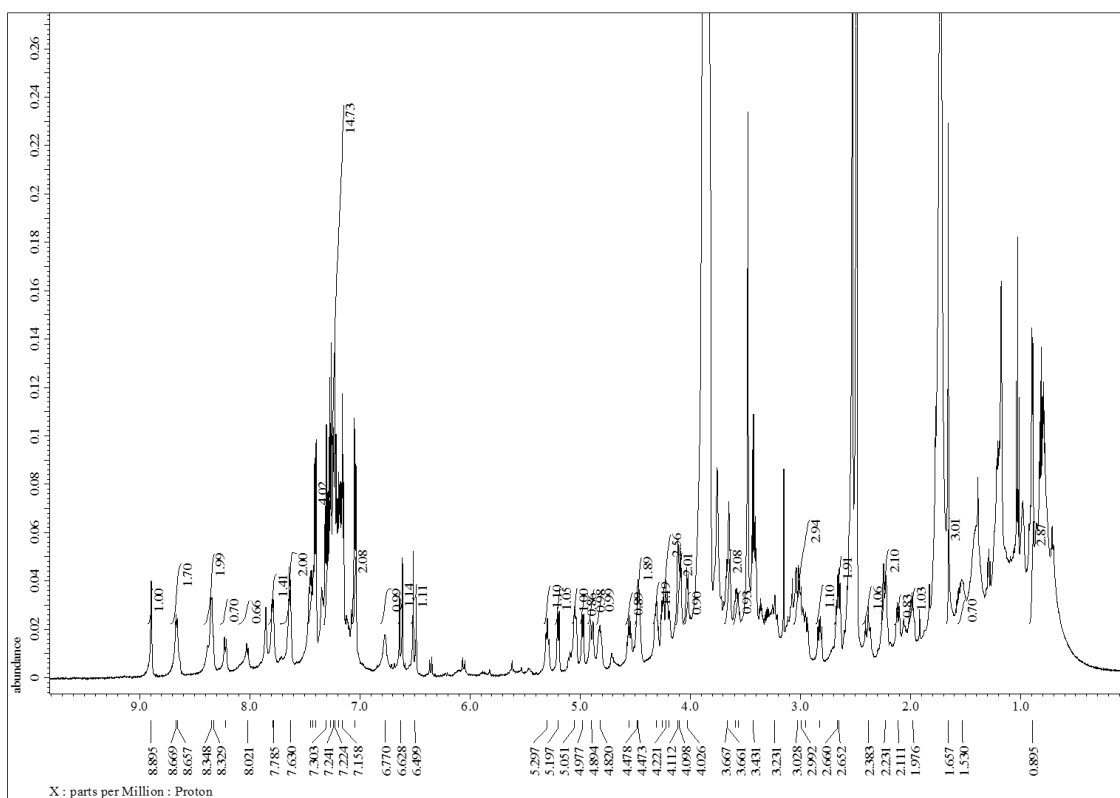


Figure S4-5. ^1H NMR spectrum of theonellamide H (4-1) in DMSO- d_6 /H $_2$ O (4:1) (600 MHz, 50 °C).

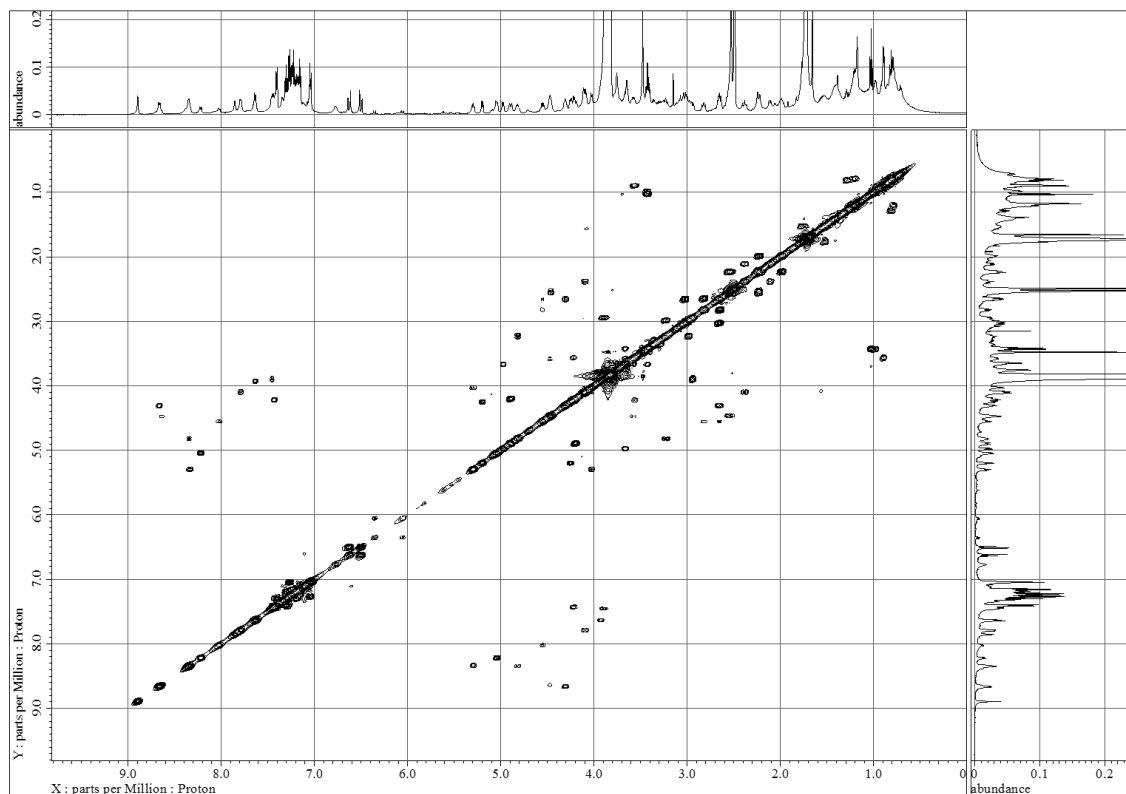


Figure S4-6. COSY spectrum of theonellamide H (4-1) in DMSO- d_6 /H $_2$ O (4:1) (600 MHz, 50 °C).

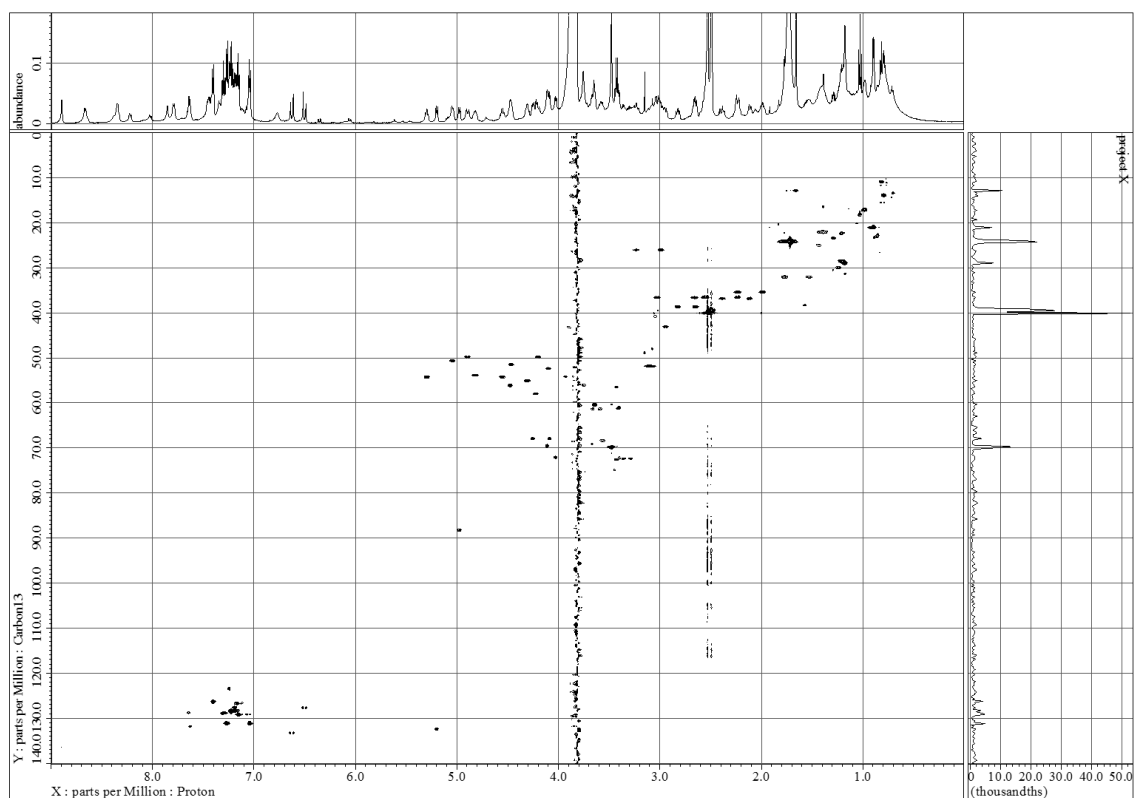


Figure S4-7. HSQC spectrum of theonellamide H (**4-1**) in DMSO- d_6 /H $_2$ O (4:1) (600 MHz, 50 °C).

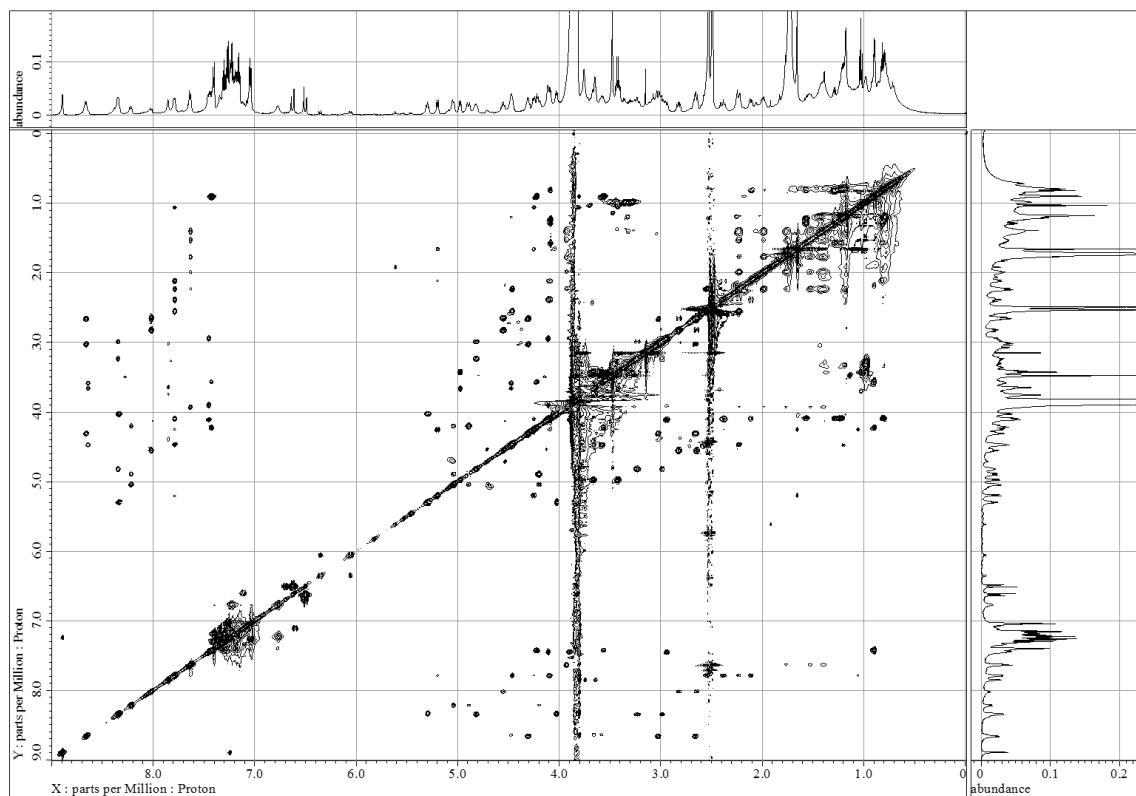


Figure S4-8. TOCSY spectrum of theonellamide H (**4-1**) in DMSO- d_6 /H $_2$ O (4:1) (600 MHz, 50 °C).

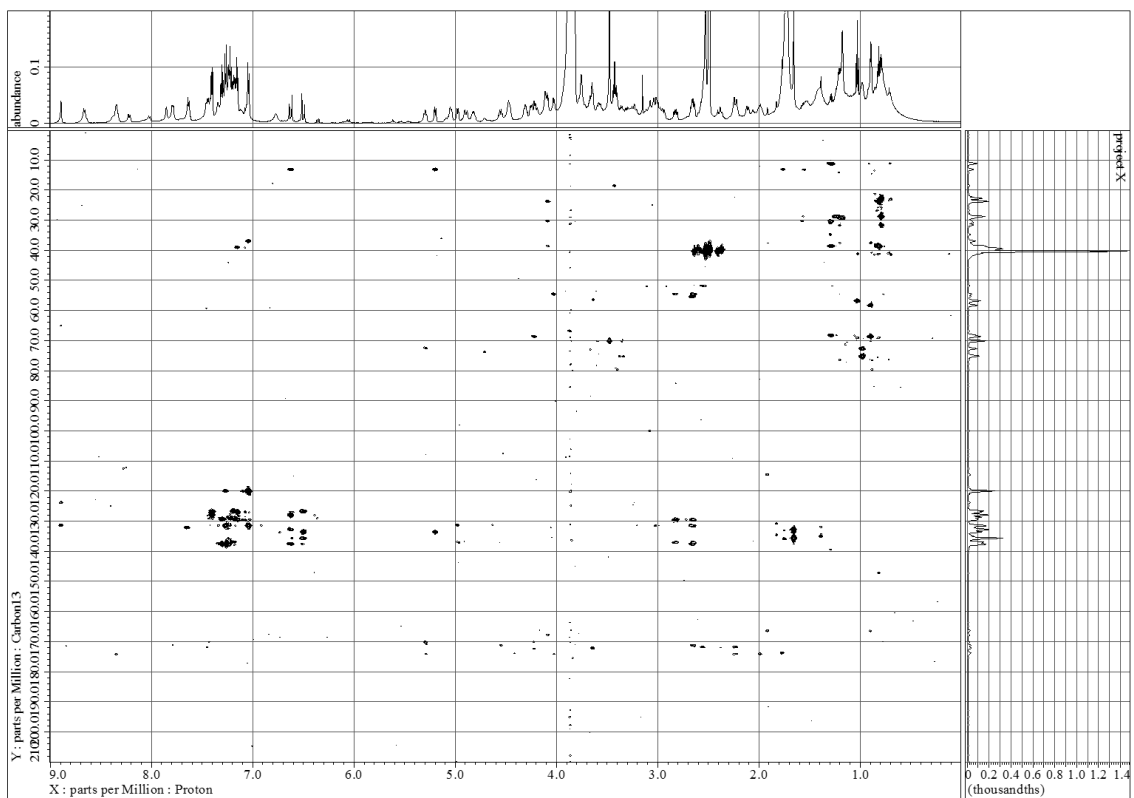


Figure S4-9. HMBC spectrum of theonellamide H (**4-1**) in DMSO- d_6 /H₂O (4:1) (600 MHz, 50 °C).

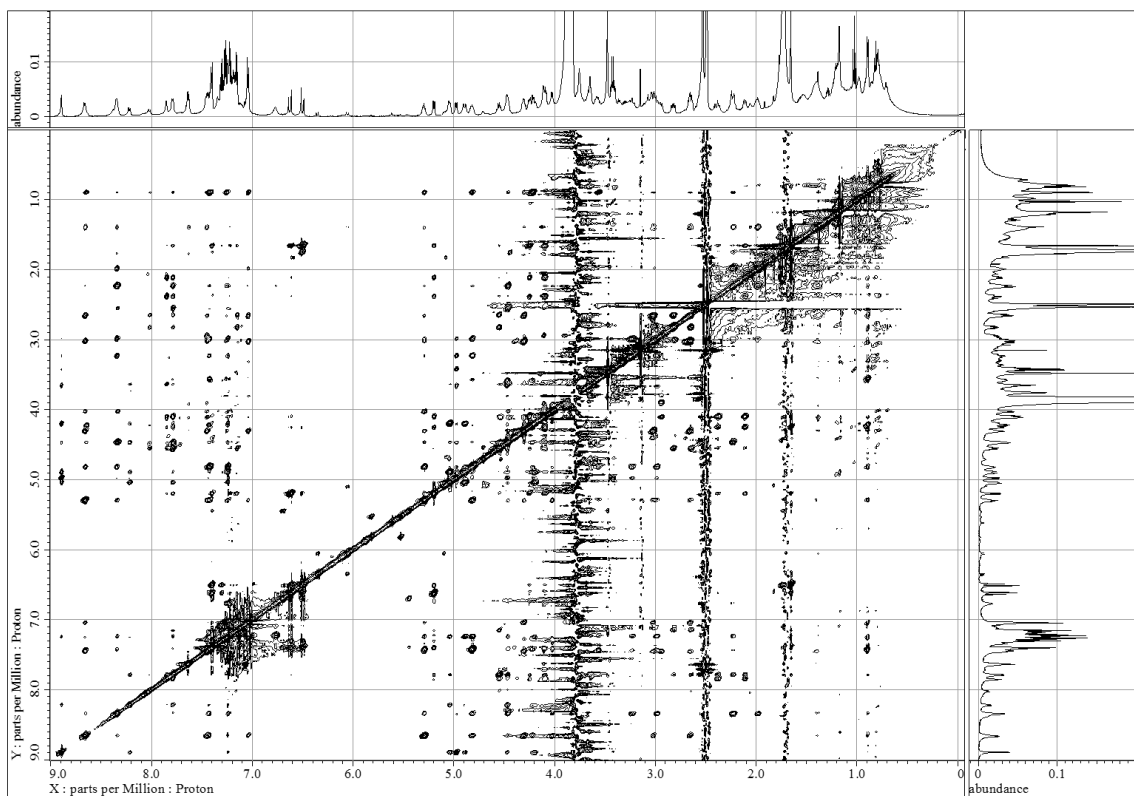


Figure S4-10. NOESY spectrum of theonellamide H (**4-1**) in DMSO- d_6 /H₂O (4:1) (600 MHz, 50 °C).

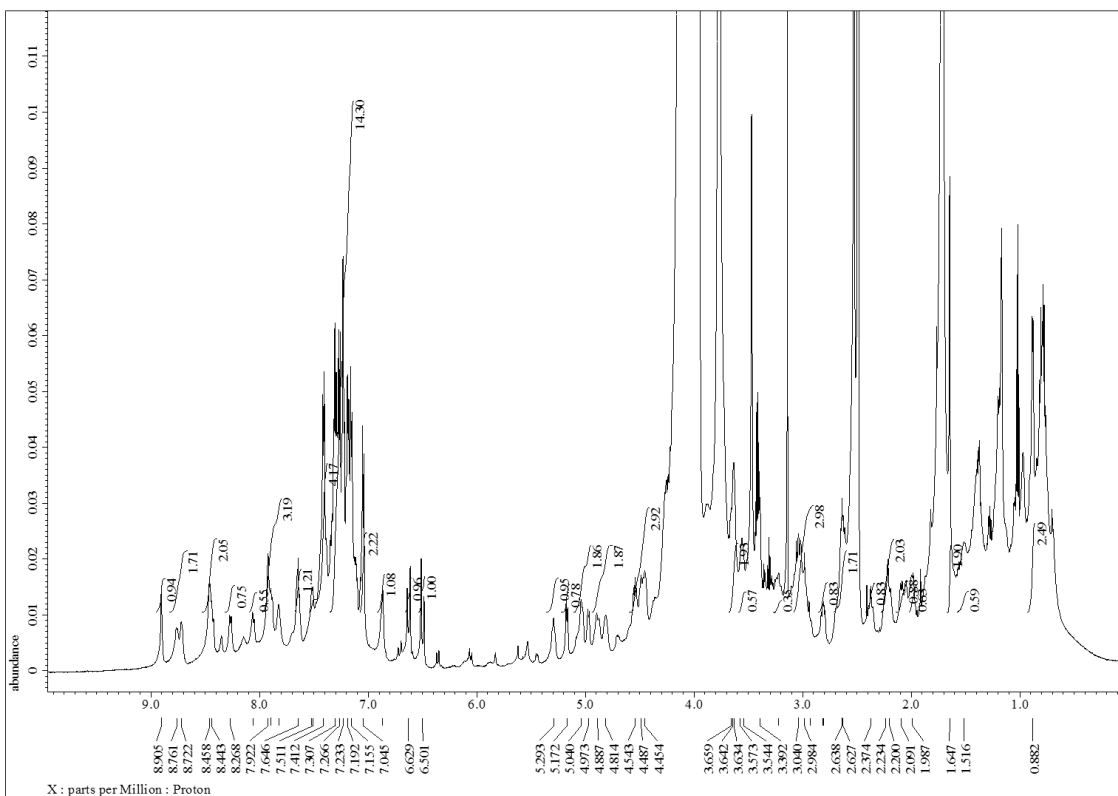


Figure S4-11. ^1H NMR spectrum of theonellamide H (**4-1**) in $\text{DMSO-}d_6/\text{H}_2\text{O}$ (4:1) (600 MHz, 30 °C).

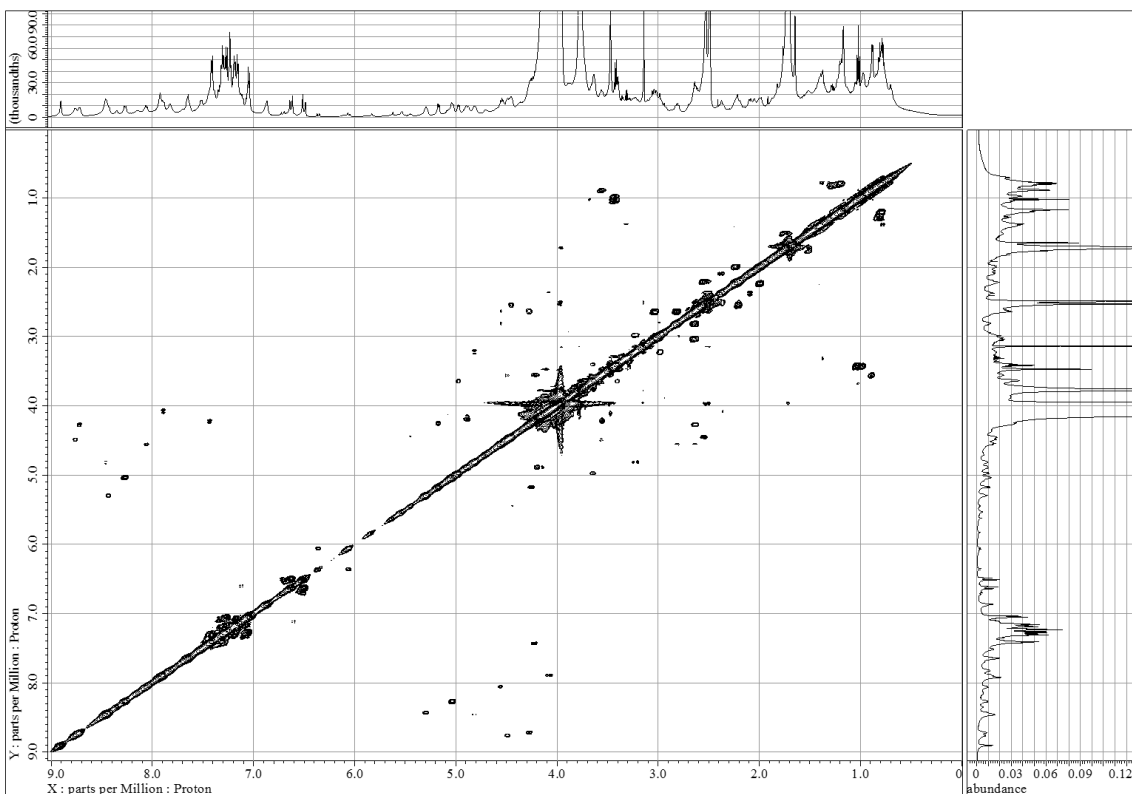


Figure S4-12. COSY spectrum of theonellamide H (**4-1**) in $\text{DMSO-}d_6/\text{H}_2\text{O}$ (4:1) (600 MHz, 30 °C).

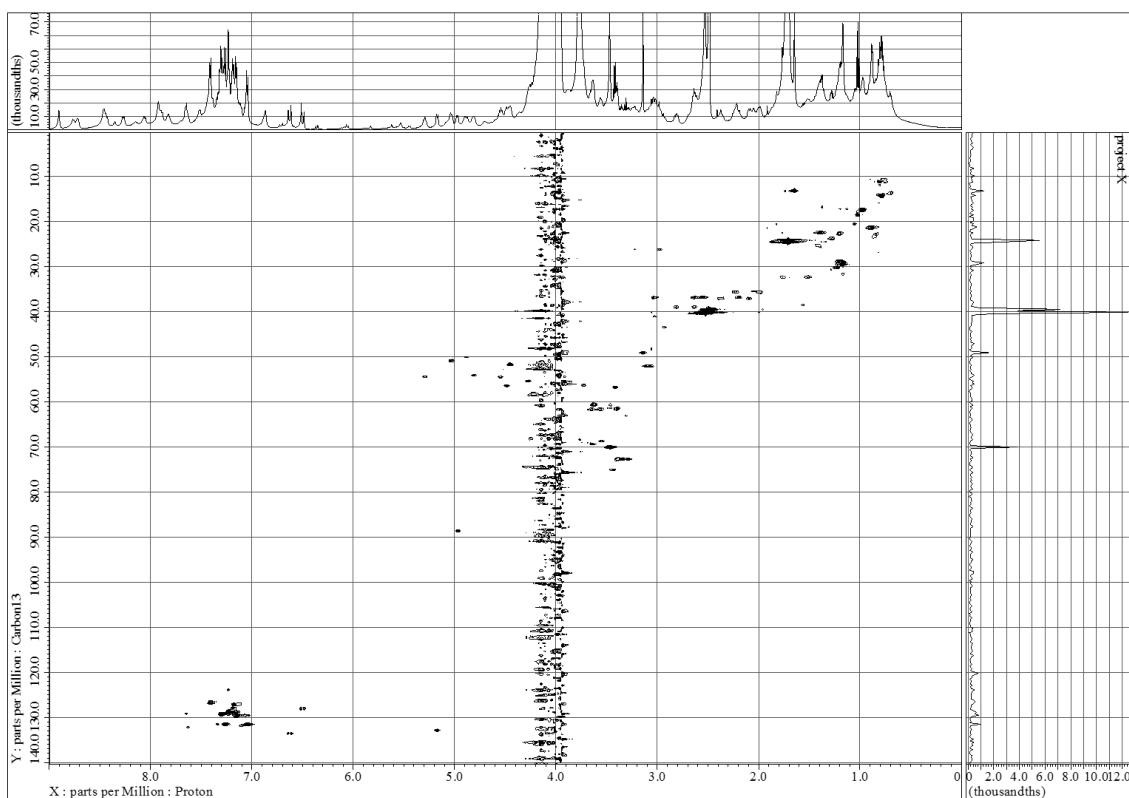


Figure S4-13. HSQC spectrum of theonellamide H (**4-1**) in DMSO-*d*₆/H₂O (4:1) (600 MHz, 30 °C).

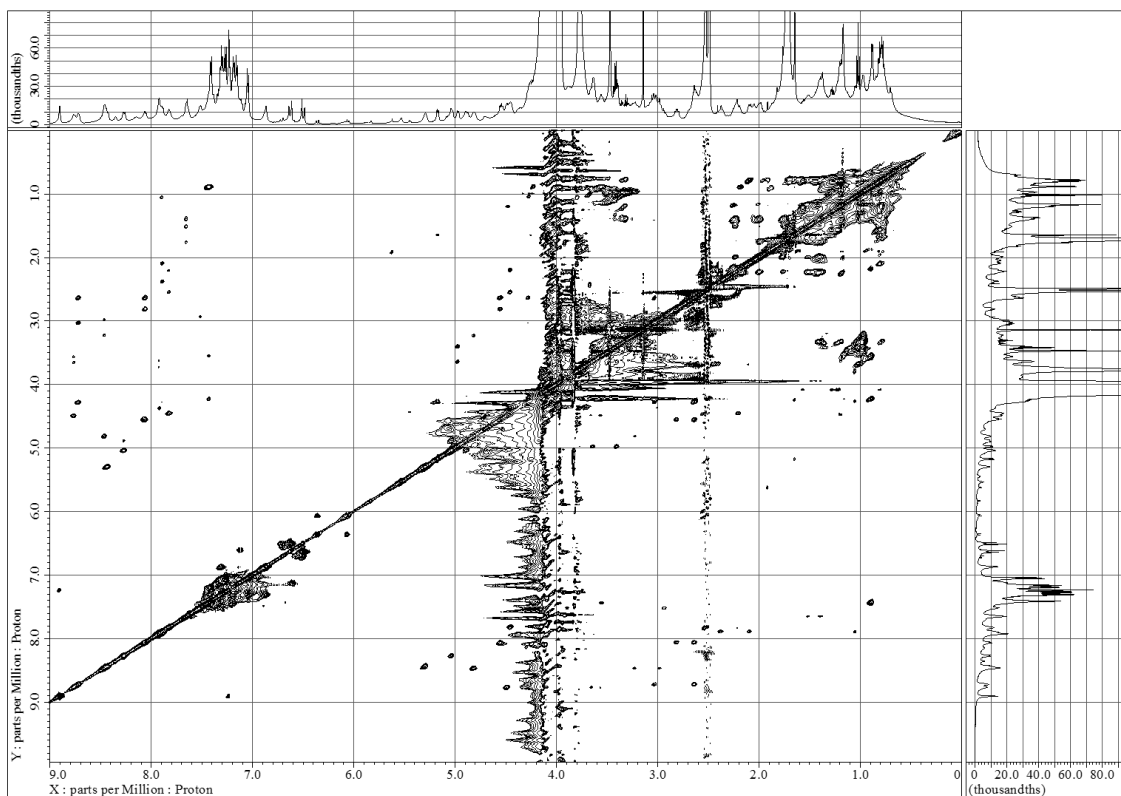


Figure S4-14. TOCSY spectrum of theonellamide H (**4-1**) in DMSO-*d*₆/H₂O (4:1) (600 MHz, 30 °C).

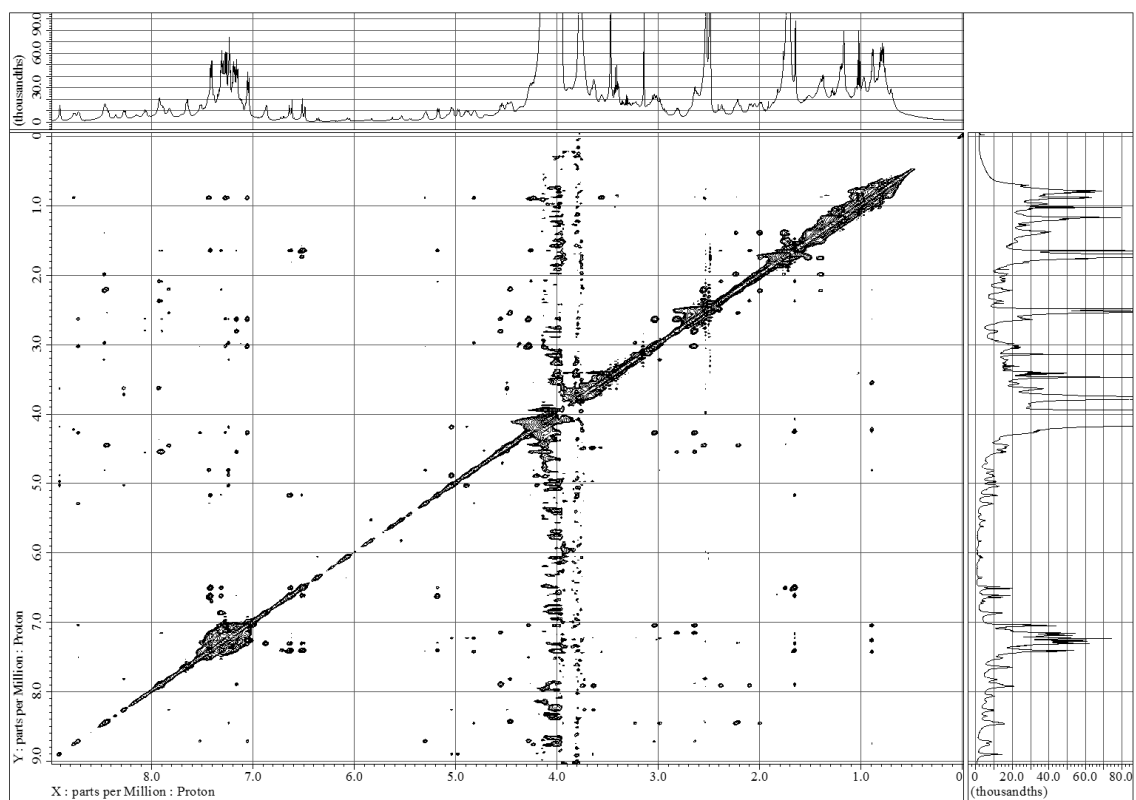


Figure S4-15. NOESY spectrum of theonellamide H (**4-1**) in DMSO-*d*₆/H₂O (4:1) (600 MHz, 30 °C).

Table S4-2. Results of Marfey's Analyses of Theonellamide H (**4-1**) and Analysis of the Absolute Configuration of the Arabinose Residue in **4-1**.

amino acid	retention time (min)		
	L	D	Sample
Aad	13.9	14.1	13.9
Asp	12.7	13.0	12.7
BrPhe	19.7	21.1	19.8
Iser	13.3	13.1	13.3
Phe	17.8	19.0	17.9
Ser	12.4	12.8	12.5
Thr	12.3	13.6	12.8
<i>allo</i> -Thr	12.8	13.3	
Arabinose	32.2	33.5	32.2

Table S4-3. Result of Marfey's Analysis of the OHAsp Residue in Theonellamide H (**4-1**).

amino acid	retention time (min)		
	(2 <i>S</i> , 3 <i>R</i>)	(2 <i>R</i> , 3 <i>S</i>)	Sample
OHAsp	12.0	11.8	12.1

Table S4-4. Result of Marfey's Analysis of the HisAla Residue in Theonellamide H (**4-1**).

amino acid	retention time (min)				Sample
	L, L	L, D	D, L	D, D	
HisAla	16.9	15.8	15.7	15.3	15.8

Table S4-5. Result of Marfey's Analysis of the H₄-Apoa Residue in Theonellamide H (**4-1**).

amino acid	retention time (min)		
	(2 <i>S</i> , 4 <i>R</i>)	(2 <i>R</i> , 4 <i>S</i>)	Sample
H ₄ -Apoa	20.1, 20.8	22.6, 23.0	20.1, 20.9

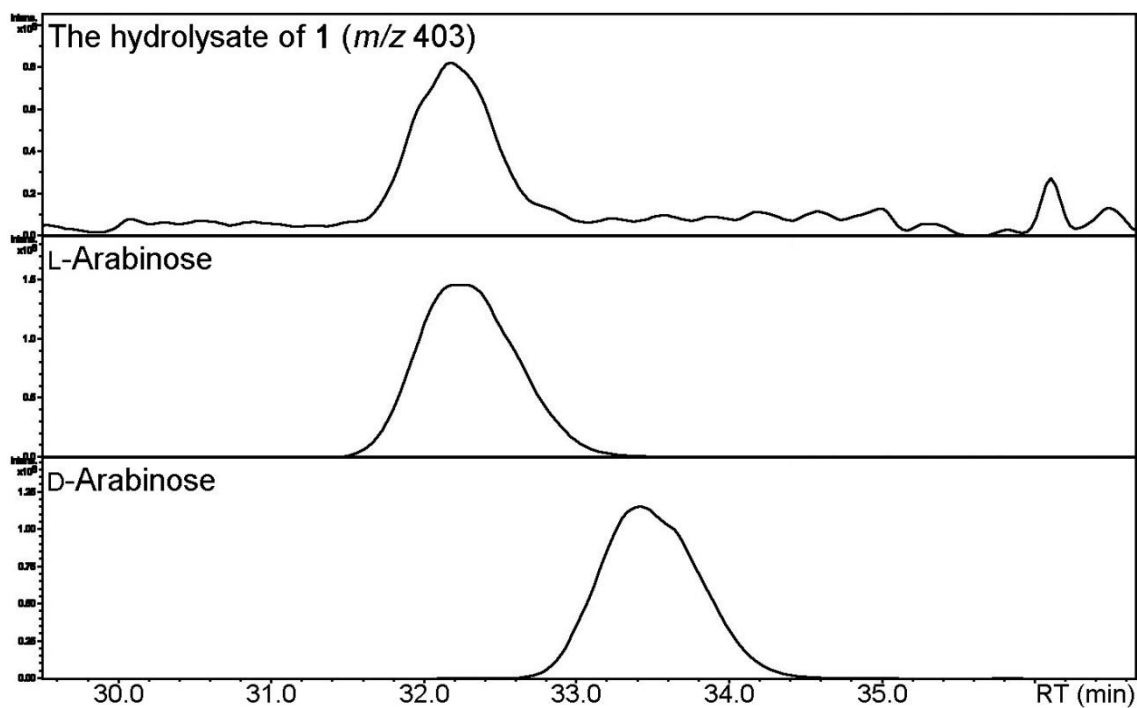


Figure S4-16. LC-MS chart of the arabinose residue after converting into the methyl 3-phenylthiocarbamoylthiazoline-4(*R*)-carboxylate derivative.

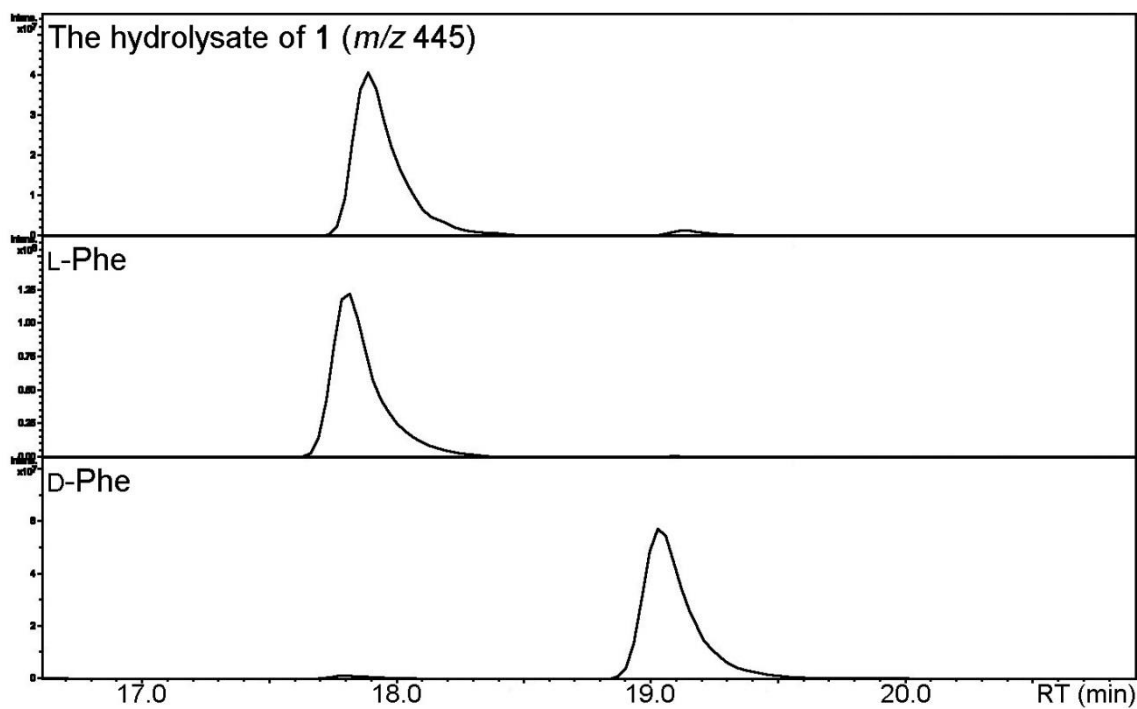


Figure S4-17. LC-MS chart of Marfey's analysis of theonellamide H (**4-1**) (Phe).

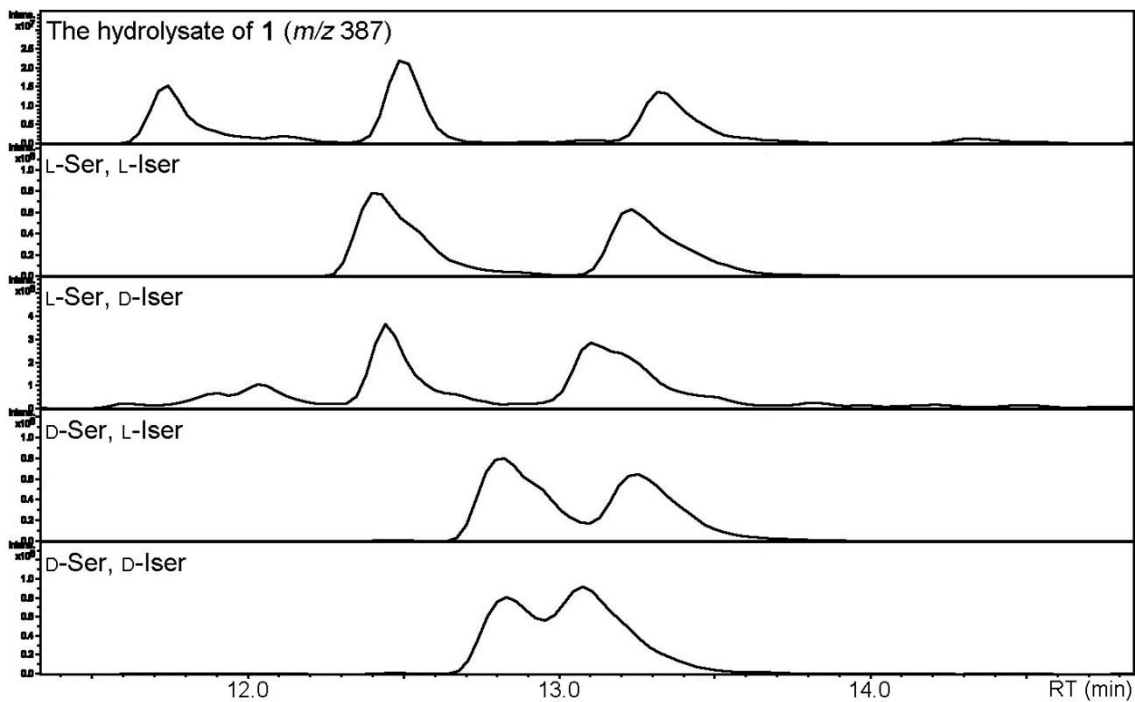


Figure S4-18. LC-MS chart of Marfey's analysis of theonellamide H (**4-1**) (Ser, Iser).

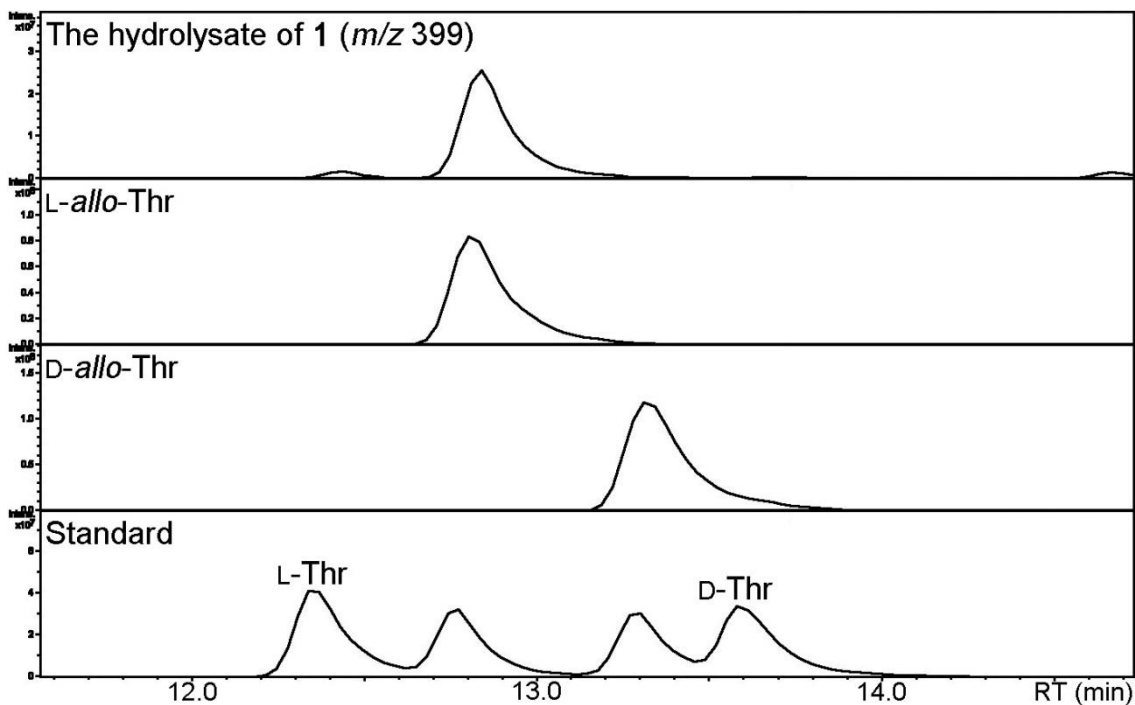


Figure S4-19. LC-MS chart of Marfey's analysis of theonellamide H (**4-1**) (Thr).

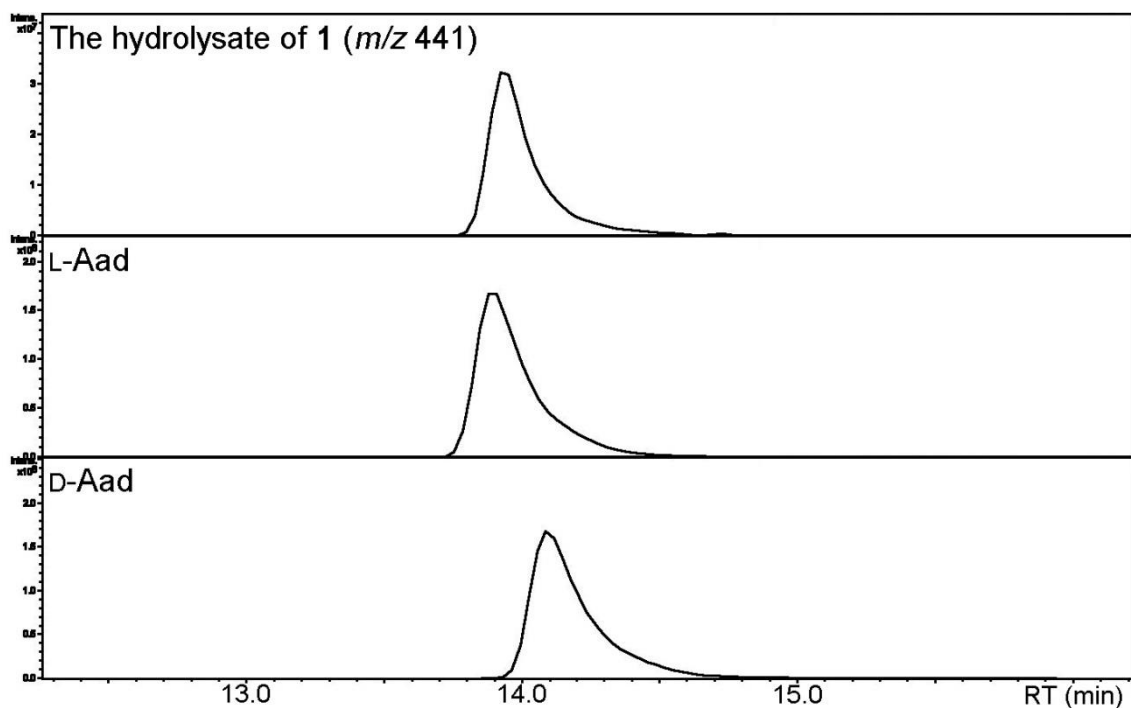


Figure S4-20. LC-MS chart of Marfey's analysis of theonellamide H (**4-1**) (Aad).

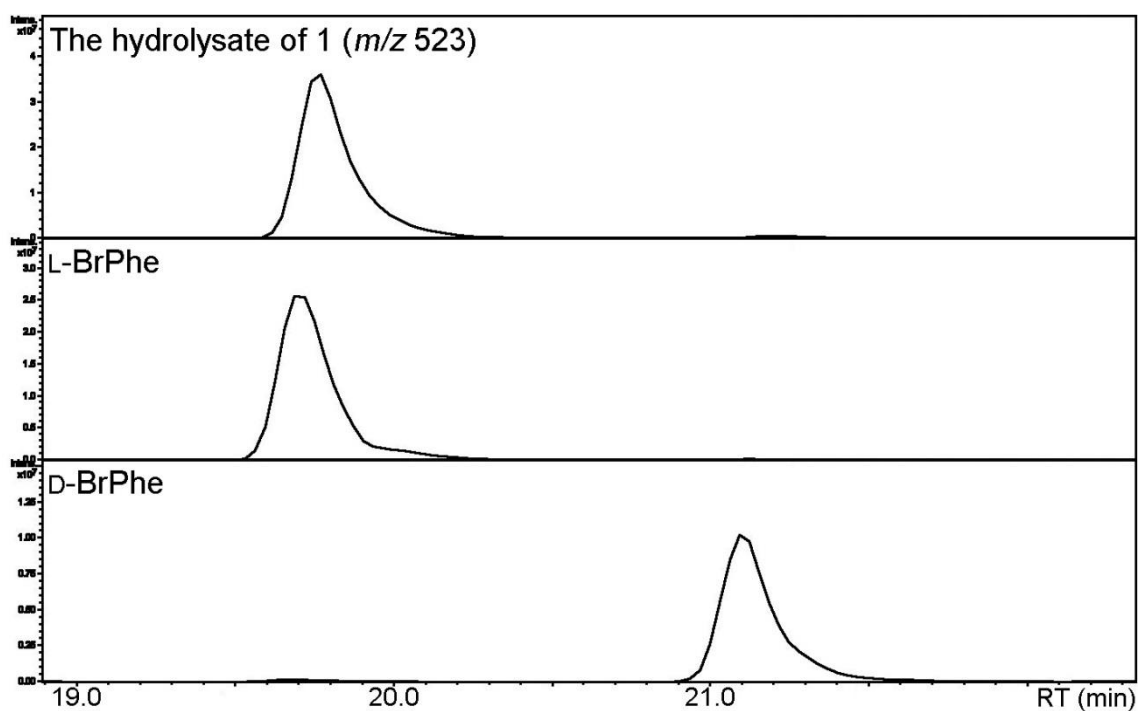


Figure S4-21. LC-MS chart of Marfey's analysis of theonellamide H (**4-1**) (BrPhe).

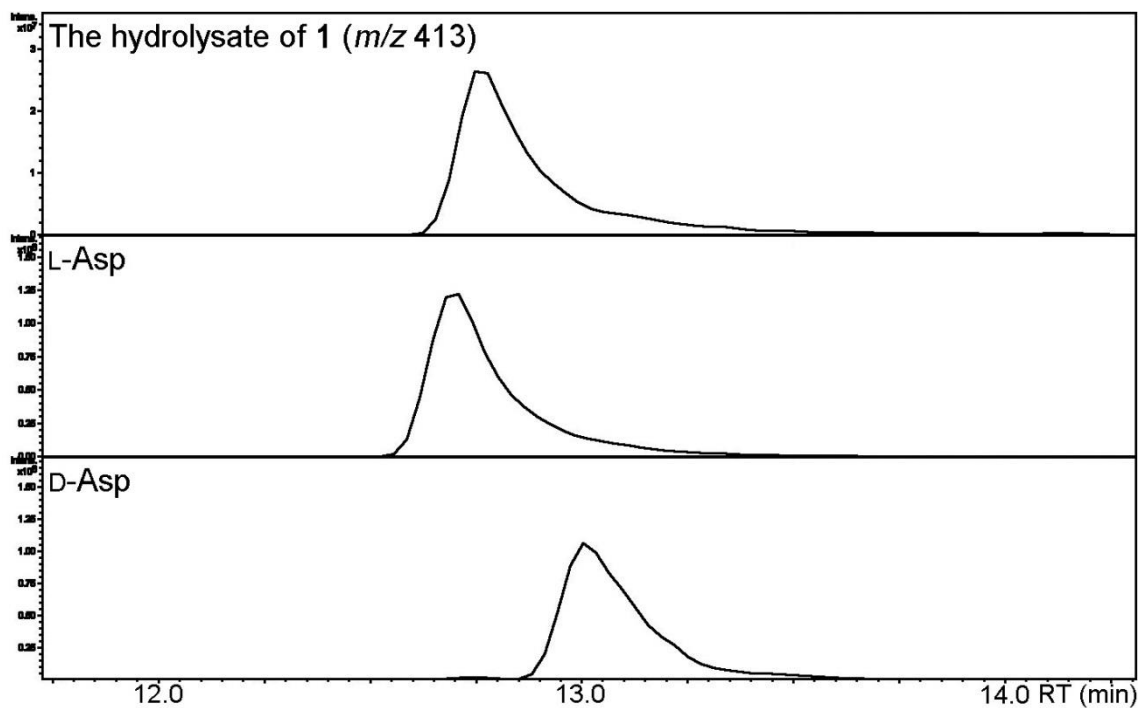


Figure S4-22. LC-MS chart of Marfey's analysis of theonellamide H (4-1) (Asp).

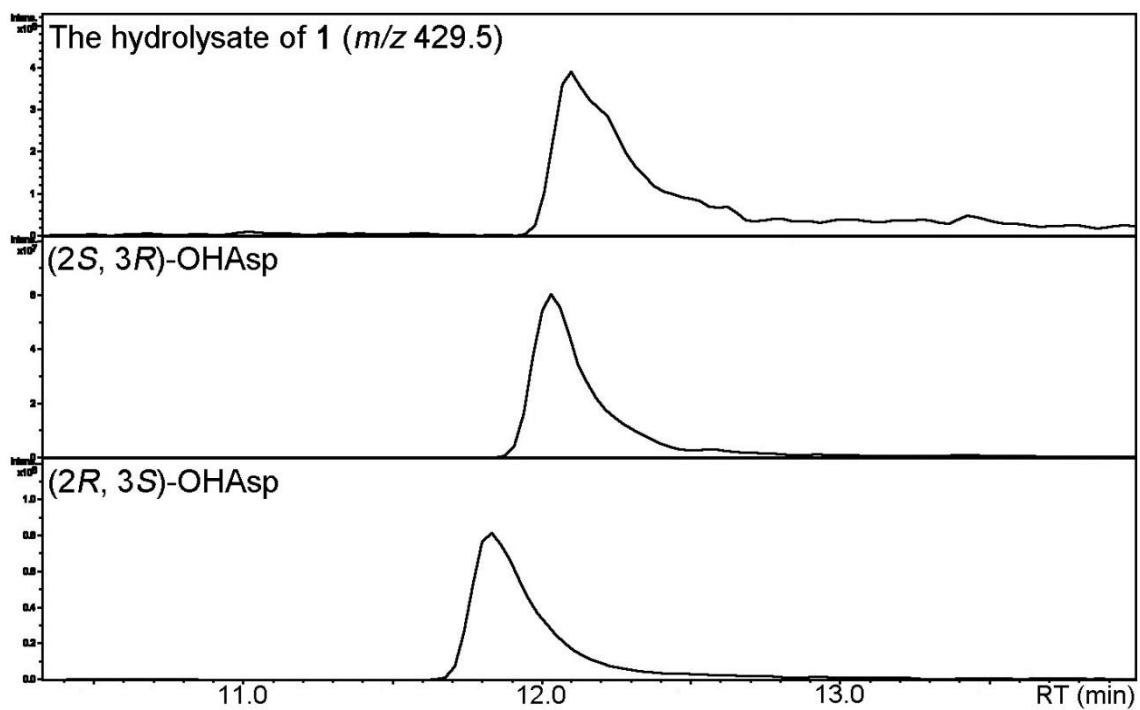


Figure S4-23. LC-MS chart of Marfey's analysis of theonellamide H (4-1) (OHAsp).

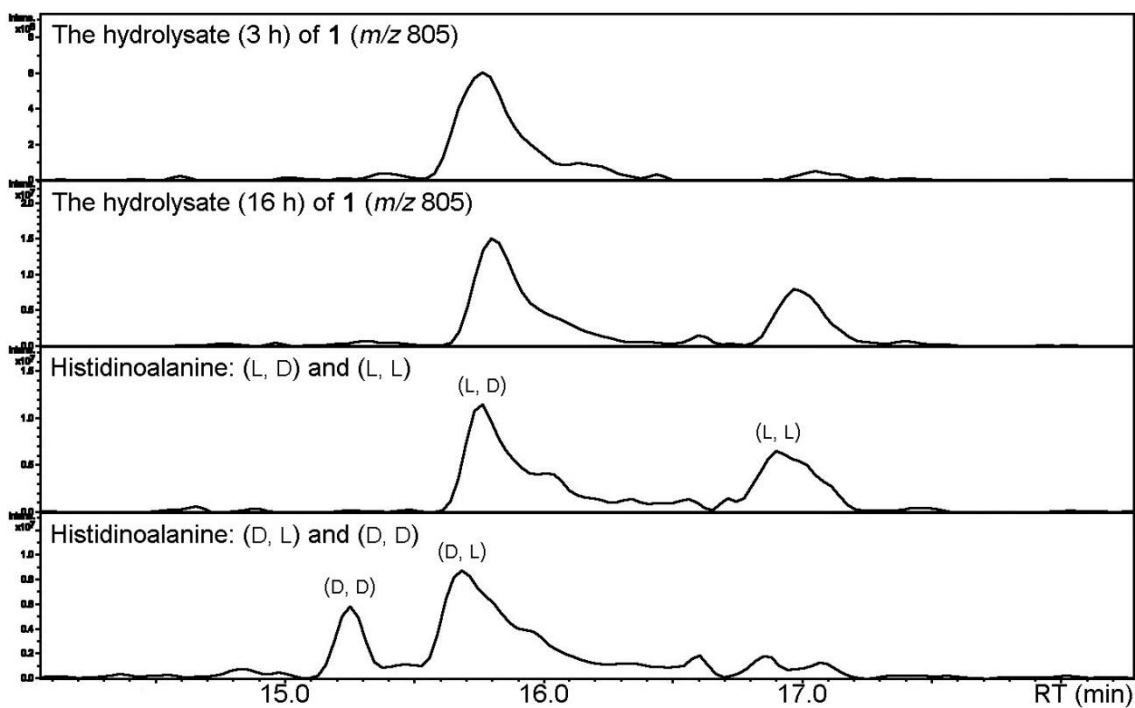


Figure S4-24. LC-MS chart of Marfey's analysis of theonellamide H (**4-1**) (HisAla).

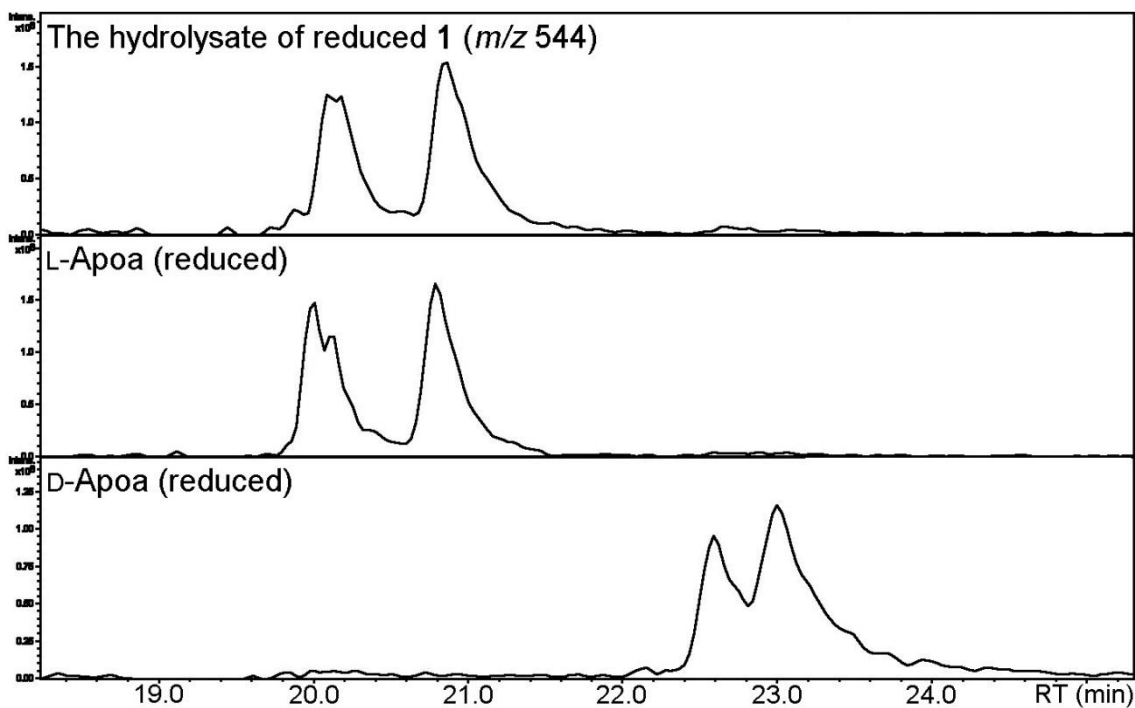


Figure S4-25. LC-MS chart of Marfey's analysis of theonellamide H (**4-1**) (H₄-Apoa.).

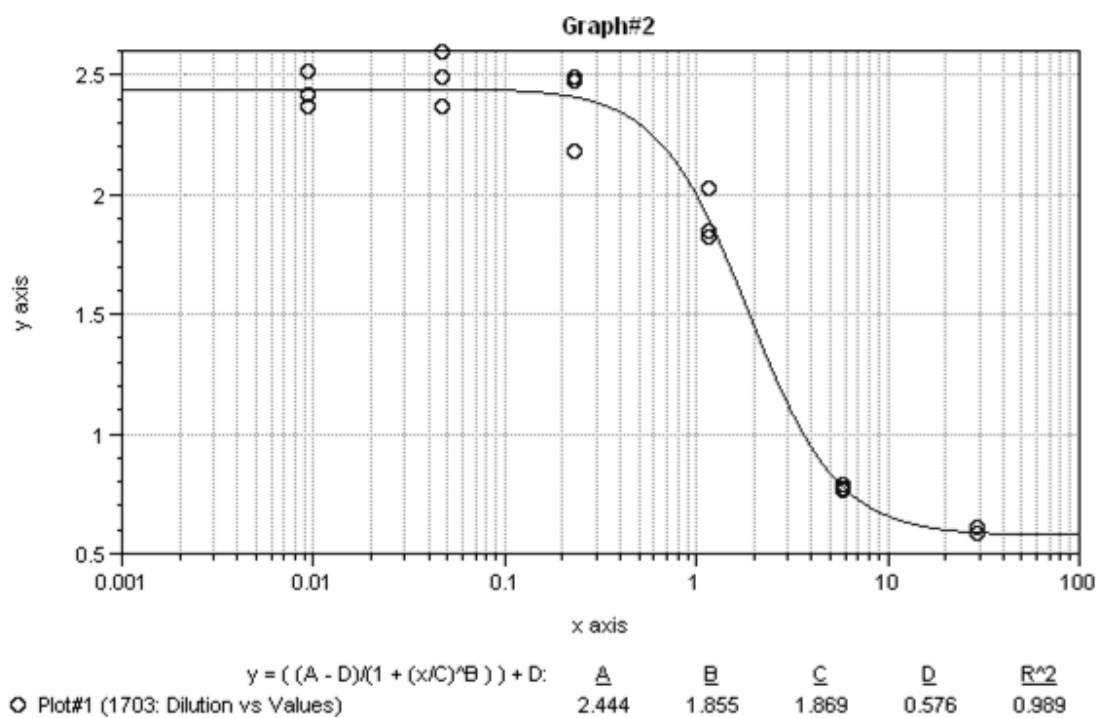


Figure S4-26. The graph of XTT assay of **4-1** against HeLa cells; x-axis is concentration and y-axis is absorption at 450 nm.

Chapter 5.

Conclusion

Traditionally, natural products have been important resource of drug discovery.⁶⁹ As the success in penicillin brought natural products in market in 1940s, many research groups and pharmaceutical companies searched for new drugs from natural sources. From 1980s, along with the improvement of NMR and MS techniques, and other biological technologies, a variety of natural products with complex structure were isolated. From 1990s, pharmaceutical industries changed their attention to synthetic compounds as drug resource because high-through put screening (HTS) system was developed and the system enabled to test a lot of drug candidates in a short time. Until now, HTS and chemical library of synthetic compounds were the main research theme of companies, however, discovery rate of novel drugs is dropping dramatically.⁷⁰ On the other hand, 40% approved drugs in U.S. were still natural products or their related compounds⁷¹, so natural products should be reexamined as drug resource.⁷² Actually, HTS hit rates of chemical library of natural products are better than those of synthetic compound chemical library.⁷³

In this research, we searched for new bioactive natural products from the sponge *Theonella swinhoei*. As a result, we found four cytotoxic compounds (nazumazoles A–C and theonellamide H) and three enzyme inhibitors (nazumazoles D–F). These compounds are difficult to detect by traditional UV- or bioassay-based separation. This result indicated that a large amount of chemical resources in sponges including *T. swinhoei* and their symbiotic bacteria are still underexplored. With progress in biological techniques, it is expected that new drugs and biological research tools will be discovered from sponges.

In 1986, the structure of a potent anti-tumor sponge metabolite, halichondrin B, was reported.⁷⁴ The total synthesis of halichondrin B was achieved six years later⁷⁵, and tested their synthetic analogues as anti-cancer agents in 2001.⁷⁶ Finally, a synthetic analogue of halichondrin B, ER-086526, was approved as an anti-cancer drug in 2010. From this success story of halichondrin B, it is indicated that structure of bioactive natural products is necessary information to synthesize natural products and provide compounds for clinical trial or drug use. In addition, the structure of natural products is important to obtain biosynthetic genes of the compounds.

Moreover, structural information of bioactive compounds is essential for *de novo* synthesis of drug candidates. To design candidates, medicinal chemists must

consider an enormous number of chemical structures (theoretically, the number of organic molecules with molecular mass of less than 500 Da could be up to 10^{60})⁷⁷. The structures of bioactive natural products and their modes of action can not only elucidate biological phenomenon at a molecular level⁷⁸, but also provide the idea of drug candidates' structure.⁷⁹

In this research, with a number of degradation studies and analysis of derivatives, we determined the structures of seven compounds including the absolute configuration. While nazumazoles A–C (**2-1-2-3**), cyclic peptide dimers, exhibited cytotoxicity against leukemia cells, nazumazoles D–F (**3-1-3-3**), monomeric analogues of **2-1-2-3**, showed no cytotoxicity against the same cell line. Recently, comparable phenomenon was observed in the study about cyclic hexapaptide dimers, antatollamides A and B.⁸⁰ These results suggested that bioactivities of cyclic peptides could be changed or improved by dimerization through disulfide bonds. Theonellamide H was a structural analogue of theonellamide family. As described in chapter 1, the molecular target of theonellamide F was revealed as 3β -hydroxysterols.²¹ By comparing the bioactivity against 3β -hydroxysterols and cell membrane among theonellamide family, it can be revealed which structure is important for binding to sterols.

Nazumazoles contain several unusual amino acids and D-amino acids, and have the structural similarity with peptides isolated from *T. swinhoei*, such as cyclotheonamide A²⁷ and orbiculamide A.⁵⁰ In addition, the absolute configurations of nazumazoles were conserved regardless of replacements of amino acids. These results indicated that nazumazoles should be non-ribosomal peptide. 4-methylproline is one of the most characteristic amino acids in nazumazoles. A few peptides isolated from *T. swinhoei* contain this amino acid (perthamides⁸¹ and mutremdamide A⁸²), and this amino acid is mainly found in peptides isolated from cyanobacteria.⁸³ While biosynthetic gene cluster of this amino acid was identified in cyanobacteria⁸⁴, that has not been found in metagenome of *T. swinhoei*. If biosynthetic gene cluster of nazumazoles and 4-methylproline is established, it is expected not only to provide nazumazoles for biological research to reveal the mode of action, but also to find new class of active peptides in *T. swinhoei* by genome mining.

As mentioned in chapter 4, theonellamide H is the first analogue of theonellamides which was isolated from *T. swinhoei* Y. Both *T. swinhoei* Y and *T. swinhoei* W contain *Ca. Entotheonella* bacteria in their tissues, but their metabolic profiles are clearly different (chapter 1, figure 1-3).^{41,42} From the discovery of theonellamide H, it is supposed that the horizontal transmission of genes or bacteria

occurs among bacteria in sponges. We would like to compare metagenome or bacterial composition among colonies of *T. swinhoei* Y, and examine if there is a difference between the colony containing theonellamide H and the colony not containing the compound.

In summary, we found seven bioactive peptides from the sponge *T. swinhoei* Y and determined their structures. They have potential for being drug candidates or biological research tools. In addition, their information about structure and bioactivities will provide new insights into biochemistry and design of (semi)synthetic drug candidates. The result of this work is beneficial for development of chemistry, pharmacology, and biology.

References and Notes

1. Li, C.-W.; Chen, J.-Y.; Hua, T.-E. *Science* **1998**, *279*, 879–882.
2. Love, G. D.; Grosjean, E.; Stalvies, C.; Fike, D. A.; Grotzinger, J. P.; Bradley, A. S.; Kelly, A. E.; Bhatia, M.; Meredith, W.; Snape, C. E.; Bowring, S. A.; Condon, D. J.; Summons, R. E. *Nature* **2009**, *457*, 718–721.
3. Van Soest, R. W. M.; Boury-Esnault, N.; Vacelet, J.; Dohrmann, M.; Erpenbeck, D.; De Voogd, N. J.; Santodomingo, N.; Vanhoorne, B.; Kelly, M.; Hooper, J. N. A. *PLoS One* **2012**, *7*, e35105
4. Pechenik, J. A. *Biology of the invertebrates*. **2010**, McGraw-Hill, New York.
5. Verma, A. *Invertebrates Protozoa to Echinodermata*. **2005**, Alpha Science International, Oxford.
6. Vos, L. D.; Rützler, K.; Boury-Esnault, N.; Donadey, C.; Vacelet, J. *Atlas of sponge morphology*. **1991**, Smithsonian institution press, Washington and London.
7. Hentschel, U.; Piel, J.; Degnan, S. M.; Taylor, M. W. *Nat. Rev. Microbiol.* **2012**, *10*, 641–654.
8. Bewley, C. A.; Faulkner, D. J. *Angew. Chem. Int. Ed.* **1998**, *37*, 2162–2178.
9. Furrow, F. B.; Amsler, C. D.; McClintock, J. B.; Baker, B. J. *Mar. Biol.* **2003**, *143*, 443–449.
10. Porter, J. W.; Targett, N. M.; *Biol. Bull.* **1988**, *175*, 230–239.
11. Lee, O. O.; Yang, L. H., Li, X.; Pawlik, J. R.; Qian, P.-Y. *Mar. Ecol. Prog. Ser.* **2007**, *339*, 25–40.
12. Pawlik, J. R. *BioScience* **2011**, *61*, 888–898.
13. Molinski, T. F.; Dalisay, D. S.; Lievens, S. L.; Saludes, J. P. *Nat. Rev. Drug Discov.* **2009**, *8*, 69–85.
14. Blunt, J. W.; Copp, B. R.; Keyzers, R. A.; Munro, M. H. G.; Prinsep, M. R. *Nat. Prod. Rep.* **2017**, *34*, 235–294.
15. Marinlit: <http://pubs.rsc.org/marinlit/>
16. Sakai, R.; Higa, T.; Kashman, Y. *Chem. Lett.* **1986**, *15*, 1499–1502.
17. Kato, Y.; Fusetani, N.; Matsunaga, S.; Hashimoto, K.; Sakai, R.; Higa, T.; Kashman, Y. *Tetrahedron Lett.* **1987**, *28*, 6225–6228.
18. Tanaka, J.; Higa, T.; Kobayashi, M.; Kitagawa, I. *Chem. Pharm. Bull.* **1990**, *38*, 2967–2970.

19. (a) Carmely, S.; Kashman, Y. *Tetrahedron Lett.* **1985**, *26*, 511–514. (b) Kobayashi, M.; Tanaka, J.; Katori, T.; Matsuura, M.; Kitagawa, I. *Tetrahedron Lett.* **1989**, *30*, 2963–2966. (c) Kitagawa, I.; Kobayashi, M.; Katori, T.; Yamashita, M. Tanaka, J.; Doi, M.; Ishida, T. *J. Am. Chem. Soc.* **1990**, *112*, 3710–3712.
20. Matsunaga, S.; Fusetani, N.; Hashimoto, K.; Wälchli, M. *J. Am. Chem. Soc.* **1989**, *111*, 2582–2588.
21. Nishimura, S.; Arita, Y.; Honda, M.; Iwamoto, K.; Mastuyama, A.; Shirai, A.; Kawasaki, H.; Kakeya, H.; Kobayashi, T.; Matsunaga, S.; Yoshida, M. *Nat. Chem. Biol.* **2010**, *6*, 519–526.
22. Sakemi, S.; Ichiba, T.; Kohmoto, S.; Saucy, G.; Higa, T. *J. Am. Chem. Soc.* **1988**, *110*, 4851–4853.
23. Burrell, N. S.; Clement, J. J. *Cancer Res.* **1989**, *49*, 2935–2940.
24. Lee K.-H.; Nishimura, S.; Matsunaga, S.; Fusetani, N.; Horinouchi, S.; Yoshida, M. *Cancer Sci.* **2005**, *96*, 357–364.
25. Piel, J.; Hui, D.; Wen, G.; Butzke, D.; Platzer, M.; Fusetani, N.; Matsunaga, S. *Proc. Natl. Acad. Sci. USA* **2004**, *101*, 16222–16227.
26. Matsunaga, S.; Fusetani, N.; Kato, Y.; Hirota, H. *J. Am. Chem. Soc.* **1991**, *113*, 9690–9692.
27. Fusetani, N.; Matsunaga, S.; Matsumoto, H.; Takebayashi, Y. *J. Am. Chem. Soc.* **1990**, *112*, 7053–7054.
28. Hagihara, M.; Schreiber, S. L. *J. Am. Chem. Soc.* **1992**, *114*, 6570–6571.
29. (a) Lee, A. Y.; Hagihara, M.; Karmacharya, R.; Albers, M. W.; Schreiber, S. L.; Clardy, J. *J. Am. Chem. Soc.* **1993**, *115*, 12619–12620. (b) Maryanoff, B. E.; Qiu, X.; Padmanabhan, K. P.; Tulinsky, A.; Almond, H. R. Jr.; Andrade-Gordon, P.; Greco, M. N.; Kauffman, J. A.; Nicolaou, K. C.; Liu, A.; Brungs, P. H.; Fusetani, N. *Proc. Natl. Acad. Sci. USA* **1993**, *90*, 8048–8052.
30. Hamada, T.; Matsunaga, S.; Yano, G.; Fusetani, N. *J. Am. Chem. Soc.* **2005**, *127*, 110–118.
31. Hamada, T.; Matsunaga, S.; Fujiwara, M.; Fujita, K.; Hirota, H.; Schmucki R.; Güntert, P.; Fusetani, N. *J. Am. Chem. Soc.* **2010**, *132*, 12941–12945.
32. Inoue, M.; Shinohara, N.; Tanabe, S.; Takahashi, T.; Okura, K.; Itoh, H.; Mizoguchi, Y.; Iida, M.; Lee, N.; Matsuoka, S. *Nat. Chem.* **2010**, *2*, 280–285.
33. Freeman, M. F.; Gurgui, C.; Helf, M. J.; Morioka, B. I.; Uria, A. R.; Oldham, N. J.; Sahi, H.-G.; Matsunaga, S.; Piel, J. *Science* **2012**, *338*, 387–390.
34. Kobayashi, J.; Ishibashi, M. *Chem. Rev.* **1993**, *93*, 1753–1789.

35. Fusetani, N.; Matsunaga, S. *Chem. Rev.* **1993**, *93*, 1793–1806.
36. Bewley, C. A.; Holland, N. D.; Faulkner, D. J. *Experientia* **1996**, *52*, 716–722.
37. Schmidt, E. W.; Bewley, C. A.; Faulkner, D. J. *J. Org. Chem.* **1998**, *63*, 1254–1258.
38. Schmidt, E. W.; Obraztsova, A. Y.; Davidson, S. K.; Faulkner, D. J.; Haygood, M. G. *Mar. Biol.* **2000**, *136*, 969–977.
39. Piel, J. *Proc. Natl. Acad. Sci. USA* **2002**, *99*, 14002–14007.
40. Fusetani, N.; Sugawara, T.; Matsunaga, S. *J. Org. Chem.* **1992**, *57*, 3828–3832.
41. Wilson, M. C.; Mori, T.; Rückert, C.; Uria, A. R.; Helf, M. J.; Takada, K.; Gernert, C.; Steffens, U. A. E.; Heycke N.; Schmitt, S.; Rinke, C.; Helfrich, E. J. N.; Brachmann, A. O.; Gurgui, C.; Wakimoto, T.; Kracht, M.; Crüsemann, M.; Hentschel, U.; Abe, I.; Matsunaga, S.; Kalinowski, J.; Takeyama, H.; Piel, J. *Nature* **2014**, *506*, 58–62.
42. Ueoka, R.; Uria, A. R.; Reiter, S.; Mori, T.; Karbaum, P.; Peters, E. E.; Helfrich, E. J. N.; Morinaka, B. I.; Gugger, M.; Takeyama, H.; Matsunaga, S.; Piel, J. *Nat. Chem. Biol.* **2015**, *11*, 705–712.
43. Kato, Y.; Fusetani, N.; Matsunaga, S.; Hashimoto, K.; Fujita, S.; Furuya, T. *J. Am. Chem. Soc.* **1986**, *108*, 2780–2781.
44. Ishida, K.; Murakami, M. *J. Org. Chem.* **2000**, *65*, 5898–5900.
45. Wakimoto, T.; Egami, Y.; Nakashima, Y.; Wakimoto, Y.; Mori, T.; Awakawa, T.; Ito, T.; Kenmoku, H.; Asakawa, Y.; Piel, J.; Abe, I. *Nat. Chem. Biol.* **2014**, *10*, 648–655.
46. Nakashima, Y.; Egami, Y.; Kimura, M.; Wakimoto, T.; Abe, I. *PLoS One* **2016**, *11*, e0164468.
47. Lackner, G.; Peters, E. E.; Helfrich, E. J. N.; Piel, J. *Proc. Natl. Acad. Sci. USA* **2017**, *114*, E347–E356
48. Matsunaga, S.; Fusetani, N.; Nakao, Y. *Tetrahedron* **1992**, *48*, 8369–8376.
49. (a) Kobayashi, J.; Sato, M.; Ishibashi, M.; Shigemori, H.; Nakamura, T.; Ohizumi, Y. *J. Chem. Soc. Perkin Trans. 1* **1991**, 2609–2611. (b) Itagaki, F.; Shigemori, H.; Ishibashi, M.; Nakamura, T.; Sasaki, T.; Kobayashi, J. *J. Org. Chem.* **1992**, *57*, 5540–5542. (c) Kobayashi, J.; Itagaki, F.; Shigemori, H.; Takao, T.; Shimonishi, Y. *Tetrahedron* **1995**, *51*, 2525–2532.
50. Fusetani, N.; Sugawara, T.; Matsunaga, S.; Hirota, H. *J. Am. Chem. Soc.* **1991**, *113*, 7811–7812.

51. The presence of Kle and Knv residues was confirmed by the Marfey's analysis of the hydrolysate which gave peaks for of DAA-derivatized rKlv (m/z 400) and DAA-derivatized rKle (m/z 414) (c.f. the experimental section). This was confirmed by the HMBC data of **2-4a**, **2-4b**, **2-5a**, and **2-5b**.
52. The reduced products of **2-1–2-3** with DTT only gave broad peaks in ODS-HPLC [m/z 594 and 608 ($M + H$)⁺] and could not be separated.
53. Each peak in Figure S2-2 contains four diastereomers which were not separable by ODS-HPLC. Each peak gave two sets of NMR signals depending on the configuration of the secondary alcohol.
54. Marfey, P. *Carlsberg Res. Commun.* **1984**, *49*, 591–596.
55. Murphy, A. C.; Mitova, M. I.; Blunt, J. W.; Munro, M. H. G. *J. Nat. Prod.* **2008**, *71*, 806–809.
56. The mixture of nazumazoles A–C also inhibit chymotrypsin (IC_{50} : 3.9 μ M), and do not inhibit trypsin or thrombin at a concentration of 50 μ M.
57. Ireland, C. M.; Durso, A. R. Jr.; Newman, R. A.; Hacker, M. P. *J. Org. Chem.* **1982**, *47*, 1807–1811.
58. (a) Schmidt, E. W.; Sudek, S.; Haygood, M. G. *J. Nat. Prod.* **2004**, *67*, 1341–1345. (b) Schmidt, E. W.; Nelson, J. T.; Rasko, D. A.; Sudek, S.; Eisen, J. A.; Haygood, M. G.; Ravel, J. *Proc. Natl. Acad. Sci. USA* **2005**, *102*, 7315–7320.
59. Sakai, R.; Kamiya, H.; Murata, M.; Shimamoto, K. *J. Am. Chem. Soc.* **1997**, *119*, 4112–4116.
60. Sakai, R.; Yoshida, K.; Kimura, A.; Koike, K.; Jimbo, M.; Koike, K.; Kobiyama, A.; Kamiya, H. *ChemBioChem* **2008**, *9*, 543–551.
61. Fusetani, N.; Nakao, Y.; Matsunaga, S. *Tetrahedron Lett.* **1991**, *32*, 7073–7074.
62. To increase the yield of the compound, we isolated the compound from the extract of *T. swinhoei* Y made in 1999. The detail of extraction and isolation procedure was described in the Experimental section.
63. Bewley, C. A.; Faulkner, D. J. *J. Org. Chem.* **1994**, *59*, 4849–4852.
64. (a) Matsunaga S.; Fusetani N. *J. Org. Chem.* **1995**, *60*, 1177–1181. (b) Youssef, D. T. A.; Shaala, L. A.; Mohamed, G. A.; Badr, J. M.; Bamanie, F. H.; Ibrahim, S. R. M. *Mar. Drugs* **2014**, *12*, 1911–1923.
65. The weak NOESY correlation was observed between the signal of NH proton of Iser residue (δ_H 7.45) and the signal of g-proton of Aad residue (δ_H 1.40) at 50 °C.

66. The relative stereochemistry of OHAsp and ApoA residues was determined as same as that of theonellamide A based on the coupling constants ($^3J_{H-\alpha/H-\beta} = 7.2$ Hz and $^3J_{H-\beta/H-\gamma} = 3.9$ Hz, respectively) and almost identical chemical shifts.
67. Tanaka, T.; Nakashima, T.; Ueda, T.; Tomii, K.; Kouno, I. *Chem. Pharm. Bull.* **2007**, *55*, 899–901.
68. Wang, Y.-H.; Avula, B.; Fu, X.; Wang, M.; Khan, I. A. *Planta Med.* **2012**, *78*, 834–837.
69. Katz, L.; Baltz, R. H. *J. Ind. Microbiol. Biotechnol.* **2016**, *43*, 155–176.
70. Scannell, J. W.; Blanckley, A.; Boldon, H.; Warrington, B. *Nat. Rev. Drug Discov.* **2012**, *11*, 191–200.
71. Newman, D. J.; Cragg, G. M. *J. Nat. Prod.* **2016**, *79*, 629–661.
72. Harvey, A. L.; Edrada-Ebel, R.; Quinn, R. J. *Nat. Rev. Drug Discov.* **2015**, *14*, 111–129.
73. Sukuru, S. C. K.; Jenkins, J. L.; Beckwith, R. E. J.; Scheiber, J.; Bender, A.; Mikhailov, D.; Davis, J. W.; Glick, M. *J. Biomol. Screen.* **2009**, *14*, 690–699.
74. Hirata, Y.; Uemura, D. *Pure Appl. Chem.* **1986**, *58*, 701–710.
75. Aicher, T. D.; Buszek, K. R.; Fang, F. G.; Forsyth, C. J.; Jung, S. H.; Kishi, Y.; Matelich, M. C.; Scola, P. M.; Spero, D. M.; Yoon, S. K. *J. Am. Chem. Soc.* **1992**, *114*, 3162–3164.
76. Towle, M. J.; Salvato, K. A.; Budrow, J.; Wels, B. F.; Kuznetsov, G.; Aalfs, K. K.; Welsh, S.; Zheng, W.; Seletsky, B. M.; Palme, M. H.; Habgood, G. J.; Singer, L. A.; DiPietro, L. V.; Wang, Y.; Chen, J. J.; Quincy, D. A.; Davis, A.; Yoshimatsu, K.; Kishi, Y.; Yu, M. J.; Littlefield, B. A. *Cancer Res.* **2001**, *61*, 1013–1021.
77. Bohacek, R. S.; McMartin, C.; Guida, W. C. *Med. Res. Rev.* **1996**, *16*, 3–50.
78. Dobson, C. M. *Nature* **2004**, *432*, 824–828.
79. Wetzel, S.; Bon, R. S.; Kumar, K.; Waldmann, H. *Angew. Chem. Int. Ed.* **2011**, *50*, 10800–10826.
80. Salib, M. N.; Molinski, T. F. *J. Org. Chem.* **2017**, *82*, 10181–10187.
81. (a) Gulavita, N. K.; Pomponi, S. A.; Wright, A. E.; Yarwood, D.; Sills, M. A. *Tetrahedron Lett.* **1994**, *35*, 6815–6818. (b) Festa, C.; Marino, S. D.; Sepe, V.; D'Auria, M. V.; Bifulco, G.; Andrés, R.; Terencio, M. C.; Payá, M.; Debitus, C.; Zampella, A. *Tetrahedron* **2011**, *67*, 7780–7786.
82. Plaza, A.; Bifulco, G.; Masullo, M.; Lloyd, J. R.; Keffer, J. L.; Colin, P. L.; Hooper, J. N. A.; Bell, L. J.; Bewley, C. A. *J. Org. Chem.* **2010**, *75*, 4344–4355.

83. Liu, L.; Jokela, J.; Herfindal, L.; Wahlsten, M.; Sinkkonen, J.; Permi, P.; Fewer, D. P.; Døskeland, S. O.; Sivonen, K. *ACS Chem. Biol.* **2014**, *9*, 2646–2655.
84. Luesch, H.; Hoffmann, D.; Hevel, J. M.; Becker, J. E.; Golakoti, T. Moore, R. E. *J. Org. Chem.* **2003**, *68*, 83–91.